

HEPATITIS C VIRUS NS3/4A PROTEASE AND THE INTRACELLULAR
ANTIVIRAL RESPONSE: MAPPING COMPLEX
VIRUS-HOST INTERACTIONS

APPROVED BY SUPERVISORY COMMITTEE

Michael J. Gale, Jr., Ph.D. (Supervisor)

Iwona Stroynowski, Ph.D. (Chair)

Nitin Karandikar, M.D., Ph.D.

Kim Orth, Ph.D

DEDICATION

I would like to dedicate this dissertation to my family, without whose love and support I would not have been able to complete this endeavor. My mother, Muriel, endowed me with excellent grammar skills that I have put to good use during my graduate education. Her belief in me has never faltered and for that I am grateful. In spite of having dropped me on my head when I was a baby, my brother Eric and I have always been close friends and allies. He, along with my father, Kenneth, are my computer experts, and over the last four years, I have had multiple, catastrophic technical difficulties that they have helped me solve. I would like to thank all of them for instilling in me a good work ethic and an unfailing moral compass.

I am very grateful to my mentor, Dr. Michael Gale, for the opportunities he gave me in his lab. I have learned a great deal from Mike, most importantly, how to ask the right questions and then go about answering them. His insights into the pathways we study, support, and guidance have been invaluable to me. My time in the lab was a very rewarding experience and has taught me how to become a great scientist and mentor.

The entire Gale Lab, past and present have all contributed to this work. Dr. Brenda Fredericksen was an invaluable source of techniques and reference material, and helped me when I first came to the lab as a rotation student. Dr. Penny Fish taught me how to use the confocal microscope, without which many of these experiments would not have been possible. Angela Collins, an MSTP summer rotation student, was truly critical in advancing the NS3/4A localization story, making many of the constructs that were used. Dr. Eileen Foy was an inspiration for me but down-to-earth and always available when I needed help or advice. Brian Keller, my fellow Medical Scientist Training

Program (MSTP) classmate, friend and expert proofreader, has always been there to discuss data. Andrea Erickson is also a great friend and source of support and amusement, as well as a valuable technical resource. Dr. Takeshi Saito exhibited a rare degree of quirkiness (insanity), and it was always a challenge to keep up with him. Innumerable times Takeshi has sat down with me and hashed out experimental designs or discussed confusing results. Eileen, Andrea, Brian, and Takeshi were also delightful traveling companions on conference trips and will always have a special place in my heart for the support they gave me during a difficult time. Nanette Crochet has been the rock of Gibraltar since the Gale lab move to Seattle, taking care of us orphans left in Dallas. Eileen, Takeshi, and Nanette provided me with hours of entertainment and I will miss their practical jokes, pranks, and mischievous spirit when I return to medical school. David Owen was very helpful in establishing the HCV infectious clone and aided me in the NS3/4A structure-function study. Dr. Yueh-Ming Loo and Kristan Hagan made several IPS-1 constructs, and the latter has been a fount of information about NF- κ B. Jill Pfluegheber and Drs. D. Spencer Carney, Mehul Suthar, Chunfu Wang, Rhea Sumpter, and Juniche Tanabe have also contributed to my work intellectually and have my thanks. Andrea and Dr. Stacy Horner have my gratitude for their input and critical reading of this thesis.

I would be remiss if I did not acknowledge all my teachers who have instilled in me my love for science, fostered my curiosity, and answered innumerable questions, and especially I would like to thank the Science Investigations instructors in high school: Mr. Reule, Mr. Price, and Dr. McLaughlin.

I am also extremely grateful to Julie Pfeiffer for taking me in for the last few months and even giving up her lab bench so that I would have a place to work. Kristie Ibarra, Sharon Kuss, and Chris Etheredge have been wonderful new lab mates.

The members of my advisory committee, Iwona Stroynowski, Nitin Karandikar, and Kim Orth, have always been helpful and I thank them for their comments, criticism, and suggestions.

I would also like to acknowledge Tom Januszewski and the Molecular and Cellular Imaging Facility at the University of Texas Southwestern Medical Center for their help with TEM sample processing and image analysis. Rachel Cassady in the Department of Microbiology office has gone above and beyond in helping me with forms, flights, and reimbursements for the numerous conferences I attended during graduate school. Finally, I would like to thank the MST Program for funding and especially Robin Downing and Stephanie Robertson for their assistance and support.

HEPATITIS C VIRUS NS3/4A PROTEASE AND THE INTRACELLULAR
ANTIVIRAL RESPONSE: MAPPING COMPLEX
VIRUS-HOST INTERACTIONS

by

CYNTHIA L. JOHNSON

DISSERTATION

Presented to the Faculty of the Graduate School of Biomedical Sciences

The University of Texas Southwestern Medical Center at Dallas

In Partial Fulfillment of the Requirements

For the Degree of

DOCTOR OF PHILOSOPHY

The University of Texas Southwestern Medical Center at Dallas

Dallas, Texas

June, 2009

Copyright

by

CYNTHIA L. JOHNSON, 2009

All Rights Reserved

HEPATITIS C VIRUS NS3/4A PROTEASE AND THE INTRACELLULAR
ANTIVIRAL RESPONSE: MAPPING COMPLEX
VIRUS-HOST INTERACTIONS

Publication No. .

Cynthia L. Johnson, M.D., Ph.D.

The University of Texas Southwestern Medical Center at Dallas, 2009

Supervising Professor: Michael Gale, Jr., Ph.D.

Virus infection triggers an innate immune response characterized by host cell production of interferon (IFN). Intermediates of viral replication, including dsRNA, initiate a signaling cascade that is amplified within the cell and alerts neighboring cells of viral invaders. Recognition of dsRNA intermediates occurs through retinoic acid inducible gene-1 (RIG-I). RIG-I elicits an antiviral state by binding to the IFN- β Promoter Stimulator-1 (IPS-1) adaptor protein, activating the latent downstream transcription factors IRF-3 and NF- κ B. These transcription factors bind to the promoter

region of effector genes including IFN- β , producing an antiviral amplification loop within and around the infected cell. This response is critical for immunity to infection.

Hepatitis C virus (HCV) is a serious global health problem with 170 million people chronically infected. HCV persistence is linked to viral regulation of innate host defenses by the nonstructural 3/4A protein complex (NS3/4A) cleavage of IPS-1. NS3 structural composition includes an amino-terminal serine protease and a carboxy-terminal RNA helicase. A structure-function analysis of NS3/4A truncation and deletion mutations was conducted. Mutants lacking the helicase domain retained the ability to control RIG-I signaling, but this regulation was abrogated by truncation of the protease domain. Furthermore, treatment of HCV-infected cells with a NS3/4A protease inhibitor prevented IPS-1 proteolysis, restored RIG-I signaling, and decreased viral protein levels. These results indicate that the NS3/4A protease domain alone can target IPS-1 on the mitochondrial membrane.

Current dogma holds that NS3/4A is located on the endoplasmic reticulum, thus the mechanism of NS3/4A targeting IPS-1, a mitochondrial membrane protein, remains unexplained. We have shown that NS3/4A distributes on mitochondria independently of the previously identified NS4A membrane localization motif, in a manner dependent on the first twenty amino acids of the NS3 protease domain.

The functional domains of IPS-1 that direct the immune response have not been elucidated. We conducted a structure-function study of IPS-1 that revealed distinct processes of IRF-3 and NF- κ B activation. Mutational analyses further identified areas of IPS-1 critical for mitochondrial localization, dimerization, and uncoupling IRF-3 and NF-

κ B signaling. These findings improve our understanding of IPS-1 function in innate immunity to virus infection.

TABLE OF CONTENTS

PRIOR PUBLICATIONS	xv
LIST OF FIGURES	xvi
LIST OF TABLES	xx
ABBREVIATIONS	xxi
CHAPTER 1: INTRODUCTION	1
HEPATITIS C VIRUS	1
Discovery of HCV	1
Clinical aspects of HCV	2
<i>Epidemiology</i>	2
<i>Clinical presentation and progression of disease</i>	2
<i>Economic burden of HCV</i>	5
Molecular Biology of HCV	5
<i>HCV genome structure and function</i>	6
<i>The HCV replication complex</i>	10
<i>The HCV replicon system and cell-culture infections HCV 2a clone</i>	11
<i>Animal models of HCV infections</i>	12
<i>Current and future therapy</i>	13
INNATE INTERFERON ANTIVIRAL RESPONSE	15
Pathogen recognition receptors (PRRs)	15
<i>RIG-I</i>	16
<i>HCV RNA triggers RIG-I</i>	18
<i>MDA5</i>	19

Interferon Regulatory Factors	20
<i>IRF-3</i>	21
<i>IRF-7</i>	24
<i>IRF-9</i>	25
NF- κ B	27
IPS-1	28
EFFECT OF HCV ON THE INTERFERON ANTIVIRAL RESPONSE.....	31
HCV infection in human patients	31
Disruption of RIG-I signaling by HCV NS3/4A	32
CHAPTER 2: MATERIALS AND METHODS	35
PLASMIDS AND TRANSFECTION	35
NS3/4A PROTEASE INHIBITORS	36
CELLS	36
VIRUSES	37
CONFOCAL MICROSCOPY	37
IMMUNOBLOTTING	38
IMMUNOPRECIPITATION ANALYSIS	39
PROMOTER LUCIFERASE REPORTER ASSAY	40
ELECTROPHORETIC MOBILITY SHIFT ASSAY (EMSA)	41
CHAPTER 3: FUNCTIONAL AND THERAPEUTIC ANALYSIS OF HCV NS3/4A PROTEASE CONTROL OF ANTIVIRAL IMMUNE DEFENSE	43

INTRODUCTION	43
EXPERIMENTAL PROCEDURES	46
Expression Cloning and Site-directed Mutagenesis	46
Statistical Analysis	48
RESULTS	50
Characterization of NS3/4A constructs	50
The helicase domain is dispensable for inhibition of innate defense signaling .	54
The functional NS3/4A protease domain inhibits signaling by RIG-I and MDA5	57
The SC Protease blocks activation of IRF-3 and exhibits a subcellular localization pattern similar to wt NS3/4A	62
Regulation of NF- κ B by NS3/4A	63
The protease domain of NS3/4A is sufficient to target and cleave IPS-1	67
NS3/4A protease inhibitor treatment prevents cleavage and restores localization of IPS-1	75
ITMN-C restores the endogenous host response triggered by HCV RNA replication and HCV infection	78
DISCUSSION	79
CHAPTER 4: LOCALIZATION AND MEMBRANE TARGETING BY NS3/4A	85
INTRODUCTION	85
NS4A	85
NS3 Serine Protease	85
EXPERIMENTAL PROCEDURES	88

Expression cloning and site-directed mutagenesis	88
<i>Cloning from PCR products</i>	88
<i>Primer subcloning</i>	89
<i>Site-directed mutagenesis</i>	91
Transmission Electron Microscopy (TEM)	91
RESULTS	93
NS4A is necessary for NS3-dependent inhibitions of IRF-3 activation and for targeting NS3 to the mitochondrial membrane	93
The SC Protease colocalizes with IPS-1	96
The amino-terminus of NS3 encodes a potential transmembrane motif	99
Potential ER to mitochondria transport mechanism	104
DISCUSSION	105
CHAPTER 5: STRUCTURE/FUNCTION ANALYSIS OF INTEFERON-β PROMOTER STIMULATOR-1, A KEY MODULATOR OF INNATE ANTIVIRAL IMMUNITY.....	109
INTRODUCTION	109
EXPERIMENTAL PROCEDURES	110
Plasmids	110
Expression Cloning and Site-directed Mutagenesis	110
Cells	112
Statistical analysis.....	112
RESULTS	114

Creation of IPS-1 mutation constructs	114
Deletion of the IPS-1 CARD domain confers a dominant-negative phenotype	116
IPS-1 oligomerization occurs through two multimerization motifs	120
NS3/4A inhibits carboxy-terminal multimerization of IPS-1	122
Uncoupling IRF-3 and NF- κ B signaling	124
Identification of the IPS-1 mitochondrial signal sequence	128
DISCUSSION	131
CHAPTER 6: DISCUSSION AND FUTURE DIRECTIONS	138
DISCUSSION	138
Structural analysis of NS3/4A regulation of the host response	138
Mitochondrial localization and targeting by NS3/4A	140
Structural analysis of IPS-1 signaling	142
CURRENT AND FUTURE DIRECTIONS	144
Involvement of TRAFs in IPS-1 signaling	144
Downstream effector molecules and their involvement in IPS-1 signaling	146
LGP2	148
ISG15 interaction with IPS-1	149
APPENDIX A: ALIGNMENT OF IPS-1 SEQUENCES ACROSS SPECIES	151
BIBLIOGRAPHY	154

PRIOR PUBLICATIONS

Johnson CL, Erickson A, Hagan KA, Saito T, and Gale M Jr. Structure-Function analysis of Interferon- β Promoter Stimulator-1 signaling. In preparation.

Johnson CL, Horner S, Collins A, Seiwert S, Gale M Jr Membrane targeting of hepatitis C virus NS3/4A protease. In preparation.

Keller BC, **Johnson CL**, Erickson A, and Gale M Jr. (2007) Innate immune evasion by Hepatitis C Virus and West Nile Virus. *Cytokine and Growth Factor Reviews*. 2007 Oct-Dec;18(5-6):535-44.

Johnson CL, Owen DM, Gale M Jr. (2007) Functional and therapeutic analysis of hepatitis C virus NS3/4A protease control of antiviral immune defense. *J Biol Chem*. 2007 Apr 6; 282(14):10792-803.

Saito T, Hirai R, Loo YM, Owen D, **Johnson CL**, Sinha SC, Akira S, Fujita T, Gale M Jr. Regulation of innate antiviral defenses through a shared repressor domain in RIG-I and LGP2. *Proc Natl Acad Sci U S A*. 2007 Jan 9;104(2):582-7

Johnson CL and Gale M Jr. CARD games between virus and host get a new player. *Trends in Immunology*. 2006 Jan; 27(1):1-4.

Chien Y, Kim S, Bumeister R, Loo YM, Kwon SW, **Johnson CL**, Balakireva MG, Romeo Y, Kopelovich L, Gale M Jr, Yeaman C, Camonis JH, Zhao Y, White MA. RalB GTPase-mediated activation of the IkappaB family kinase TBK1 couples innate immune signaling to tumor cell survival. *Cell*. 2006 Oct 6;127(1):157-70

Loo YM, Owen DM, Li K, Erickson AK, **Johnson CL**, Fish PM, Carney DS, Wang T, Ishida H, Yoneyama M, Fujita T, Saito T, Lee WM, Hagedorn CH, Lau D, Weinman SA, Lemon SM, and Gale M Jr. Viral and therapeutic control of IFN- β promoter stimulator 1 during hepatitis C virus infection. *Proc Natl Acad Sci U S A*. 2006 Apr 11;103: 6001 - 6006.

Foy E, Li K, Sumpter R Jr., Loo YM, **Johnson CL**, Wang C, Fish PM, Yoneyama M, Fujita T, Lemon SM, and Gale M Jr. Control of antiviral defenses through hepatitis C virus disruption of retinoic acid-inducible gene-I signaling. *Proc Natl Acad Sci U S A*. 2005 Feb 22; 102:2986-2991.

Brzostowski JA, **Johnson C**, Kimmel AR. Galpha-mediated inhibition of developmental signal response. *Curr Biol*. 2002 Jul 23;12(14):1199-208.

Henderson CW, **Johnson CL**, Lodhi, SA, Bilimoria SL. Replication of *Chilo* iridescent virus in the cotton boll weevil, *Anthonomus grandis*, and development of an infectivity assay. *Arch Virol*. 2001; 146(4): 767-775.

FIGURES

FIGURE 1-1.	HEPATITIS C VIRUS: PROGRESSION OF DISEASE	4
FIGURE 1-2.	SCHEMATIC OF THE HCV GENOME AND SUBGENOMIC REPLICON	7
FIGURE 1-3.	MEMBRANE ASSOCIATION OF HCV PROTEINS.....	10
FIGURE 1-4.	STRUCTURE OF THE CARD-CONTAINING MOLECULES IPS-1, RIG-I AND MDA5	17
FIGURE 1-5.	INTRACELLULAR RECOGNITION AND RESPONSE TO VIRUS INFECTION .	23
FIGURE 1-6.	VIRUS INFECTION TRIGGERS A POSITIVE IFN FEEDBACK LOOP	26
FIGURE 1-7.	EFFECTS OF PHARMACOLOGICAL TREATMENT ON HCV REPLICATION AND THE INNATE IMMUNE RESPONSE.....	34
FIGURE 3-1.	DIAGRAM OF WT NS3/4A AND NS3/4A MUTANTS	47
FIGURE 3-2.	EFFECT OF NS3 EXPRESSED WITH NS4A IN <i>CIS</i> OR IN <i>TRANS</i> ON INDUCTION OF ISG56 PROMOTER AND CLEAVAGE OF NS5AB	51
FIGURE 3-3.	EXPRESSION AND CLEAVAGE OF A NS5AB SUBSTRATE BY NS3/4A CONSTRUCTS	53
FIGURE 3-4.	FOLD ACTIVATION OF THE IFN β -LUC REPORTER IN RESPONSE TO SENDAI VIRUS (SenV) INFECTION AS COMPARED TO MOCK INFECTION	54
FIGURE 3-5.	LOCALIZATION OF SELECTED NS3/4A CONSTRUCTS	55
FIGURE 3-6.	EFFECT OF NS3/4A MUTANTS ON VIRUS-INDUCED ISG EXPRESSION ..	56
FIGURE 3-7.	EFFECT OF THE NS3/4A PROTEASE ON RIG-I SIGNALING	58
FIGURE 3-8.	IMMUNOBLOT ANALYSIS OF ISG PRODUCTION IN RESPONSE TO N-RIG STIMULATION	59

FIGURE 3-9.	NS3/4A PROTEASE REGULATION OF MDA5 SIGNALING	61
FIGURE 3-10.	NS3/4A PROTEASE CONTROL OF MDA5-INDUCED ISG PRODUCTION...	62
FIGURE 3-11.	EFFECT OF THE NS3/4A PROTEASE DOMAIN ON THE SUBCELLULAR DISTRIBUTION OF IRF-3	63
FIGURE 3-12.	NS3/4A REGULATION OF NF- κ B SIGNALING	65
FIGURE 3-13.	EFFECT OF THE SC PROTEASE ON SENV- AND N-RIG-MEDIATED ACTIVATION OF AN NF- κ B-DEPENDENT PROMOTER	66
FIGURE 3-14.	EFFECT OF NS3/4A CONSTRUCTS ON PHOSPHORYLATION OF I κ B α , THE INHIBITOR OF NF- κ B	66
FIGURE 3-15.	TARGETING AND CLEAVAGE OF IPS-1 BY THE SC PROTEASE	68
FIGURE 3-16.	THE SC PROTEASE CLEAVES IPS-1 AT CYSTEINES 283 AND 508	69
FIGURE 3-17.	NS3/4A CONSENSUS AND IPS-1 CLEAVAGE SITES	70
FIGURE 3-18.	INHIBITION OF IPS-1 SIGNALING BY THE SC PROTEASE	71
FIGURE 3-19.	THE SC PROTEASE ACTIVE SITE MUTANT EFFECTIVELY BLOCKS ISG PRODUCTION BY ECTOPIC IPS-1	72
FIGURE 3-20.	THE SC PROTEASE S1165A BLOCKS SENV AND N-RIG DOWNSTREAM SIGNALING	73
FIGURE 3-21.	EFFECT OF NS3/4A MUTANTS ON ACTIVATION OF AN NF- κ B PROMOTER ELEMENT	74
FIGURE 3-22.	COLOCALIZATION OF ENDOGENOUS RIG-I AND NS3/4A IN SENV- INFECTED HCV REPLICON CELLS	75
FIGURE 3-23.	IPS-1 LOCALIZATION IS DISRUPTED BY NS3/4A	76

FIGURE 3-24.	EFFECT OF PROTEASE INHIBITOR TREATMENT ON SUBGENOMIC HCV REPLICON DISPERSION OF IPS-1	77
FIGURE 3-25.	CHARACTERIZATION OF NS3/4A PROTEASE INHIBITOR TREATMENT ON THE HOST RESPONSE TO HCV	79
FIGURE 4-1.	SCHEMATIC OF NS4A AND THE SC PROTEASE	86
FIGURE 4-2.	DIAGRAM OF STRUCTURAL DOMAINS OF THE NS3/4A PROTEASE	87
FIGURE 4-3.	PROTEIN SEQUENCE OF THE NS3 AMINO-TERMINUS	87
FIGURE 4-4.	NS4A IS REQUIRED FOR NS3 TO INHIBIT IRF-3 ACTIVATION IN RESPONSE TO VIRUS	94
FIGURE 4-5.	COLOCALIZATION OF NS3/4A, MITOCHONDRIA, AND IPS-1 IN CELLS TREATED WITH PROTEASE INHIBITOR	96
FIGURE 4-6.	EFFECT OF NS3/4A AND THE SC PROTEASE ON IPS-1 INDUCTION	97
FIGURE 4-7.	EFFECT OF PROTEASE INHIBITOR TREATMENT ON LOCALIZATION OF THE SC PROTEASE	98
FIGURE 4-8.	HYDROPHOBICITY PLOT OF THE NS3 PROTEASE DOMAIN (A.A. 1-180)	100
FIGURE 4-9.	EFFECT OF AMINO-TERMINAL NS3 TRUNCATIONS ON VIRUS-MEDIATED ACTIVATION OF THE IFN- β PROMOTER	101
FIGURE 4-10.	EFFECT OF AMINO-TERMINAL NS3 DELETION CONSTRUCTS ON LOCALIZATION AND CLEAVAGE OF IPS-1	103
FIGURE 4-11.	ELECTRON MICROGRAPH OF HUH7 CELLS	105
FIGURE 4-12.	STRUCTURE OF HCV NS3/4 INCLUDING THE PUTATIVE MEMBRANE TARGETING REGION	108
FIGURE 5-1.	DIAGRAM OF IPS-1 CONSTRUCTS	115

FIGURE 5-2.	DOMINANT-NEGATIVE IPS-1 CONSTRUCTS INHIBIT IFN- β PROMOTER INDUCTION	117
FIGURE 5-3.	DOMINANT-NEGATIVE IPS-1 SIGNALING TO NF- κ B	119
FIGURE 5-4.	COIMMUNOPRECIPITATION ANALYSIS OF IPS-1	121
FIGURE 5-5.	DELETION OF THE CARD ABLATES AMINO-TERMINAL OLIGOMERIZATION OF IPS-1	122
FIGURE 5-6.	NS3/4A INHIBITS IPS-1 DIMERIZATION	123
FIGURE 5-7.	EFFECT OF CONSTITUTIVELY ACTIVE IPS-1 CONSTRUCTS ON IRF-3 ACTIVATION	125
FIGURE 5-8.	EFFECT OF CONSTITUTIVELY ACTIVE IPS-1 CONSTRUCTS ON NF- κ B ACTIVATION	126
FIGURE 5-9.	EFFECT OF THE DOMINANT-NEGATIVE IPS-1 CONSTRUCT Δ CARD ON VSV-GFP INFECTIVITY.....	127
FIGURE 5-10.	LOCALIZATION OF SELECTED IPS-1 MUTANTS	130
FIGURE 5-11.	AMINO ACID SEQUENCE OF IPS-1 CARBOXY-TERMINAL 50 RESIDUES	131
FIGURE 5-12.	OLIGOMERIZATION-DEPENDENT ACTIVATION OF ENDOGENOUS IPS-1	133
FIGURE 5-13.	IPS-1 ACTIVATION BY DELETION CONSTRUCTS	135

LIST OF TABLES

TABLE 3-1. PRIMER SEQUENCES FOR NS3 CLONING	49
TABLE 4-1. PRIMERS USED FOR PCR	89
TABLE 4-2. PRIMERS USED FOR DIRECT SUBCLONING	90
TABLE 4-3. SITE-DIRECTED MUTAGENESIS PRIMERS	92
TABLE 4-4. SUMMARY OF NS3/4A AND SC PROTEASE DELETION CONSTRUCT ACTIVITY	104
TABLE 5-1. PRIMERS FOR EXPRESSION CLONING OF IPS-1	111
TABLE 5-2. PRIMERS FOR SITE-DIRECTED AND DELETION MUTAGENESIS OF IPS-1	113

ABBREVIATIONS

a.a. – amino acid
ANOVA – one-way analysis of variance
 Δ Arg – full-length NS3/4A lacking the arginine-rich region
CARD – caspase activation and recruitment domain
CIP – calf intestinal alkaline phosphatase
dsRNA – double-stranded RNA
EMSA – electrophoretic mobility shift assay
ER – endoplasmic reticulum
FITC – fluorescein isothiocyanate
GAPDH – glyceraldehyde 3-phosphate dehydrogenase
HAU – hemagglutinin units
HCV – hepatitis C virus
Hel – NS3 helicase domain
HRP – horse-radish peroxidase
IFN – interferon
IFNAR – interferon alpha/beta receptor
I κ B α – inhibitor of κ B α
I κ B α -M – dominant-negative I κ B α
IPS-1 – interferon- β promoter stimulator 1
IRF-3 – Interferon regulatory factor-3
ISG – interferon stimulated gene
ISRE – interferon stimulated response element
MAM – mitochondria-associated ER membrane
MDA5 – melanoma differentiation associated gene 5
MEF – mouse embryo fibroblast
MOI – multiplicity of infection
MOM – mitochondrial outer membrane

NF- κ B – nuclear factor- κ B
NS – nonstructural
NTPase – nucleoside triphosphatase
PRR – pathogen recognition receptor
PAMP – pathogen-associated molecular pattern
poly(I:C) – polyinosinic:polycytidylic acid
Prot – NS3 protease domain
RER – rough ER
RIG-I – retinoic acid-inducible gene I
RLU – relative luciferase units
RT – room temperature
S1165A – NS3/4A protease active site mutation
SC – single-chain
SDS – sodium dodecyl sulfate
SenV – Sendai virus
SFM – serum-free media
ssRNA – single-stranded RNA
TIM – TRAF interaction motif
TLR – toll-like receptor
TM – transmembrane domain
TNF- α – tumor necrosis factor- α
TRAF – tumor necrosis factor receptor-associated factor
UTR – untranslated region
VSV – vesicular stomatitis virus
WT – wild-type

CHAPTER ONE

Introduction

HEPATITIS C VIRUS

Discovery of HCV

Prior to the early 1990s, blood transfusions and use of clotting factors derived from blood products carried a considerable risk of developing an acute or chronic hepatitis, which can lead to cirrhosis, hepatocellular carcinoma, and death. With the advent of specific screening tests for hepatitis A virus (HAV) and hepatitis B virus (HBV) in the 1970s, it rapidly became apparent that there was an unidentified virus responsible for the majority of cases of hepatitis spread by blood products (designated non-A, non-B hepatitis)^{3,38}. All that was known was that the etiological agent might be a small, enveloped virus that could be transmitted to chimpanzees²⁰. However, immunological studies consistently failed to identify novel viral antibodies or antigens in the serum of infected individuals. Then in 1989 a seminal paper appeared in *Science* where researchers at Chiron Corporation used a cDNA screen to identify a novel 10kb positive-sense RNA virus from the serum of a chronically infected non-A, non-B hepatitis patient²⁷, which they called hepatitis C virus (HCV). This was the first time that a virus was identified entirely by molecular cloning technology without propagating virus using tissue culture or small animal models, representing a scientific landmark. By 1992, second generation screening tests had virtually eliminated HCV from the nation's blood supply¹⁰⁶.

Clinical aspects of HCV infection

Epidemiology

HCV is a life-threatening disease with an estimated 3% of the world's population currently infected¹⁶⁸. In the United States, it causes 15% of acute viral hepatitis, 60-70% of chronic hepatitis, and the majority of cases of cirrhosis, end-stage liver disease, and hepatocellular carcinoma, making liver disease the tenth leading cause of death for adults^{22,115}.

HCV is the most common persistent blood-borne pathogen in the United States²². The main risk factor for acquisition of HCV infection is intravenous drug use (IVDU), but hemophiliacs treated with clotting factor concentrates prior to 1987 and recipients of blood transfusions or organs prior to 1992 have high prevalence of HCV^{1,22,115}. Transmission of HCV during sexual intercourse has also been reported, but is not as common as with other viruses, such as human immunodeficiency virus (HIV)²³. Isolated studies have suggested HCV may be spread by percutaneous exposures such as body piercing and tattooing, but in fact the risk is considered negligible¹⁰⁶.

Clinical presentation and progression of disease

HCV infection follows a slowly progressing course. Acute infection is asymptomatic in most cases, or if present, symptoms are mild, nonspecific, and intermittent. Most often the initial infection goes unrecognized¹¹⁵. Without treatment the majority of patients develop a persisting infection, and at least 20% of chronic hepatitis C patients develop cirrhosis, putting them at risk for the development of hepatocellular carcinoma, one of the sequelae of this disease (**Figure 1-1**). HCV-related

liver failure is the most common indication for liver transplantation in the United States^{22,115}.

Identification of infected individuals is difficult because HCV is usually clinically silent for decades after infection¹⁰⁶. At least 3.9 million Americans have been exposed to HCV, but because many high-risk populations such as prisoners, intravenous drug users, and the homeless are generally excluded from surveys, these estimates are likely conservative^{22,106}. In the rare instance that acute infection is recognized, symptoms appear a few weeks after exposure and may include jaundice, fatigue, anorexia, dark urine, or abdominal pain. HCV RNA can be detected in human serum within 1-3 weeks of exposure^{1,127}. Elevated serum alanine aminotransferase (ALT) levels are the most characteristic feature of acute infection, indicating liver damage has already occurred^{22,115}.

Hepatitis C: Progression of Disease

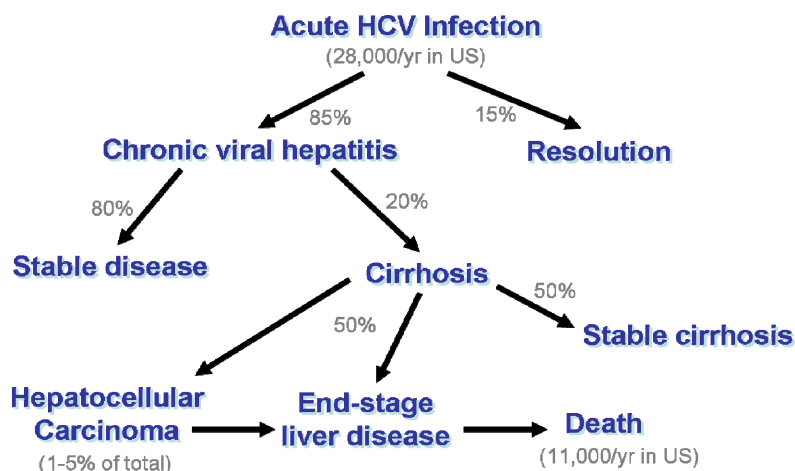


Figure 1-1: Hepatitis C virus: progression of disease. HCV infection most often causes a chronic viral hepatitis, which over the course of decades can lead to cirrhosis, hepatocellular carcinoma, end-stage liver failure, and death. Adapted from ^{23,72}

Liver pathology in chronic HCV-infected patients shows an inflammatory infiltrate in the portal tracts and hepatic lobules. With progression of the disease, inflammation and hepatocyte necrosis lead to fibrosis and later, cirrhosis. Complications secondary to liver failure, such as jaundice, variceal hemorrhage, ascites, and encephalopathy mark the transition to decompensated cirrhosis, which is associated with increased mortality and necessitates liver transplantation. However, reinfection with HCV after liver transplantation is common ¹⁰⁶. The incidence of hepatocellular carcinoma in chronically infected patients with cirrhosis is 1-4% per year, with 5-year survival rates less than 5% ^{1,22}.

Economic burden of HCV

In 1995 there were at least 26,700 hospitalizations for liver disease caused by HCV, costing an estimated \$514 million. Extrapolating from these inpatient costs, the total cost of all morbidity associated with HCV was \$1.5 billion in 1995. Conservative estimates for the next decade (2010-2019) have suggested that cirrhosis will increase by 61%, decompensated liver disease by 279%, hepatocellular carcinoma by 68%, and the requirement for liver transplantation will skyrocket at least 500% ¹. HCV-associated liver disease is projected to cause 165,900 deaths, plus an additional 27,200 deaths from hepatocellular carcinoma ¹⁶⁷. Therefore HCV represents a substantial current and future public health burden.

Molecular Biology of HCV

HCV is a small, single-stranded (ss) positive-sense RNA hepatotropic virus. Belonging to the Flaviviridae family of enveloped viruses, this virus measures around 40-60nm in diameter ¹²⁷. HCV possesses a 9.6 kb genome which is translated as a single polyprotein and post-translationally processed by viral and cellular proteases into at least 10 structural and nonstructural (NS) proteins (**Figure 1-2A**) ¹²⁸. It is divided into 6 major genotypes (1 through 6) based on sequence homology, with numerous subtypes. HCV genotypes 1, 2, and 3 are distributed throughout the world, whereas genotypes 4 and 5 are confined mainly to Africa, and genotype 6 to Asia ^{1,127}. Genotype 1 is the most prevalent genotype in the United States, accounting for 70% of all infections, and is also the most refractory to treatment ^{1,103,106}. Due to the high error rate of the viral polymerase and selective pressure by the host immune response, viral quasispecies, a mixture of closely

related but distinct genomes, occur within an infected individual^{52,103,153}. Quasispecies evolution has hampered the development of an HCV vaccine¹⁰³.

HCV genome structure and function

Translation of the HCV genome depends on an internal ribosomal entry site (IRES) within the 5' untranslated region (UTR) that directs cap-independent translation of the HCV open reading frame. The HCV IRES contains four highly structured, dsRNA domains. It directly binds the 40S ribosomal subunits, bypassing the need for pre-initiation factors^{96,124,127}. The amino-terminal one-third of the HCV polyprotein encodes the structural proteins, including the highly basic core protein, the envelope glycoproteins E1 and E2, and the small integral membrane protein p7 (**Figure 1-2A**). The core protein is the major constituent of the viral nucleocapsid¹⁰. E1 and E2 form heterodimers that are involved in attachment and entry of the virus into cells¹⁵². The p7 protein has been shown to function as an ion channel and is necessary for HCV replication in cell culture^{58,76,123}. The remaining two-thirds of the genome consists of the nonstructural (NS) proteins NS2, NS3, NS4A, NS4B, NS5A, and NS5B, which are responsible for viral replication events within the cells. The C/E1, E1/E2, E2/p7, and p7/NS2 junctions are cleaved by the cellular signal peptidase, while the host signal-peptidase cleaves between core and the E1 signal peptide (**Figure 1-2A**). The NS2 cysteine protease cleaves between NS2 and NS3, while the NS3/4A serine protease proteolytically processes the downstream sites^{10,31,96,152}. Additionally, HCV encodes a small protein F (frameshift), also known as ARFP (alternative reading frame protein), that is produced

during ribosomal shifting to an alternate reading frame during translation of the core protein^{159,171}.

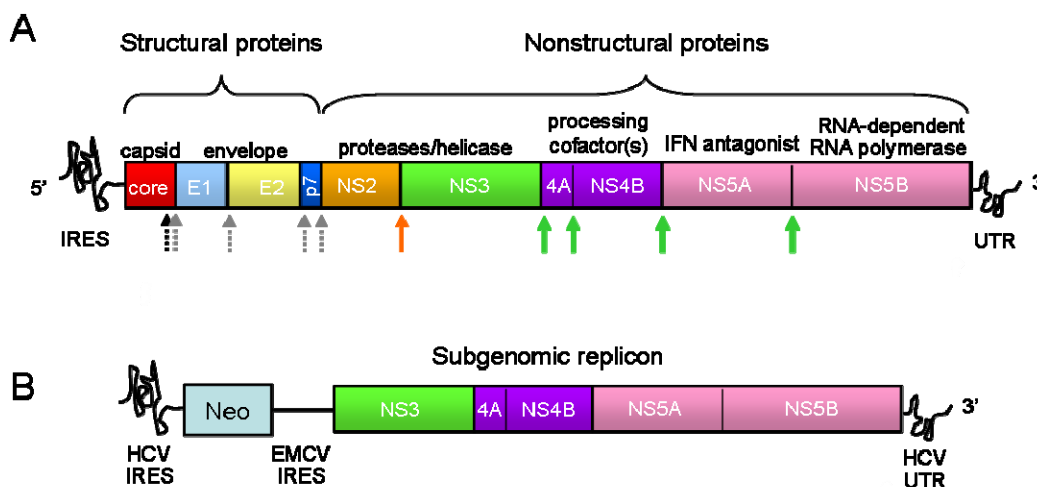


Figure 1-2: Schematic of the HCV genome and subgenomic replicon. **A.** The HCV genome is comprised of a 5' IRES; 3' untranslated region (UTR); the structural genes core, E1, E2, and p7; and the nonstructural proteins NS2-NS5. The black dotted arrow indicates the signal-peptide peptidase cleavage site; grey dotted arrows designate signal peptidase cleavage locations; the orange arrow shows the NS2 protease cleavage junction; and green arrows denote sites of NS3/4A proteolysis. **B.** HCV subgenomic replicon structure includes a selectable neomycin cassette under the control of the HCV IRES. The EMCV IRES allows constitutive expression of the HCV nonstructural proteins, which are flanked by the HCV 3' UTR.

NS2 contains a cysteine protease in the carboxy terminus required for cleavage of the polyprotein between NS2/3. Also required for this activity is the amino-terminal serine protease domain of NS3, but not the NS3 serine protease catalytic activity. Since proteolytic activity of NS2 is enhanced by addition of Zn^{2+} , a NS3 protease cofactor, it is believed that the NS3 protease domain may be required for correct folding of the NS2 protease^{96,152}. Interestingly, NS2 is not necessary for HCV RNA replication in the

subgenomic replicon system, but is required for viral replication in the HCV cell culture model ⁷⁶.

NS3 is a bifunctional protein with an amino-terminal protease and a carboxy-terminal helicase/NTPase domain. The NS3 serine protease is responsible for cleavage of virtually all the nonstructural proteins; however, differences exist in how NS3 processes each of these sites ^{31,96}. Cleavage is believed to occur in the order of NS3-4A first, followed by NS5A-B, then NS4A-B, and lastly NS4B-5A ¹³². Proteolysis at the NS3-NS4A junction occurs exclusively in *cis* (within the same molecule), while at other sites of cleavage it can be processed in *trans* ⁹. NS4A is a small, 54 amino acid peptide that is an essential cofactor for NS3-dependent polyprotein processing at most downstream sites. NS4A is not required for cleavage of the NS5A-B junction, but significantly enhances its cleavage efficiency ^{11,31,152}. High resolution crystal structure analysis of the protease domain shows that NS3 has a chymotrypsin-like fold and a tetrahedrally-coordinated zinc-binding site. The protease domain consists of dual β -barrels, with the catalytic triad located at the interface between the two ^{81,96,99,105,152,173}. The central portion of NS4A folds into a β -strand that intercalates into the amino-terminal β -barrel through interactions with the amino-terminus of NS3 ^{32,81,173}. NS4A is also thought to tether NS3 to intracellular membranes via its hydrophobic amino-terminus (**Figure 1-3**) ¹⁶⁶. The NS3 helicase is a member of the DExD/H-box family and is believed to be involved in RNA unwinding during replication ^{87,144}. Interestingly, it has higher processivity on DNA than RNA substrates ¹²². Movement of NS3 along the RNA strand is dependent on NTPase activity and magnesium binding, and occurs in an inchworm-like fashion ^{35,47}. Due to the viral dependence on NS3/4A protease and

helicase activities, inhibitors of both these enzymatic activities are active areas of pharmaceutical interest^{30,33}.

NS4B is a hydrophobic integral membrane protein (**Figure 1-3**) and component of the replication complex with unknown function⁹⁶. It contains a nucleotide binding motif that binds and hydrolyses GTP, and mutations that abrogate GTPase activity decrease HCV replication¹²⁷. NS4B has been proposed to play a role in the membrane alterations that serve as a scaffold for the HCV replication complex¹¹².

NS5A is a multiply-phosphorylated protein that contains a region thought to be involved in interferon (IFN) sensitivity^{96,152}. It also has been shown to interact with and inhibit the dsRNA-dependent protein kinase (PKR), an antiviral mediator which serves to inhibit translation initiation⁵¹. NS5A is tethered to membranes via its amino-terminal region (**Figure 1-3**)^{112,127}.

NS5B is a RNA-dependent RNA polymerase (RdRp) and is essential for synthesis of both the negative-stranded RNA intermediate as well progeny positive-sense RNA genomes. It is a tail-anchored integral membrane protein. Membrane association occurs post-translationally, and it functions in the membrane-bound replication complex^{33,95,112,152}. NS5B may function as a homo-oligomer. Like other RdRps, NS5B is error-prone with a misincorporation rate of 10^{-3} per nucleotide per generation. This promotes rapid evolution of HCV and leads to the production of divergent variants known as viral quasispecies within an infected individual. These likely provide a selective advantage by increasing replication fitness and enabling viral escape from immune detection^{52,103,127}. This enzyme is also a current target for anti-HCV therapeutics^{30,33}.

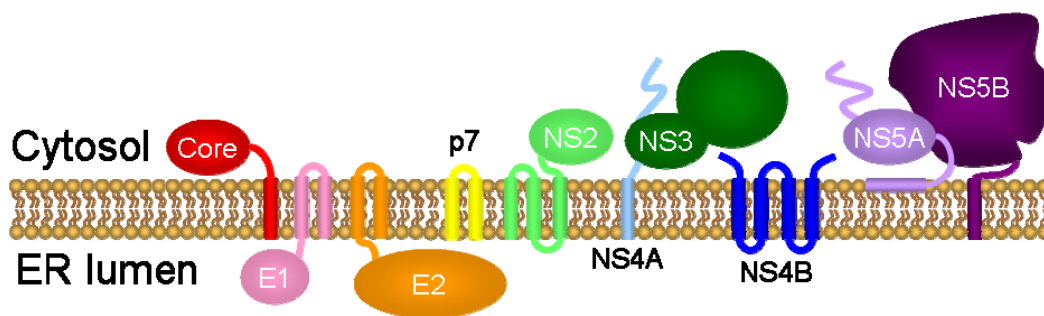


Figure 1-3: Membrane association of HCV proteins. All the HCV structural and nonstructural proteins are believed to be associated with intracellular membranes either directly or indirectly (as in the case of NS3). This has important implications for the viral replication complex, which is thought to be composed of altered endoplasmic reticulum (ER) membranes. Adapted from ⁹⁶.

The HCV replication complex

Similar to other positive-sense ssRNA viruses, HCV genome replication takes place on altered rough endoplasmic reticulum (ER) membrane structures (called the membranous web) by a replication complex ^{37,56}. These structures were similar to those observed in the liver of HCV-infected chimpanzees ^{112,127}. Compartmentalization of the viral replicase offers the virus an increased local concentration of viral proteins, viral RNA tethering during unwinding, and protection of the viral RNA from dsRNA-mediated host defense pathways ¹²⁴. Expression of NS4B alone is able to promote the formation of the membranous web, although other viral and cellular proteins are found associated with the replication complex. Manufacturing of these altered membranes appears to be dependent on the lipid content, favoring saturated and monounsaturated fatty acids, suggesting membrane fluidity is important for replicase function ^{96,127}.

The HCV replicon system and cell-culture infectious HCV 2a clone

Until recently the absence of an infectious cell culture system or small animal model of infection hampered investigation into the HCV lifecycle and development of antiviral compounds. The first breakthrough came with the development of a replicon capable of stable viral RNA replication in a human hepatoma cell line (Huh7 cells or derivatives)⁹⁷. These subgenomic replicons consisted of a bicistronic RNA encoding the nonstructural proteins from HCV genotype 1b linked to a selectable Neomycin cassette in place of the structural genes (**Figure 1-2B**). The neomycin cassette was put under the control of the HCV IRES, while the nonstructural genes were expressed using the heterologous encephalomyocarditis virus (EMCV) IRES. These replicons harbored cell-culture adaptive mutations which allowed higher RNA replication, but attenuated viral production and infectivity in experimentally infected chimpanzees^{96,111,127,132}. However, full-length genomic replicons lacking the adaptive mutations replicated poorly in cell culture⁹⁶. Despite the lack of infectious virus production, the replicon system provided a cell-based system to study HCV RNA replication and evaluate potential antiviral compounds.

The discovery of an HCV cell culture infectious clone in 2005, however, has allowed studies into the HCV lifecycle and viral infectivity. The HCV genotype 2a JFH-1 strain was isolated from a Japanese patient with fulminant hepatitis. For unknown reasons, full-length JFH-1 RNA produces infectious HCV particles in cell culture, and subgenomic replicons derived from the JFH-1 strain do not require adaptive mutations for cell culture propagation¹⁶². Since then a variety of groups have synthesized chimeric viruses with partial genotype 1 genomes and viruses that reach higher titer in cell culture

^{95,127,180}. While cell culture systems do not completely replicate conditions *in vivo*, they are invaluable tools for studying HCV and investigating novel antiviral agents.

Animal models of HCV infections

There has been only limited success in developing a small animal model of HCV infection despite numerous attempts. Even though HCV does not infect mice, a chimeric mouse model of infection was developed, in which SCID mice overexpressing the urokinase plasminogen activator (uPA) transgene (causing hepatocellular atrophy from birth) are transplanted with human hepatocytes that repopulate the mouse liver¹⁰⁸. These human hepatocytes are capable of replicating HCV and produce infectious progeny virus. This model system should provide an attractive approach to studying HCV infection of hepatocytes.

Currently the chimpanzee (*Pan troglodyte*) is the only primate animal model for HCV infection⁸³. Primates other than the chimpanzee do not appear to be susceptible to HCV. Due to the high cost and limited availability of chimpanzees, most studies have used two to four animals, limiting statistical significance of conclusions and leaving results open to interpretation as biological variation among animals²⁰. Despite these problems, studies in chimpanzees have been invaluable in determining that the active sites of the protease, helicase, and polymerase are critical to HCV infectivity (Kolykhalov AA, et al Rice CM J. Virol 2000 74), as is the p7 protein (Sakai A Claire M, Faulk K et al PNAS 2003), and the 3' UTR (Kolykhalov AA, et al Rice CM J. Virol 2000 74; Yanagi M St. Clair M Emerson SU et al PNAS 1999).

Chimpanzees represent an effective way to study acute infection with HCV, which is otherwise difficult to detect and study in humans as mentioned previously. Acute infection of chimpanzees is similar to acute infection in humans; however, chimpanzees have a lower rate of development of chronic infection (33% compared to 85% in humans; **Figure 1-1**)¹³. Chimpanzees who cleared infection had a high induction of IFN-stimulated genes (ISGs)^{16,88}. Interestingly, chronically-infected chimps analyzed by microarray also showed a significant increase in a large number of ISGs, although not statistically significant increase in levels of IFN- α , IFN- β , or IFN- γ ¹⁵. Parenchymal cells represent ~80% of the cells in the liver, thus the increase in ISGs could result from expression in uninfected neighboring cells or due to expression of IFN from plasmacytoid dendritic cells (pDCs), the major Type I IFN producers in the body. Despite the obvious benefits of the chimpanzee model, their scarcity and high cost necessitate development of better HCV infection models.

Current and future therapy

Current treatment for HCV infection is once weekly injections of pegylated IFN- α in combination with daily oral dosing of ribavirin, a nucleoside analog, for 48 weeks. Combination therapy has a sustained response rate of 54-56% depending on genotype^{7,39,106}. While genotypes 2 and 3 are highly susceptible to IFN- α and ribavirin combination therapy (response rate of about 76%), genotype 1 sustained response rate was significantly lower, around 42% depending on the study¹⁰⁶. A sustained response is defined as undetectable serum HCV RNA 6 months after discontinuation of therapy, with 99% of patients meeting this requirement remaining virus-free indefinitely^{7,106}.

Adherence to the regimen also had a significant effect on response rate¹⁰⁶. This therapy is expensive and side effects are considerable, and include fatigue, nausea, muscle aches, depression, fever, neutropenia, and anemia, limiting patient compliance^{106,115}. Therefore better therapeutic options are necessary.

An ideal antiviral candidate would be against a target protein that was a vital part of the viral lifecycle, yet distinct enough from cellular proteins that its inhibition would not effect cellular functioning. The life cycle of HCV, as with other RNA viruses, involves 1) binding to a cell surface receptor and internalization; 2) uncoating of the virus and release of viral RNA; 3) IRES-mediated translation and processing of the polyprotein; 4) RNA replication; 5) packaging and assembly of nascent virions; and 6) virion maturation and release from the cell. Each of these steps could potentially be targeted by antiviral therapy, but the viral NS3/4A protease and the NS5B RdRp enzymes are the most popular current targets of therapy^{30,111}.

BILN 2061 (Boehringer Ingelheim) is a peptidomimetic active site inhibitor of the HCV NS3/4A protease, and was the first HCV protease inhibitor to enter clinical trials. When administered twice daily for two days, it induced a rapid decline in the viral load in a dose-dependent manner, with a drop of two orders of magnitude in the higher doses. However, side effects were observed in laboratory animals that included cardiac toxicity, and clinical development of this drug was halted^{66,131}. VX-950 (Vertex/Mitsubishi), another peptidomimetic inhibitor of NS3/4A, also showed promising results in a two week clinical trial, with two- to four-log drops in HCV titers¹²⁹. Similar compounds have been advanced by other companies and are in various stages of development³⁰.

While these drugs show promise as antiviral treatments, the emergence of drug-resistant viruses under the selective pressure of these antiviral compounds is a constant worry. The rapid mutation rate (about one nucleotide per genome) endows the virus the ability to quickly change to new environmental conditions and escape antiviral pressure. Studies in our lab have shown that IFN-resistant HCV replicon strains were produced by long-term cell culture treatment with IFN- α ¹⁵⁰. Similarly, single point mutations were found to confer resistance of HCV replicons to certain NS3/4A protease inhibitors ⁹², suggesting that these drugs should be used in combination with other treatment options.

INNATE INTERFERON ANTIVIRAL RESPONSE

Pathogen recognition receptors (PRRs)

Virus infection triggers an innate immune response characterized by the production of interferon (IFN) by the host cell. IFN is a secreted, immunomodulatory cytokine that serves as an antiviral warning system. Type I IFNs, including IFN- α and IFN- β , are produced by most cells in the body in response to infection ¹⁵⁵. How this process is initiated and carried out is incompletely understood. Recent developments have shown that intermediates of viral replication, including dsRNA, act as pathogen-associated molecular patterns (PAMPs) to initiate a signaling cascade that is amplified within the cell and serves to alert neighboring cells and tissue of virus invaders. Recognition of dsRNA intermediates can occur through any of several pathogen recognition receptors (PRRs), including toll-like receptor 3 (TLR3) ², protein kinase R

(PKR)⁵³, retinoic acid inducible gene I (RIG-I)¹⁷⁵, and melanoma differentiation-associated gene 5 (MDA5)¹⁷⁴.

RIG-I

RIG-I and MDA5 are homologous cytoplasmic proteins containing two tandem amino-terminal caspase activation and recruitment domains (CARDs) and a carboxy-terminal DExD/H box RNA helicase (**Figure 1-4**). They initiate the IFN regulatory factor-3 (IRF-3) and nuclear factor- κ B (NF- κ B) antiviral effector pathways by binding dsRNA intermediates that accumulate during viral replication via their helicase domain, and activate a downstream component through the CARDs (**Figure 1-5**)^{174,175}. The helicase contains ATPase activity, and mutations in the Walker ATP-binding site abrogates activation by RIG-I and MDA5¹⁷⁵. CARDs are signaling motifs that interface with other CARD-containing molecules to direct their actions. RIG-I and MDA5 CARD signaling occurs through interaction with an adapter protein, interferon- β promoter stimulator-1 (IPS-1), which recruits a macromolecular complex to coordinate innate immune signaling in response to dsRNA stimulation^{74,80,134}.

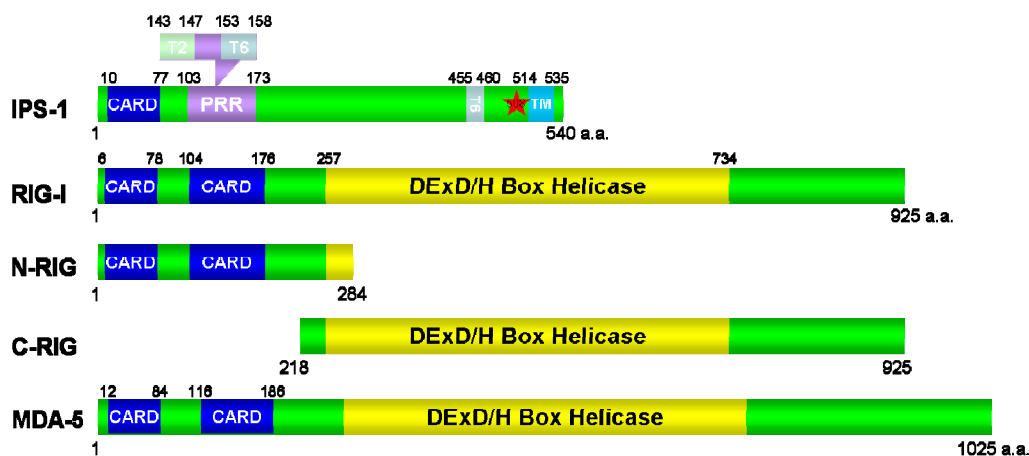


Figure 1-4: Structure of the CARD-containing molecules IPS-1, RIG-I, and MDA5. The amino acid (a.a.) number and position of each CARD and helicase domain is indicated. Abbreviations: T2, TRAF2 binding motif; T6, TRAF6 binding motif; TM, mitochondrial outer membrane transmembrane domain; PRR, proline-rich region. The star indicates the site of IPS-1 cleavage by HCV (cysteine 508). Adapted from ⁷⁴.

Discerning self from non-self is one of the main objectives of the immune system surveillance mechanism. Recent studies suggest that RIG-I may discriminate self from non-self RNA substrates in part through recognition of free 5' triphosphates ^{73,126} and specific RNA secondary structures ¹³⁵.

When overexpressed in cells, RIG-I does not constitutively signal to IRF-3 or NF- κ B, but instead amplifies viral activation of these pathways ^{44,175}. These observations implicate an internal mechanism for repression of RIG-I signaling in the absence of viral stimulus. Expression of an amino-terminal form of RIG-I containing the CARDS results in constitutive activation of the IFN- β promoter and a high-level production of IFN; expression of RIG-I lacking the CARDS confers a dominant negative phenotype for virus-mediated signaling (**Figure 1-4**) ¹⁷⁵. Dissecting this region further revealed that the carboxy-terminal 190 amino acids (a.a.) of RIG-I serves as a repressor domain and

ablated virus-mediated signaling¹³⁵. The repressor domain was found to interact with both the amino-terminal CARDs as well as the helicase domain. Furthermore, deletion of the repressor domain rendered RIG-I constitutively active, suggesting that it holds RIG-I in a closed conformation in the absence of a dsRNA ligand. However, when expressed in *trans*, it was unable to inhibit IFN- β promoter activation by the CARDs, but blocked virus-induced signaling by wt RIG-I. This indicates that RIG-I activation is positively controlled through tandem CARDs but is negatively modulated by internal repressor domain interactions¹³⁵. Taken together, these data suggest a model for RIG-I activation wherein RIG-I exists as a monomer in resting cells, but self-associates upon virus infection or high levels of expression. This multimerization is necessary but insufficient for RIG-I activation, and a further viral RNA binding event by the helicase domain releases the repressor domain inhibition of the CARDs and results in an active RIG-I complex that can signal downstream¹³⁵. RIG-I is normally expressed at low levels in cells, but is increased in response to IFN, thus it acts to upregulate its own expression to better respond to a continuing virus threat⁵².

HCV RNA triggers RIG-I

HCV RNA has been shown to activate IRF-3 and IFN production early in infection through the PAMP receptor, RIG-I^{135,149}. The HCV genome contains regions of dsRNA secondary structure in its 5' and 3' UTRs that are required for HCV RNA replication and protein translation⁹⁷. When transfected into cells, HCV replicon RNA as well as the HCV 5' or 3' UTR can transiently activate the IFN- β promoter and turn on transcription of ISG56 and ISG15 mRNA¹⁴⁹. The RIG-I helicase recognizes and binds

the highly-structured 3' and 5' UTRs of the HCV genomic RNA but not a linear, nonstructured domain of the HCV genome^{135,149}. A human hepatoma cell line previously determined to be highly permissive for HCV RNA replication (the Huh 7.5 cell line) was discovered to contain a mutation in RIG-I that ablates activation and downstream signaling to IRF-3 by virus and HCV RNA¹⁴⁹. Therefore, RIG-I is essential for triggering innate defenses against HCV infection.

MDA5

Like RIG-I, MDA5 is also an ISG. But in contrast to RIG-I, MDA5 does not contain a functional repressor domain and thus constitutively activates the IFN- β promoter when overexpressed^{75,135}. While MDA5 lacks an internal repressor domain, a recent study found that MDA5 is negatively regulated by the cellular protein dihydroxyacetone kinase, thus inhibiting constitutive activation of the antiviral pathways by endogenous MDA5³⁴. Of clinical interest, researchers found a nonsynonymous single-nucleotide polymorphism in the MDA5 locus that associated with Type I diabetes, though how MDA5 may contribute to the development of this disease is unknown¹⁴⁷.

While their similarity would suggest redundant functions, RIG-I and MDA5 seem to recognize disparate and distinct dsRNA motifs and viruses. They both bind to the synthetic dsRNA, poly inosine:cytosine (pIC). However, MDA5 preferentially binds pIC, whereas RIG-I is more responsive to in vitro transcribed RNA^{78,174}. MDA5 has also been shown to be important for the host response to the picornavirus encephalomyocarditis virus (EMCV); RIG-I, on the other hand, is essential for triggering interferon production in response to paramyxoviruses including Sendai virus, influenza

virus, and flaviviruses such as Japanese encephalitis virus and HCV^{55,78,135,149}. RIG-I binds to HCV RNA encoding dsRNA motifs whereas MDA5 mediates only weak binding of the HCV 3' UTR and not at all to the 5' UTR^{135,149}. Studies in RIG-I-deficient mouse embryo fibroblasts (MEFs) indicated that Mda5 was incapable of signaling to the IFN- β promoter when transfected with HCV RNA, indicating that RIG-I is an essential PRR for HCV¹³⁵.

Interferon Regulatory Factors

IFN regulatory factors (IRFs) are transcription factors vital in mediating the IFN response. IRF-3, IRF-7, and NF- κ B are transcription factors vital in the production of type I IFNs, which, through a JAK-STAT signaling cascade, mediate induction of gene products important in establishing an antiviral state. This pathway is key in regulating host defense, and several groups have shown that specific viruses interfere with signaling through this pathway, including paramyxovirus V protein⁵, HAV⁴⁰, and HCV⁴⁴.

There are thirteen IFN- α subtypes in humans, but only one IFN- β gene⁷⁰. Type I IFN production is regulated at the transcriptional level; hence the mechanisms used to induce gene transcription has been avidly pursued. The IFN- β gene promoter contains at least four positive regulatory domains (PRDs): PRDI through IV (**Figure 1-5**)⁷⁰. The promoter of the IFN- α gene, however, contains PRDI-and PRDII-like elements (PRD-LEs). PRDI, PRDIII, and PRD-LEs are binding sites for IRF family members, whereas PRDII is bound by NF- κ B, and PRDIV binds to activating transcription factor-2 (ATF-2) and c-Jun heterodimers (also called in combination AP-1)⁷⁰. Together these proteins

form the IFN- β enhanceosome¹⁶⁵. Interestingly, the IFN- β promoter is only weakly activated by TNF- α , an inducer of NF- κ B and AP-1⁷⁰, suggesting that production of IFN- β is dependent on the involvement of IRFs.

All members of the IRF family of transcription factors have an amino-terminal DNA-binding domain (DBD) containing five tryptophan repeats^{70,130,155}. Their cellular localization and activation are regulated by their expression, inducible phosphorylation, nuclear localization sequences (NLS) and nuclear export signals (NES), and association with other proteins¹³⁰. The first IRF family member to be discovered, IRF-1, is found at low or undetectable levels in cells, but can be induced in response to a variety of stimuli including IFN and dsRNA stimulation¹³⁰. IRF-1 is constitutively localized to the nucleus, and has a short half life of around 30 minutes^{130,155}. Overexpression of IRF-1 constitutively activates IFN- β production through binding at the PRDI locus, but gene-targeting studies revealed that while IFN transcription in response to dsRNA was impaired in IRF-1 $-/-$ mice, it was normal in cells infected with NDV, suggesting another factor was important in virus-induced IFN production^{70,155}.

IRF-3

IRF-3 is a 44 kDa protein that is constitutively expressed at high levels and found mainly in the cytoplasm of uninfected cells^{130,142,176}. In addition to the amino-terminal DBD, IRF-3 has a carboxy-terminal IRF associate domain (IAD) that mediates protein-protein interactions including dimerization^{142,155}. It also contains a transactivation domain and two autoinhibitory domains that interact with each other to mask the DBD and IAD^{67,142,155}. Latent IRF-3 is basally phosphorylated and shuttles in and out of the

nucleus due to NLS (a.a. 72-83) and NES (a.a. 139-149) sequences, but export predominates^{130,176}. In its inactive state, however, it cannot bind DNA. Upon virus infection, IRF-3 becomes hyperphosphorylated (serine 385/386 and serine 396/398 appear to be important in this) by the IκB kinase homologs TANK-binding kinase 1 (TBK1; also known as NF-κB-activating kinase (NAK)) or IκB kinase ε (IKKε; also known as IKKi)^{42,130,176}. Virus-induced phosphorylation unmasks the IAD and DNA-binding domains allowing IRF-3 to homodimerize and translocate to the nucleus where it then is able to interact with the nuclear histone acetyltransferases CREB binding protein (CBP) and p300^{130,155,176}. This association requires the phosphorylated carboxy-terminus of IRF-3 and is essential for transcriptional activation of IRF-3 target genes¹³⁰. The association of IRF-3 with CBP/p300 retains it within the nucleus^{130,142,176}. The IRF-3 holocomplex binds direct repeats on the IFN-β promoter at PRD I or PRDIII and palindromic IFN-stimulated response elements (ISREs) of several genes including ISG56 and ISG15 (**Figure 1-5**)^{57,137,142,176}. Activated IRF-3 is rapidly ubiquitinated and targeted for degradation; however, one of its target genes, ISG15, can inhibit this action. ISG15 is a small ubiquitin-like protein that can be conjugated with IRF-3, subverting its proteasome-mediated degradation and thus prolonging IRF-3-dependent transcriptional activity¹⁰¹. Targeted gene disruption of IRF-3 revealed that these mice are more susceptible to virus infection, and type I IFN levels were dramatically decreased^{130,155}.

Figure 1-5 (previous page): Intracellular recognition and response to virus infection. Virus infection of a cell produces replication products, such as dsRNA intermediates, that are recognized and bound by the intracellular PRRs, RIG-I or MDA5. This drives a conformation change in RIG-I/MDA5 that promotes interaction with IPS-1, a downstream adapter protein anchored on the mitochondria outer membrane, and results in recruitment of signaling components that activate the transcription factors IRF-3 and NF- κ B. Nuclear translocation of IRF-3 and NF- κ B induces IFN- β expression and secretion from the infected cell. IFN- β binds to the type I IFN receptor, triggering a downstream Jak-Stat signaling pathway that leads to expression of interferon stimulated genes (ISGs), potent antiviral effector molecules. HCV disrupts RIG-I-dependent signaling through cleavage of IPS-1 by the viral NS3/4A protease. Abbreviations: P, phosphorylation; Ubq, ubiquitin modification; CBP, CREB-binding protein.

IRF-7

IRF-7 is a 67 kDa protein structurally similar to IRF-3, and functions to induce the second wave of IFN production after viral infection^{142,155}. IRF-7 is constitutively expressed in B cells and dendritic cells, but can be induced by IFN in all cell types^{67,142,155}. Therefore in most cells, IRF-7 is regulated at two levels: transcription and activation. Additionally, a number of IRF-7 splice variants are produced, though the functions that differentiate each of these are unknown¹⁴². In the face of a continuing viral threat, IRF-7, induced by IRF-3-dependent IFN- β production, is phosphorylated by TBK1 or IKK ϵ on carboxy-terminal serine residues, which results in its homo- or heterodimerization with IRF-3 and translocation to the nucleus (**Figure 1-6**)^{142,155}. It then binds to PRD-LEs in the IFN- α promoter and to PRDI and PRDIII on the IFN- β promoter. IRF-7 has a short half life of 30 min to 1 hour due to its susceptibility to ubiquitination and degradation^{67,70}. This allows the host cell to quickly shut down the pathway once virus is cleared. Genetic-deletion of IRF-7 revealed that IRF-7 was vital

for both early and late phases of type I IFN secretion during virus infection, indicating the importance of the IFN amplification loop (**Figure 1-6**)⁷¹.

IRF-9

IRF-9 (also known as p48) is a subunit of the transcription factor interferon stimulated gene factor 3 (ISGF3) (**Figure 1-5**)^{130,155}. ISGF3 is activated in response to type I IFN binding the type I IFN receptor (IFNAR), which stimulates the receptor-associated Janus kinases, Jak1 and Tyk2. These kinases catalyze the tyrosine phosphorylation of signal transducer and activator of transcription 1 (STAT1) and STAT2¹⁵⁵. IRF-9 and STAT2 are associated basally in the cell, and upon activation, STAT1 and STAT2/IRF-9 form the stable ISGF3 complex¹³⁰. ISGF3 then translocates into the nucleus where it binds the ISRE of interferon stimulated genes (ISGs)^{130,155}. ISGs are immunomodulatory effector molecules of the cell, and direct antiviral programs that limit HCV infection^{45,52,125,164}. IRF-9-deficient mice are defective in an IFN-induced antiviral response and thus are more susceptible to viral killing¹³⁰.

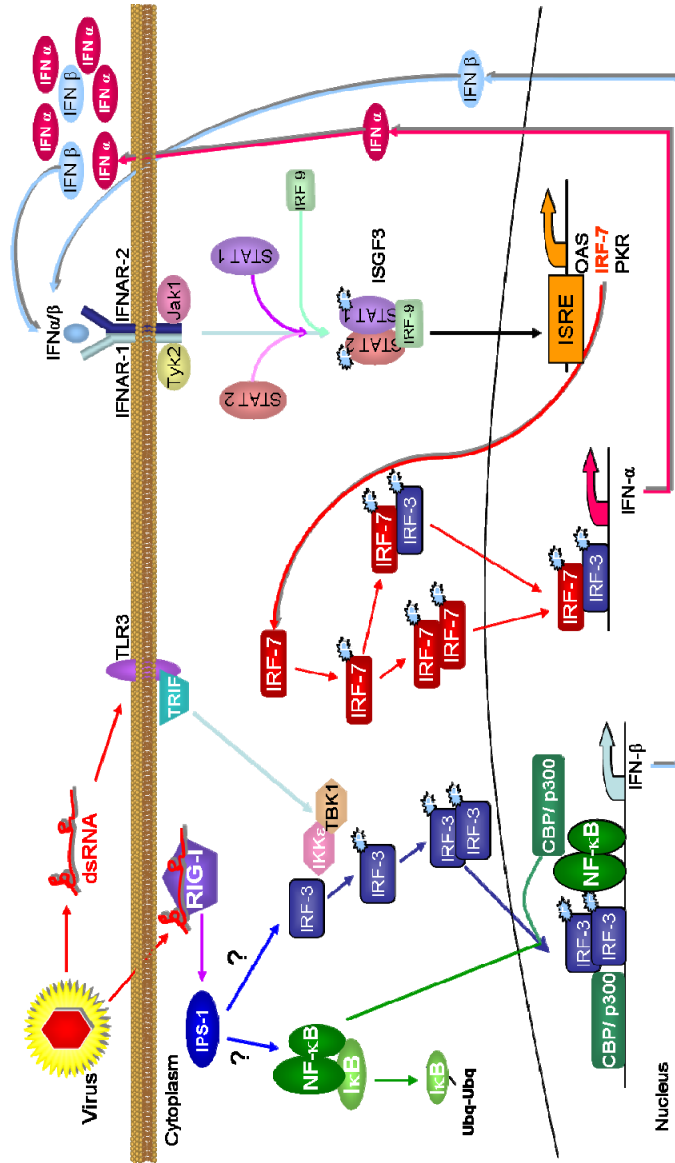


Figure 1-6: Virus infection triggers a positive IFN feedback loop. Virus infection causes replicative intermediates to accumulate, and these are potent inducers of antiviral pathways. dsRNA intermediates can bind to the pattern recognition receptors (PRRs) TLR3 or RIG-I to activate a complex that phosphorylates IRF-3, a latent cytoplasmic protein, leading to its dimerization and nuclear translocation. Similarly, activation of these PRRs also leads to the phosphorylation, ubiquitination, and subsequent degradation of IκBα, the inhibitor of another transcription factor, NF-κB. Liberated NF-κB then translocates to the nucleus. Binding of IRF-3 and NF-κB, along with other transcription factors, to the IFN-β promoter results in the production of IFN-β. IFN-β, acting in an autocrine or paracrine manner, binds to the type I IFN receptor (IFNAR) of the infected cell and surrounding tissues, activating a Jak/STAT signaling cascade. This results in production of interferon stimulated genes (ISGs), including IRF-7. IRF-7 activation, through processes that parallel the activation of IRF-3, stimulates the production of IFN-α subtypes, amplifying the IFN antiviral response and creating a positive feedback loop. Abbreviations: P, phosphorylation event.

NF- κ B

NF- κ B induces a variety of proinflammatory genes and cooperates with IRF-3 to induce IFN- β expression⁶². NF- κ B refers to a highly-regulated superfamily of proteins that possess an N-terminal Rel homology domain (RHD), a highly conserved DNA-binding/dimerization/nuclear localization domain^{54,69}. Of relevance to innate immune signaling are the subunits p65 (RelA) and p50. p65 contains a C-terminal transactivation domain, which enables it to induce target gene expression⁶³. p50 originally starts as a longer protein, p105, that contains multiple carboxy-terminal copies of autoinhibitory ankyrin repeats⁵⁴. Through limited proteolysis, p105 becomes p50, the active DNA-binding form; however, since it does not contain a transactivation domain, p50 cannot activate transcription without p65⁶³. NF- κ B heterodimers bind 9-10 base pair DNA sites. Both p50 and RelA can form heterodimers and homodimers in vivo⁵⁴.

NF- κ B is held quiescent in the cytoplasm by sequestration with I κ B α . I κ B α interacts with NF- κ B via multiple contacts, covering the NLS and interfering with its DNA-binding capability. I κ B α is an NF- κ B-dependent gene, and its expression is induced by NF- κ B activation, lending inherent negative feedback to the pathway^{54,69}.

Virus infection activates p50/p65 heterodimers through the canonical NF- κ B pathway (**Figure 1-5**). Detection of dsRNA by RIG-I leads to the induction of the I κ B kinase (IKK) complex, which consists of the catalytic kinase subunits IKK α and IKK β and two molecules of the scaffolding, regulatory protein called NF- κ B essential modulator (NEMO; also known as IKK γ)^{54,63,68}. NEMO is regulated by oligomerization and K63-ubiquitin binding activity⁴³. IKK mediates phosphorylation of I κ B α at serines

32 and 36, which induces its K48 ubiquitination and degradation, enabling NF- κ B to enter the nucleus and bind to target genes. NF- κ B activation is most often transient and cyclic in the presence of a continuous inducer due to repeated degradation and re-synthesis of I κ B α ⁵⁴.

IPS-1

While it was speculated that the downstream adaptor molecule linking RIG-I and MDA-5 to IRF-3 and NF- κ B was a CARD-containing protein ¹⁴⁹, the identity of this molecule remained elusive. In 2005 four independent groups, using genome database bioinformatics searches or cDNA screens, identified a 62 kDa protein as the downstream adapter and dubbed it (in order of publication acceptance dates) interferon- β promoter stimulator 1 (IPS-1) ⁸⁰, mitochondrial antiviral signaling protein (MAVS) ¹⁴³, virus-induced signaling factor (VISA) ¹⁷⁰, or CARD adaptor inducing IFN- β (Cardif) ¹⁰⁹ (reviewed in ⁷⁴). This protein had previously been established as a regulator of NF- κ B ¹⁰⁴, and is expressed in multiple tissues ^{80,170}. IPS-1 contains an amino-terminal CARD with homology to the RIG-I and MDA5 CARDS and a proline-rich region (PRR) ^{80,109,143,170}. It also possesses a carboxy-terminal transmembrane domain (TM) targeting IPS-1 to the outer mitochondrial membrane ¹⁴³ (**Figure 1-4**). IPS-1 overexpression constitutively activated IRF-3 and NF- κ B and resulted in reduced vesicular stomatitis virus (VSV) titers, suggesting that IPS-1 conferred antiviral activity through induction of type I IFN ^{80,143}. Co-immunoprecipitation studies showed that IPS-1 associated with amino-terminal, constitutively active RIG-I, and, to a lesser extent, amino-terminal

MDA5⁸⁰. This suggested a model in which dsRNA binds to RIG-I or MDA5, resulting in a conformational change that allows the CARD of IPS-1 to interact with one or more CARDS of RIG-I or MDA5. Activated IPS-1 can then bind downstream effector molecules, inducing antiviral response programs (**Figure 1-5**)⁸⁰.

Studies using mice deficient in functional IPS-1 revealed that IPS-1 was the sole adaptor for both RIG-I and MDA5 signaling to IRF-3 and NF- κ B, but it was not required for TLR signaling or the DNA-dependent activation of IRF-3 and NF- κ B^{86,151}. Importantly, this pathway is not important in plasmacytoid dendritic cells (pDCs), which signal IFN production via TLRs. Infection of IPS-1 knockout mice with VSV was 100% lethal, whereas most wt mice survived, suggesting the importance of the RIG-I pathway in protecting from lethal virus infection^{86,151}. However, a dose-dependent effect of VSV infection was observed, in which lower doses resulted in similar levels of type I IFN secretion in infected wt and IPS-1-null mice despite higher viral loads and increased mortality in the IPS-1-deficient mice. This continued IFN secretion was presumably due to pDCs, and indicates that secretion of IFN by pDCs is not sufficient to protect mice from virus-induced death¹⁵¹. However, type I IFN secretion was completely ablated in IPS-1^{-/-} MEFs in response to a variety of viruses⁸⁶. This suggests that either IPS-1 is essential for virus-mediated type I IFN secretion by every relevant signaling pathway in non-hematopoietic cells, or that the RIG-I pathway is the only pathway that recognizes RNA virus infection and hence that dsRNA is the only viral PAMP recognized by these cells to initiate IFN signaling^{86,151}.

Whether or not IPS-1 directly interacts with the IKK complex to activate NF- κ B or TBK1/IKK ϵ to phosphorylate IRF-3 is currently controversial. Several groups have

reported direct interactions while others have found no interaction occurring between these proteins. For example, Kawai et al. observed no evidence of direct association of IPS-1 with TBK1 or IKK ϵ ⁸⁰, while Xu et al. determined IPS-1 interacted with TBK1¹⁷⁰, and others found it bound to IKK ϵ but not TBK1^{93,109}.

IKK ϵ but not TBK1 was found to colocalize with IPS-1 in response to VSV infection⁹³, a surprising finding since genetic deletion of IKK ϵ previously was shown to have minimal effect on IFN production in response to virus infection, suggesting it functions in an accessory role to TBK1⁶⁵. Additionally, TBK1 is ubiquitously expressed in most cells, whereas constitutive IKK ϵ expression only occurs in a subset of hematopoietic cells, but can be induced in an NF- κ B-dependent fashion in other cells by virus infection⁶⁷. This suggests that IKK ϵ binding to IPS-1 may only be important in hematopoietic cells or the later stages of infection. Indeed, a recent article found that IKK ϵ activated a particular subset of ISGs, believed to be in part due to IKK ϵ phosphorylation of STAT1¹⁵⁷, suggesting there may be differential activation mechanisms of the two kinases promoting their differing functions.

There have been a number of downstream proteins proposed to indirectly mediate the interaction between IPS-1 and the kinases responsible for activating IRF-3 and NF- κ B^{80,109,133,136,143,170,179}. It is probable that different molecules are recruited depending on cell type and/or stimulus, and since many studies were performed in cancer cell lines, some interactions may be an artifact of disease. A major focus of future publications will be to identify the downstream interacting partners of IPS-1.

EFFECT OF HCV ON THE INTERFERON ANTIVIRAL RESPONSE

HCV infection in human patients

Current HCV combination therapy, interferon- α and ribavirin, has a response rate of around 50%³⁹, suggesting that HCV may encode mechanisms to hamper or evade the action of IFN. Several groups have looked at the effect of HCV infection in chronically infected patients and their response to IFN therapy. Surprisingly, many have found increased ISG expression in patients where therapy is ineffective. Examination of nine chronically-infected livers compared to healthy controls showed that a significant number of ISGs were expressed during HCV infection⁶⁴. In another report, liver biopsy specimens taken from HCV-infected patients before combination therapy showed that patients who subsequently did not respond to therapy had high baseline expression of ISGs, whereas responders and relapsers more closely resembled healthy controls³⁹. These studies suggest that non-responders have an upregulated and largely ineffective IFN response. HCV pseudotype particles have been shown to bind dendritic cells, one of the major type I IFN-producing cell types, causing their activation¹². Infiltration of immune effector cells, such as dendritic cells, could explain increased ISGs found in infected patients. Additionally, it suggests that the virus is able to inhibit downstream signaling pathways in infected hepatocytes, rendering both endogenous and exogenous IFN useless⁷.

Disruption of RIG-I signaling by HCV NS3/4A

Type I IFN genes are expressed at low levels during chronic HCV infection, with ISG expression varying widely among patients^{110,146}, suggesting that HCV may regulate the innate immune response to infection. RIG-I has been shown to control intracellular permissiveness to HCV RNA replication¹⁴⁹. Studies in HCV replicon cells revealed that HCV imparted a blockade on IRF-3 and NF- κ B activation⁴⁵. Further work showed that HCV NS3/4A, the essential viral protease and RNA helicase, antagonized RIG-I and MDA-5 signaling during infection^{44,45,174}, thereby preventing induction of antiviral response programs. Protease activity of NS3/4A was necessary for inhibition of this pathway, while the helicase activity was dispensable⁴⁵. However, NS3/4A did not cleave RIG-I or MDA5, suggesting that the proteolytic target was one or more effector molecules downstream of RIG-I and MDA-5^{44,45,174}. Indeed, it was discovered that NS3/4A cleaves IPS-1, the adapter molecular downstream of RIG-I, at a.a. cysteine 508 both in vitro and in livers from chronically-infected patients. Proteolysis of IPS-1 removes the TM domain from the effector portions of the molecule, disrupting its normal localization on mitochondrial membranes. Additionally, this action by NS3/4A ablates signaling to both IRF-3 and NF- κ B, effectively shutting down the host intracellular antiviral response and enabling HCV replication to continue^{91,98,109}. Interestingly, hepatocyte-specific ablation of NF- κ B activation by genetic disruption of NEMO in mice induced a disease resembling steatohepatitis in humans, and ultimately led to hepatocellular carcinoma¹⁰². Since HCV NS3/4A ablates NF- κ B activation, this could

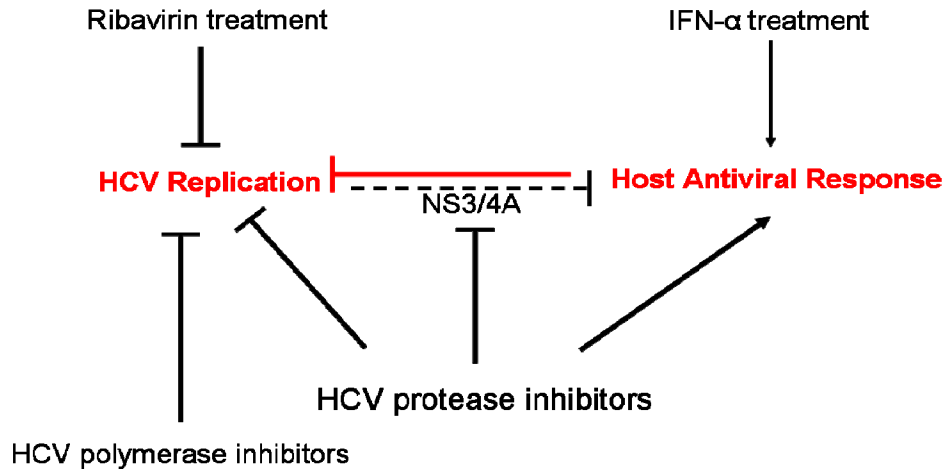
represent one mechanism by which the virus contributes to induction of hepatocellular carcinoma in humans.

Despite our advances, there is no clear picture of the number of infected hepatocytes during in vivo HCV infection or the characteristics of these HCV-infected cells. Confocal microscopy analysis of chronically infected HCV patient livers showed focal areas of infection, with IPS-1 absent from cells staining positive for HCV NS3/4A. Surrounding areas contained normal IPS-1 localization⁹⁸. This suggests that cells with active infection are able to block innate immune signaling.

Combined, these observations suggest a model for HCV interaction with the innate immune system. While HCV RNA recognition by RIG-I can initially control cellular permissiveness to HCV replication, HCV persists by evading the immune response through regulation of downstream effector molecules. The HCV NS3/4A protein complex blocks activation of the downstream transcription factors IRF-3 and NF- κ B, thereby preventing production of IFN- β and other ISGs, and terminating the IFN amplification loop mediated by IRF-7 that is critical in the innate antiviral response^{44,45}.

Treatment with NS3/4A peptidomimetic protease active site inhibitors restores the host response to HCV RNA replication⁴⁵. Current therapy for HCV infection, interferon- α and ribavirin combination therapy, is only effective in half of patients³⁹. The ability of HCV to establish persistent infection may be due to its propensity to block innate antiviral signaling pathways⁵². Therefore NS3/4A protease inhibitors offer great potential as novel therapeutic agents against HCV through their immunomodulatory activity (**Figure 1-7**).

Current Therapy



Future Therapy Options (in clinical trials)

Figure 1-7: Effects of pharmacological treatment on HCV replication and the innate immune response. Current combination therapy of IFN- α and ribavirin target both HCV replication and the host antiviral response. However, profound side effects of IFN treatment often result in patient non-compliance. Therefore new therapies are necessary. HCV polymerase inhibitors only target HCV replication. HCV protease inhibitors, on the other hand, target HCV replication, through decreased proteolysis of the viral polypeptide, and restore the host antiviral response, offering a great therapeutic advantage.

CHAPTER TWO

Materials and Methods[§]

PLASMIDS AND TRANSFECTION

pFLAG NS4A, pFLAG NS5A, and pFLAG NS5A/B were previously described^{44,45,163}. pEFBos-RIG-I, pEFBos-N-RIG, and pEFBos-C-RIG expression plasmids¹⁷⁵ as well as pEFBos-MDA5, pEFBos-N-MDA5, and pEFBos-C-MDA5¹⁷⁴ are amino-terminally FLAG-tagged. pEFBos, pEFBos-IPS-1, pMyc-IPS-1 were described previously^{98,175}. pCMV-IRF-3 5D, encoding the phospho-mimetic, constitutively active IRF-3, and pIRF-3-ΔN a dominant-negative truncation mutant of IRF-3 lacking the DBD, were a generous gift by Dr. John Hiscott. IκBα-M (Clontech) is a dominant-negative IκBα construct that inhibits activation of NF-κB. The luciferase reporter constructs pIFN-β-luc and PRDII-luc were kindly provided by Dr. Zhijian Chen; p561-luc was a generous gift of Dr. Ganes Sen. pCMV-Renilla was purchased from Promega. Mouse luciferase reporter constructs, p55A2-luc (repeated PRDII sites), p55C1B-luc (repeated PRDI sites), and p125-luc (IFN-β promoter) were obtained from T. Fujita¹⁷⁷. pEFTak vector (encoding a N-terminal FLAG tag) and pCDNA3.1 Myc-His vector were described¹³⁵. GenElute Endotoxin-free Plasmid Midiprep kit (Sigma) was used to prepare plasmid DNA for transfections. Transfections in mammalian cells were performed using Fugene 6 transfection reagent (Roche Molecular Biochemicals) or Lipofectamine 2000 (Invitrogen) according to manufacturer's protocol, using a 3:1 ratio

[§] Portions of this chapter are copyrighted to ASBMB Journals [[J. Biol. Chem.](#) 2007 Apr; 282(14): 10792-803] and used with permission

of transfection reagent (μl) to DNA (μg). Transfections in murine cell lines were performed using Liptofectamine LTX, with Plus reagent (Invitrogen) as per manufacturer's specifications.

NS3/4A PROTEASE INHIBITORS

SCH6 (kindly provided by Schering-Plough)⁴⁵ and ITMN-C (a gift from Dr. S. Seiwert at Intermune, Brisbane, CA) protease inhibitor treatments were conducted by replacing culture medium with medium containing 20 μM SCH6 or the indicated amount of ITMN-C.

CELLS

Huh7 human hepatoma cells¹¹⁴, Huh7.5, and HEK 293 cells were propagated in Dulbecco's Modified Eagle Medium (DMEM, Cellgro) supplemented with 10% fetal bovine serum (FBS, Hyclone), 1X nonessential amino acids, 2 mM L-glutamine, antibiotic-antimycotic solution, 1 mM sodium pyruvate, and 25mM HEPES (Cellgro). Huh7.5 cells, a subline of Huh7 cells kindly provided by C. Rice, contain a defect in RIG-I and do not signal through the RIG-I pathway¹⁴⁹. UNS3/4A and UNS3 cells (a gift from D. Moradpour) are osteosarcoma cells conditionally expressing HCV 1a NS3/4A or HCV 1a NS3, respectively, described previously^{113,166} and were maintained in complete media described above supplemented with 400 $\mu\text{g/ml}$ G418, 100 $\mu\text{g/ml}$ puromycin, and 1 $\mu\text{g/ml}$ tetracycline. HP and K2040 cells are Huh7 cells harboring cell culture-adapted subgenomic HCV 1b replicons^{150,164} and were cultured in the presence of 200 $\mu\text{g/ml}$ G418. All cells were grown at 37°C under 5% CO₂ in air-jacketed incubators.

VIRUSES

For Sendai Virus infection (Cantell strain, Charles River Laboratories), 1×10^5 or 2×10^4 cells/well were seeded into 12-well or 48-well dishes respectively, and where indicated transfected with expression constructs. Twenty-four hours after seeding or transfection, cells were washed twice in PBS and mock-infected or infected with 100 hemagglutinin units (HAU) of Sendai virus per mL of serum-free media (SFM) for one hour. Three volumes of complete culture media were then added to wells and cells incubated another 17 or 19 hours as described ⁴⁵. HCV 2a stock was produced as described previously ⁹⁸. For HCV infection, approximately 4×10^4 cells seeded in a 12-well plate were infected at a MOI of 1 with HCV 2a in culture media for 3 hours, washed in PBS, and culture media added. Cells were then incubated until collection at the indicated time points.

CONFOCAL MICROSCOPY

In four-chamber slides, 2×10^4 cells/chamber were plated. Sixteen to 24 hours later, 200ng of the indicated expression plasmids were transfected into each well (unless indicated otherwise in figure legend), and cells collected 12 or 24 hours later. Where indicated, mitotracker Red (Invitrogen) was used to visualize location of mitochondria by adding 250nM diluted in DMEM to live cells for 30 minutes at 37°C. Cells were fixed in 4% paraformaldehyde and blocked in PBS containing 10% FBS and 1% Triton X-100. Antibodies against the FLAG epitope (Sigma), MAVS (a gift from Z. Chen), IRF-3 (kindly provided by M. David), Cardif (Axxora), HCV NS3 NCL (Novacastra

laboratories), and RIG-I C-terminus (a gift from T. Fujita) were used in combination with Alexa 488- or Alexa 594-conjugated secondary antibodies (Invitrogen). Slides were mounted with Prolong Gold (Invitrogen), and examined using a Zeiss Pascal Laser Scanning confocal microscope and Zeiss LSM software. The images shown are ≤ 7 micron optical slices.

IMMUNOBLOTTING

For immunoblotting, 1×10^5 cells/well were plated into 12-well culture dish as needed. The following day, cells were transfected with plasmid DNA, and if indicated, 24 hours later infected with SenV for 20 hours. Cells were then harvested into modified radioimmunoprecipitation assay (RIPA) buffer (10mM Tris pH 7.5, 150mM NaCl, 0.02% NaN_3 , 1% sodium deoxycholate, 1% Triton-X) for examining cytosolic proteins or RIPA buffer (modified RIPA buffer plus 0.1% SDS) for investigating membrane-bound proteins, supplemented with protease inhibitor cocktail (Sigma), phosphatase inhibitor cocktail II (Calbiochem), and $1 \mu\text{M}$ okadaic acid (Calbiochem), and frozen at -80°C . Lysates were spun at 4°C for 15 minutes at $\geq 18,000 \times g$ to pellet membrane fractions and unlysed cells and organelles, and protein concentrations were measured by Bradford assay. Equivalent amounts of protein (usually around 20 -35 μg /well) were resolved by SDS-polyacrylamide gel electrophoresis (PAGE) on 10% or 12% polyacrylamide gels. Immediately following electrophoresis, gels were transferred to NitroPure nitrocellulose membranes (Micron Separations, Inc.) using Towbin's transfer buffer at 110V for 1 hour at 4°C . Membranes were blocked in PBS containing 0.1% Tween-20 (TPBS) and 5%

nonfat dehydrated milk (Carnation). Blots were probed with antibodies against HCV NS3 A6 (kindly provided by J. Ye), ISG56 (a gift from G. Sen), ISG15 (kindly provided by A. Haas), Sendai virus (a gift from I. Julkunen), actin (Santa Cruz Biotechnology), NS3 goat pAb (US Biologicals), Phospho-I κ B α (Cell Signaling), I κ B α (Santa Cruz Biotechnology), GAPDH (Santa Cruz Biotechnology), HCV (a gift from W. Lee), ISG48 (Santa Cruz Biotechnology), Myc epitope (Bethyl Laboratories), phospho-serine 386 IRF-3 (T. Fujita), phospho-serine 396 IRF-3 (J. Hiscott), or those described above. Primary antibodies were prepared in TPBS supplemented with 10% FBS and 0.02% NaN₃, except FLAG-HRP conjugated antibody (Sigma) used in immunoprecipitation experiments described below, which did not receive NaN₃ and was not probed with secondary antibody. Between primary and secondary antibodies, and after secondary antibody, membranes were washed 3 x 5 min. in TPBS. Secondary antibodies were diluted 1:5000 (anti-goat antibody) or 1:10,000 (all other secondary antibodies) in blocking solution (described above). Anti-human and anti-goat HRP-conjugated secondary antibodies were obtained from Jackson Laboratories; anti-rabbit and anti-mouse HRP conjugated secondary antibodies were obtained from Perkin Elmer. Protein bands were visualized using ECL+ Western Blotting reagent (Amersham Biosciences).

IMMUNOPRECIPITATION ANALYSIS

For coimmunoprecipitations, 2×10^5 Huh7 cells or 4×10^5 HEK293 cells were seeded into 6-well culture dishes and transfected with plasmid DNA using Fugene 6 as described. At 24 hours post-transfection, cells were harvested for analysis. Cells were washed in PBS and collected by scraping (Huh7) or pipetting (HEK293 cells). Cells

were briefly spun at 2400xg for 5 min., then resuspended in 100 μ l Seize II Immunoprecipitation (IP) buffer (25mM TrisCl pH 7.5, 150 mM NaCl) with 1% Triton X-100 (Lysis Buffer) and 0.1% SDS, and supplemented with protease and phosphatase inhibitors as described for immunoblotting. Cells were disrupted by vigorous pipetting with a gel loading tip (~10 times), followed by incubation on ice for 10 minutes. Cell lysates were diluted in 300 μ l lysis buffer with protease and phosphatase inhibitors, and centrifuged at \geq 20,000xg for 15 minutes to pellet unlysed cells and membranes. Supernatants were collected and incubated with 20 μ l washed FLAG M2 agarose beads (Sigma) with rocking for 6-20 hours at 4°C. Supernatant fractions were collected, beads washed 3 x lysis buffer, and boiled in SDS sample buffer. Immunoblot analysis was conducted on IP and supernatant fractions.

PROMOTER LUCIFERASE REPORTER ASSAYS

Huh7 cells (2×10^4 cells/well) or HEK293 cells (4×10^4 cells/well) were seeded in triplicate into 48-well dishes and co-transfected with 25ng of pIFN- β -luc or pPRDII-luc and 5ng pCMV-*Renilla* per well along with the indicated amounts of expression constructs. Cells were then cultured alone or subjected to virus infection and harvested 20 hours later for luciferase assay using Promega Dual Luciferase Assay Kit as per manufacturer's protocols. MEFs (1×10^4 cells/well) were plated in triplicate into 48-well dishes and co-transfected with 100ng p55A2-luc (a mouse NF- κ B specific reporter), p55C1-luc (a mouse IRF specific reporter), or p125-luc (a mouse IFN- β specific

reporter), and 20ng pCMV-*Renilla* along with 280ng of the indicated expression constructs. For all cell types, results were calculated relative to *Renilla* luciferase values.

ELECTROPHORETIC MOBILITY SHIFT ASSAY (EMSA)

EMSA analysis of NF- κ B DNA binding activity was conducted on UNS3/4A and UNS3 nuclear extracts as described⁴⁶. Cells were grown in 10 cm dishes in the presence (-NS3/4A) or absence (+NS3/4A, +NS3) of 1 mg/ml tetracycline, and protease inhibitor (20 μ M SCH6 or 10 μ M ITMN-C) or DMSO (mock treatment) was added to the media for 24 hours. Cells were then mock-infected or infected with 100 HAU/ml of Sendai virus and infection was allowed to proceed 18 hours. As a positive control for NF- κ B activation, some wells were washed twice in PBS and treated for 30 minutes with 20 ng/mL TNF- α in SFM. Cells were harvested by scraping into ice-cold PBS and pelleted at 1850 x g for 10 min at 4°C. The supernatant was removed, 100 μ l lysis buffer (50mM Tris-HCl pH 8.0, 60mM KCl, 1mM EDTA, 2mM DTT and 0.15% NP40) added to each sample, and cells were incubated on ice 15 min to facilitate swelling. Lysates were centrifuged at 3300 x g for 15 min to separate cytosol and nuclei. Nuclei were lysed in 1 volume nuclear extract buffer (20mM Tris-Cl pH 8.0, 400mM NaCl, 1.5mM MgCl₂, 200 μ M EDTA and 25% glycerol) and incubated on ice for 2 min. NaCl was added to nuclear extracts to reach a final concentration of 400mM in order to strip proteins from DNA, and incubated on ice for 10 min. Samples were vortexed for 15 sec and centrifuged at maximum speed for 30-45 minutes to collect nuclear extract. NF- κ B consensus and mutant oligonucleotides (Santa Cruz Biotechnology) were annealed by

heating at 95°C for 10 minutes and slowly cooling to room temperature (RT). Probe labeling was performed by incubating 5 pmol dsDNA template, $^{32}\text{P}\gamma\text{-ATP}$, and T4 Kinase (GibcoBRL) for 30 min at 37°C. The probe was purified on a spin column to remove unincorporated nucleotide (BioRad). Binding reactions were carried out with 5 μg nuclear extract and 50,000 cpm radiolabeled probe in EMSA binding buffer (60mM HEPES pH 7.9, 50mM NaCl, 1mM EDTA, 0.5mM DTT, 0.3 mg/ml BSA, 52 $\mu\text{g}/\text{ml}$ salmon sperm DNA and 10% glycerol) for 30 min at 30°C. Antibody supershifts were performed using antibodies against NF- κB p50 or p65 subunits (Santa Cruz Biotechnology); non-radiolabeled, cold competitor was used as a negative control. For antibody supershift and cold competitor control, nuclear extracts were incubated with antibody or unlabeled dsDNA in EMSA buffer for 15 minutes at RT, followed by addition of 50,000 cpm radiolabeled probe and a further incubation of 30 min at 30°C. Samples were separated on a 6% TBE gel (pre-run 3hr at 200V) for 90 min at 275V at 4°C. Gels were fixed (50% methanol, 10% acetic acid) for 30 minutes and dried at 80°C for 90 min on a vacuum dryer. Autoradiography was performed on the blots.

CHAPTER THREE
Functional and Therapeutic Analysis of HCV NS3/4A Protease Control of Antiviral Immune Defense[§]

INTRODUCTION

HCV establishes persistent infections in the majority of exposed individuals. There are nearly 200 million people worldwide with chronic HCV infection, and it is a major cause of hepatitis and liver disease. Moreover, HCV is associated with the development of liver cancer and is currently the leading indication for liver transplants^{4,19}. HCV is a member of the Flaviviridae family of enveloped, single-stranded, positive-sense RNA viruses. The 9.6 kb genome of HCV encodes a single polyprotein that is post-translationally processed into at least 10 structural and nonstructural (NS) proteins by a combination of host and viral proteases¹²⁸. In addition to their primary role in HCV genome replication and virion maturation, various HCV proteins have been shown to antagonize host immune defenses. HCV control of the host response and IFN α/β antiviral defenses may provide a cellular foundation for viral persistence⁵².

The innate antiviral response to RNA virus infection is triggered when intermediates of viral replication, including viral RNA or protein products, are recognized by specific cellular pathogen recognition receptors¹³⁴. RIG-I and MDA5 are cytosolic pathogen recognition receptors that bind to viral RNA and dsRNA, albeit with variable efficiency^{174,175}. Both are DExD/H-box RNA helicases and encode tandem amino-terminal CARDs¹⁷⁴. RIG-I is an essential pathogen recognition receptor for

[§] The majority of Chapter 3 is copyrighted to ASBMB Journals [[J. Biol. Chem.](#) 2007 Apr; 282(14): 10792-803] and used with permission

various negative-strand viruses and Flaviviridae⁷⁸, including HCV^{135,149}. RNA binding by RIG-I and MDA5 promotes a conformation change that potentiates signaling by the CARDs^{135,150} to a CARD-containing adaptor protein IPS-1 (reviewed in⁷⁴), located on the mitochondrial membrane. IPS-1 confers downstream signaling to the latent cytoplasmic transcription factors IRF-3 and NF- κ B^{80,109,143,170}. IRF-3 activation commences with its virus-induced phosphorylation, dimerization, and nuclear translocation whereupon it binds to the promoter region of IRF-3-dependent genes, including IFN- β , IFN-stimulated gene (ISG) 15, and ISG56^{42,57,176}. Parallel NF- κ B activation induces a variety of proinflammatory genes and cooperates with IRF-3 to induce IFN- β expression⁶². In HCV-infected hepatocytes, IFN- β plays an important role in triggering the expression of IFN-stimulated genes (ISGs) and initiating an IFN-amplification loop that enhances ISG expression and drives the production of IFN- α subtypes⁵². ISGs have antiviral and immunomodulatory activity that limit HCV infection^{45,52,125,164}, and their expression marks the effector stage of the innate antiviral response¹⁴⁰.

HCV evades the innate antiviral response in part through the actions of the viral NS3/4A protease/helicase complex, which ablates RIG-I and MDA-5 signaling^{44,149,174} through proteolytic cleavage and inactivation of IPS-1^{91,98,109}. NS3/4A cleaves IPS-1 at C508, thereby releasing it from the mitochondrial membrane and preventing its downstream activation of immune effectors⁹⁸. However, the NS3/4A structural motifs and features that direct IPS-1 cleavage and loss of RIG-I and MDA5 signaling have not been defined.

NS3/4A is a complex, bifunctional molecule (**Figure 3-1**) that is essential for NS protein processing and viral RNA replication^{8,132}. The amino-terminal region of NS3 contains a serine protease that non-covalently binds its cofactor, NS4A. NS3/4A is a member of the chymotrypsin serine protease family, but its shallow binding pocket and structural requirement for a zinc atom distinguish it from other members of the family.⁸ It is responsible for cleavage events between NS3, NS4A, NS4B, NS5A, and NS5B and is necessary for viral RNA replication.^{8,132} NS4A is a small peptide cofactor necessary for efficient processing of the HCV polyprotein by NS3 and is thought to be involved in tethering the complex to intracellular membranes^{31,166}. The carboxy-terminus of NS3 possesses a DExD/H box helicase with nucleoside triphosphatase (NTPase) activity believed to participate in RNA unwinding during viral RNA replication⁸⁷. Its helicase activity was found to be positively modulated by the protease domain and NS4A^{48,59,85,178}. Indeed, a single point mutation within the helicase domain reduced protease activity of NS3/4A⁸⁵. Additionally, an RNA ligand added to full-length NS3 inhibited NS3 protease activity, further suggesting interdomain interactions^{49,50,118}. Moreover, structural studies of full-length NS3 indicate that the C-terminus of the helicase domain may interact with the protease active site¹⁷³, indicating a structural and functional interconnectivity of the two domains. Of note, the cellular effector molecules protein kinase A and C bind to the arginine-rich region within the NS3 helicase domain *in vivo*^{17,18}. NS3/4A interaction with its cellular targets could therefore occur through a variety of processes mediated by its helicase or protease domains.

Several peptidomimetic NS3/4A protease active site inhibitors are in preclinical development as HCV antiviral drugs¹⁵⁴. Future use of these compounds could represent

an alternative or supplement to the current treatment regimen for HCV infection, IFN- α and ribavirin combination therapy, which is only effective in about 50% of patients³⁹. NS3/4A protease inhibitors may also exhibit immunomodulatory properties by removing the protease-dependent blockade to the innate antiviral response during HCV replication^{44,45}, although the impact of IPS-1 in this process is not known. The current study was undertaken to define the domain structure and function of NS3/4A that regulates the host cell innate antiviral response.

EXPERIMENTAL PROCEDURES

Expression Cloning and Site-directed Mutagenesis

pFLAG NS3/4A and pFLAG NS3 were generated as described⁴⁵. Constructs (**Figure 3-1**) containing NS3 helicase domain truncations at amino acid (a.a.) 1206 (protease domain alone, Prot), 1238, 1486, and 1501, as well as a protease domain deletion (NS3 a.a. 1207-1658, Hel) were made as follows. NS3 mutants were cloned by PCR (with primers containing a 5'HindIII site and a 3'XbaI site) using BD Advantage-HF 2 PCR kit (BD Biosciences) into pCR2.1 vector (TA cloning kit, Invitrogen). These constructs were then subcloned into the HindIII and XbaI sites of pFLAG-CMV-2 vector (Sigma). A protease active site mutant (NS3/4A S1165A) and deletion of the arginine-rich region (a.a. 1487-1501; NS3/4A Δ 1487-1501) were constructed using QuickChange XL site-directed mutagenesis kit (Stratagene) as per manufacturer's protocol. Since NS4A forms part of the protease active site and is indispensable for full protease activity

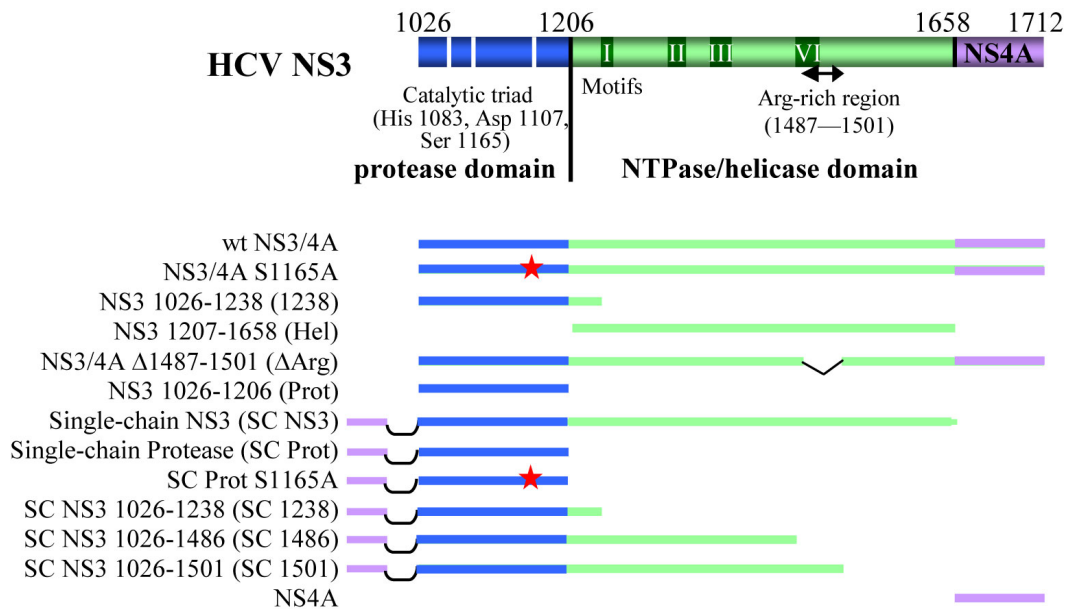


Figure 3-1: Diagram of wt NS3/4A and NS3/4A mutants. NS3 is comprised of two domains (*upper*): a serine protease domain (depicted in blue) and a NTPase/DExD/H box helicase domain (shown in lime). The three horizontal white lines in the protease domain indicate the positions of the catalytic triad. Conserved motifs in the DExD/H box helicase domain are shown in dark green. Numbers above the drawing represent the amino acid (a.a.) number of the HCV polyprotein. NS3/4A mutants (*lower*) were constructed as described in the text. The red star indicates the serine 1165 (of the catalytic triad) mutation to alanine, which ablates protease activity. NS4A (drawn in lavender) is a 54 a.a. cofactor for the NS3 serine protease domain. Single-chain constructs contain the 12 a.a. (a.a. 21-32) of NS4A essential for intercalation into the NS3 protease active site, connected to various NS3 truncation mutants via a flexible linker, enabling direct interaction of the NS4A residues with the NS3 protease without an intramolecular cleavage event. The curved semicircular line represents the flexible linker region. V-shaped lines in NS3/4A Δ 1487-1501 represent the area deleted in this construct.

³¹, a scheme was devised allowing expression of NS4A with the NS3 mutants. To circumvent this problem we created a primer containing an amino-terminal KpnI site, 12 a.a.s of NS4A (a.a. 21-32; which intercalate into the NS3 protease active site), and a flexible linker (GSGS) region, and subcloned this into the HindIII sites of the pFLAG NS3 1026-1206, creating a fully-functional, single-chain (SC) NS3/4A protease domain (SC Protease). This strategy was similar to that described by Taremi et al. ¹⁵⁶. The flexible linker was also subcloned into pFLAG NS3 (SC NS3), pFLAG NS3 1026-1238 (SC NS3 1026-1238), pFLAG NS3 1026-1486 (SC NS3 1026-1486), and pFLAG NS3 1026-1501 (SC NS3 1026-1501) to generate the SC constructs indicated in parentheses. NS3/4A, NS3/4A S1165A, the SC Protease, and the SC Protease S1165A were subcloned into pEF1/Myc-His B (Invitrogen) to allow high efficiency expression of each. NS3/4A and NS3/4A S1165A were cut with HindIII, blunt-ended with Kleenow fragment, digested with XbaI and subcloned into the EcoRV and XbaI site of pEF1/Myc-HisB. The SC Protease constructs were subcloned into the SacI and XbaI sites of pEF1/Myc-HisB. Primer sequences for all constructs are shown in **Table 3-1**.

Statistical Analysis

Differences among treatments were examined using unpaired *t*-tests, and were considered statistically significant when $P < 0.02$ and were marked with an asterisk. Statistical differences in which $P \leq 0.001$ were marked with two asterisks.

Table 3-1: Primer sequences for NS3 cloning**A. NS3 truncation mutant primers**

Mutant	Primer name	Primer sequence
NS3 1026-1206	Replicon NS3 HindIII [s]	AAG CTT GCG CCT ATT ACG GCC TAC
	HCV 1b Pr3 ter a	TCTAGACTACCGCATAGTGGTTTCCATAGACTC GACG
NS3 1026-1238	Replicon NS3 HindIII [s]	AAG CTT GCG CCT ATT ACG GCC TAC
	HCV 1b NS3 MI a	TCTAGACTAGCTCTTGCCGCTACCAGTAGGG
NS3 1026-1320	Replicon NS3 HindIII [s]	AAG CTT GCG CCT ATT ACG GCC TAC
	HCV 1b NS3 MII a	TCTAGACTAGTGGCACTCATCACATATTATGAT GTC
NS3 1026-1351	Replicon NS3 HindIII [s]	AAG CTT GCG CCT ATT ACG GCC TAC
	HCV 1b NS3 MIII a	TCTAGACTACGTAGCGGTGGCGAGCACGACGA G
NS3 1026-1486	Replicon NS3 HindIII [s]	AAG CTT GCG CCT ATT ACG GCC TAC
	HCV 1b NS3 aa1486 a	TCTAGACTACGAGCGTGACACCGCGTCTTGTG
NS3 1026-1501	Replicon NS3 HindIII [s]	aag ctt gcg cct att acg gcc tac
	HCV 1b NS3 aa1501a	TCTAGACTACCTGTAAATGCCCATCCTGCCCT ACC
NS3 1207-1658	HCV 1b HeS	AAGCTTCCCCGGTCTTCACGGACAACCTCG
	Replicon NS3 [stop] Xba1 [as]	tct aga cta cgt gac gac ctc cag gtc agc

B. NS3/4A site-directed mutants and deletions

Mutant	Primer name	Primer sequence
NS3/4A Δ1487-1501	HCV NS3 Arg rich del s	GAC GCG GTG TCA CGC TCG CAG TTT GTG ACT CCA GGA GAA CGG
	HCV NS3 Arg rich del as	CCG TTC TCC TGG AGT CAC AAA CTG CGA GCG TGA CAC CGC GTC
NS3/4A S1165A	S1165A sense	CCTACTTGAAGGGCTCTGCGGGCGGTCCACTG CTCTG
	S1165A antisense	CAGAGCAGTGGACCGCCCGCAGAGCCCTCA AGTAGG
Single-chain mutants	NS4A linker oligo S	Phospho AG CTT GGT ACC GGC AGC GTG GTC ATT GTG GGC AGG ATC ATC TTG TCC GGT AGT GGT AGT A
	NS4A linker oligo AS	Phospho AG CTT ACT ACC ACT ACC GGA CAA GAT GAT CCT GCC CAC AAT GAC CAC GCT GCC GGT ACC A

RESULTS

Characterization of NS3/4A constructs

In order to determine the minimal region of NS3/4A that could modulate the host response, a series of FLAG epitope-tagged NS3 truncation and deletion mutants were constructed (**Figure 3-1**). To assess individual domains of NS3 and NS4A in host response regulation, we produced constructs encoding NS4A alone ⁴⁵, the NS3 protease domain (Protease), helicase domain (Helicase), or full-length NS3 lacking the arginine-rich region (Δ Arg), as well as full-length NS3/4A harboring a protease activate site mutation (S1165A) as a negative control. These were placed under the control of the CMV-Immediate-Early promoter. Previous studies have identified a twelve amino acid region of NS4A (a.a. 21-32) that intercalates into the NS3 protease active site and is indispensable for full protease activity ³¹. Expressing NS4A from a separate plasmid was not sufficient to result in efficient protease activity or inhibition of antiviral signaling (**Figure 3-2**). Additionally, at the time commercially available bicistronic vectors used a viral IRES as a second promoter element. This was undesirable due to the possibility of the IRES activating the innate immune signaling pathways under study. In order to express full NS3/4A protease activity from a single plasmid, we attached these 12 a.a. of NS4A to each NS3 mutant via a flexible linker, creating a fully-functional, single-chain (SC) NS3/4A protease encoding full-length NS3 (SC NS3), progressive deletions of the NS3 helicase domain (SC 1501, SC 1486, SC 1238), the protease domain alone (SC Protease), or the protease domain with an active site mutation (SC Protease S1165A).

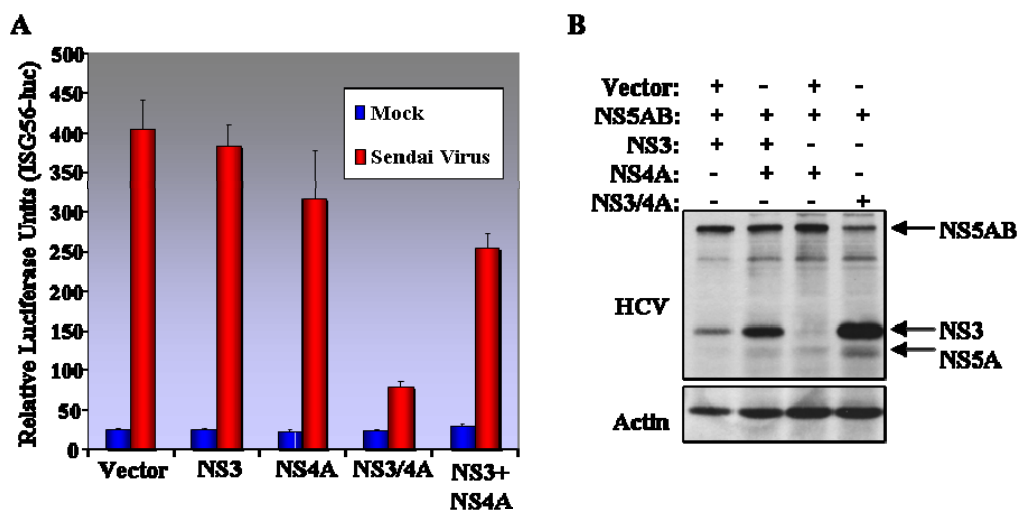


Figure 3-2: Effect of NS3 expressed with NS4A in *cis* or in *trans* on induction of ISG56 promoter and cleavage of NS5AB. *A.* Huh7 cells were co-transfected with 200 ng each of vector, NS3, or NS4A or 100 ng NS3/4A as shown along with 20 ng pCMV-Renilla and 35 ng ISG56-luc (an IRF-3-dependent promoter construct). Nineteen hours later, cells were infected with 100 HAU/mL SenV for 25 hours and lysates subjected to luciferase assay. *B.* Huh7 cells were transfected with 700 ng of the indicated plasmids and collected 24 hours later. Immunoblotting was performed using antibodies against HCV and actin as a loading control. HCV protein bands are marked.

Use of similar SC constructs as a tool for examining the NS3/4A protease structure and function has been well established in crystallization studies¹⁷³ and studies identifying small molecule protease inhibitors¹⁶⁹. Moreover, Taremi et al. found that such SC Protease constructs displayed protease activity comparable to wildtype (wt) NS3/4A¹⁵⁶. As shown in **Figure 3-3** when co-expressed in Huh7 cells, a NS5AB polyprotein substrate was efficiently cleaved by wt NS3/4A, SC Protease, SC NS3, Δ Arg, SC 1238, SC 1486, and SC 1501 constructs (*middle panel, lanes 4, 7, 9, 17, 19-21*, respectively). The NS5AB polyprotein was not cleaved by NS4A, NS3/4A S1165A, Helicase, SC Protease S1165A, SC NS3 S1165A, or Protease (*lanes 3, 5, 6, 8, 10, 18*, respectively), and when lacking NS4A was only partially cleaved (NS3 or 1238, *lanes 2*

and 11). When expressed from the elongation factor-1 promoter expression plasmid (pEF), pEF wt NS3/4A, and pEF SC Protease mediated NS5AB cleavage, but neither protease active site mutant did (compare *lanes 12-16*). These results validate the expression and cleavage activity of the NS3 constructs, and show that efficient NS3/4A proteolytic activity requires the protease domain and its NS4A cofactor but does not require the NS3 helicase domain.

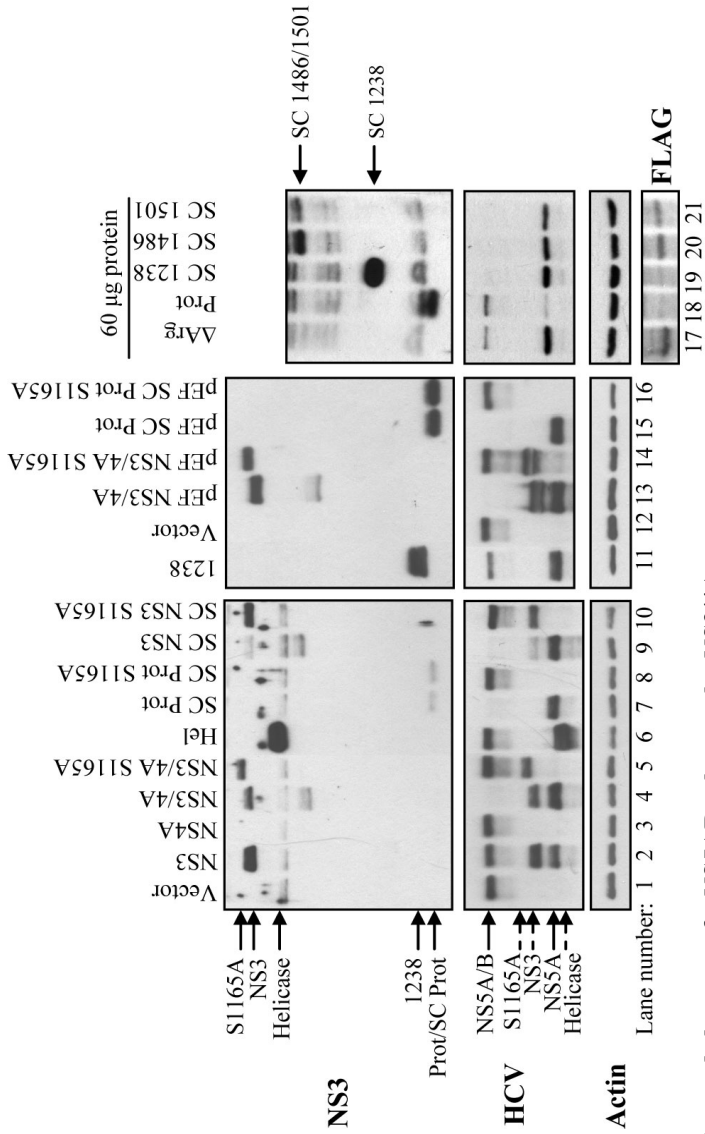


Figure 3-3: Expression and cleavage of a NS5AB substrate by NS3/4A constructs.

Huh7 cells were co-transfected with vector or a NS5AB polyprotein construct and the NS3 expression construct indicated above each lane. Twenty-four hours later, cells were collected and immunoblot analysis was performed. Unless indicated, constructs were expressed from the pFLAG-CMV2 vector. Blots were probed with antibodies against NS3 (*upper panel*), HCV (immune patient serum; *middle panel*), FLAG (M2) (*far right lower panel*) or actin as indicated. Since NS3 ΔArg, Protease (Prot), SC 1238, SC 1486, and SC 1501 were expressed at low levels from the corresponding constructs, the far right panel set, showing a blot with higher input protein, was included to demonstrate protein expression (*lanes 17-21*). Arrows to the left mark the positions of NS3 proteins, NS5AB polyprotein, or the NS5A cleavage product. NS3, S1165A, and Helicase (Hel) proteins are shown in both upper and middle panels. The identical positions of the Protease and the SC Protease (SC Prot) are marked by a single arrow. Arrows at right indicate the nearly identical positions of SC 1486 and SC 1501 (*upper*), or mark the position of the SC 1238 construct (*lower*). These abbreviations for the NS3 constructs are similarly used in all subsequent figures.

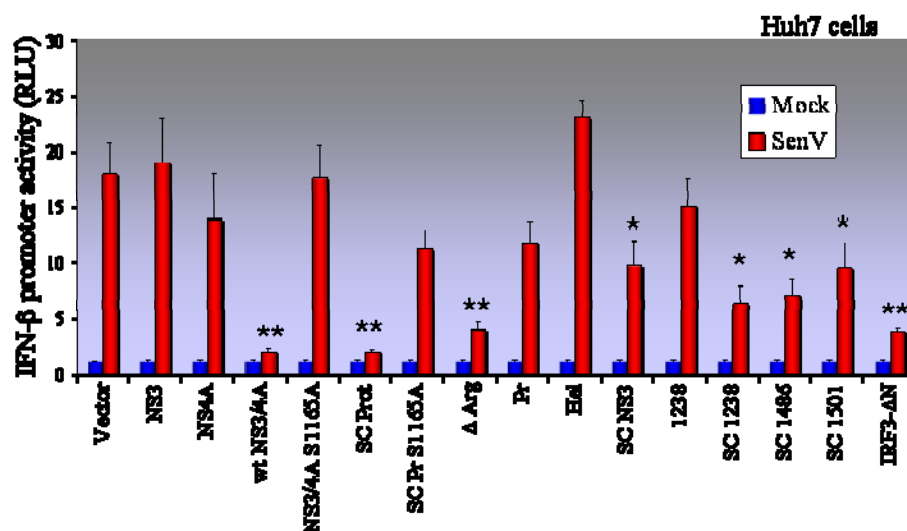


Figure 3-4: Fold activation of the IFN β -luc reporter in response to Sendai Virus (SenV) infection as compared to mock infection. Huh7 cells were co-transfected with the indicated NS3/4A mutant, CMV-*Renilla*, and IFN β -luc (containing an IRF-3 dependent promoter element) plasmids for 24 hours. Cells were then mock treated (blue bars) or infected with SenV (red bars), and infection allowed to proceed for 18 hours. Luciferase assay was performed, and results normalized to *Renilla* values and mock-infection. Bars show the mean relative luciferase units and standard deviation. Differences between SenV-infected treatments were subjected to unpaired *t*-test. Single asterisks indicate $P < 0.02$; double asterisks indicate $P \leq 0.001$.

The helicase domain is dispensable for inhibition of innate defense signaling.

To determine the NS3 structural requirements for inhibition of host antiviral signaling, we evaluated each construct for its ability to regulate IFN- β promoter induction in response to Sendai virus (SenV) infection. It should be noted that SenV and HCV trigger the host response through similar mechanisms that are blocked by NS3/4A^{44,45,149}. Wt NS3/4A significantly suppressed SenV induction of IFN- β promoter activity comparable to a dominant-negative IRF-3 control construct (**Figure 3-4**, IRF3- Δ N). However, constructs lacking NS4A and/or the intact protease domain of NS3 failed to block signaling to the IFN- β promoter. Of note, the SC NS3 construct, similar to that

used in crystallization studies ¹⁷³, mediated a weaker albeit significant suppression of virus signaling to the IFN- β promoter. Further studies revealed that the SC NS3 protein did not localize to membrane-bound compartments (**Figure 3-5**), suggesting its decreased ability to block viral activation of the IFN- β promoter could be due to aberrant localization. Of note, the SC Protease and SC Protease S1165A localize to membranes despite lack of the putative NS4A membrane targeting motif, while the NS3/4A S1165A mutants did not, suggesting a conformation change brought about by NS4A cleavage from NS3 may be responsible for membrane targeting rather than NS4A itself.

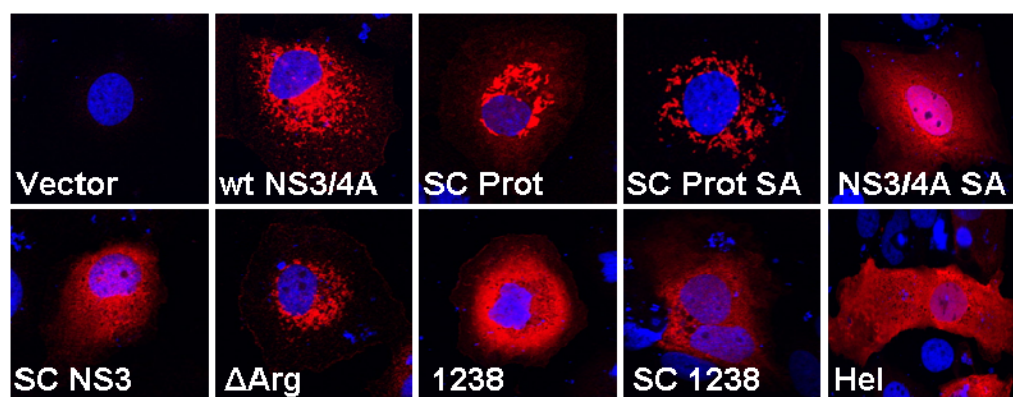


Figure 3-5: Localization of selected NS3/4A constructs. Huh7 cells were transfected with 200 ng of the indicated plasmids and collected 24 hours later for analysis by confocal microscopy. Red indicates NS3/4A mutant staining and blue is nuclear staining. Membrane localization of constructs is shown by the punctate staining pattern similar to wt NS3/4A. Diffuse staining indicates abnormal localization. Images were taken with a Zeiss Laser scanning confocal microscope and represent $\leq 7 \mu\text{m}$ sections.

We also assessed SenV-induced ISG expression in cells transfected with constructs encoding wt NS3/4A, NS3/4A S1165A, the SC Protease, or the SC Protease S1165A. As shown in **Figure 3-6**, using the highly-expressed pEF1 constructs, wt NS3/4A and the SC Protease suppressed ISG production, but ISGs were induced in cells

expressing the protease-deficient NS3/4A S1165A mutant. Interestingly, we see that with this higher expression level, the SC Protease active site mutant (SC Prot S1165A, lanes 9-10) blocked virus-mediated induction of ISGs, suggesting it is still able to target and block an essential effector function of IPS-1. Together these results indicate that the NS3 protease domain with its minimal NS4A cofactor is necessary for suppressing the host cell signaling of the IFN pathway.

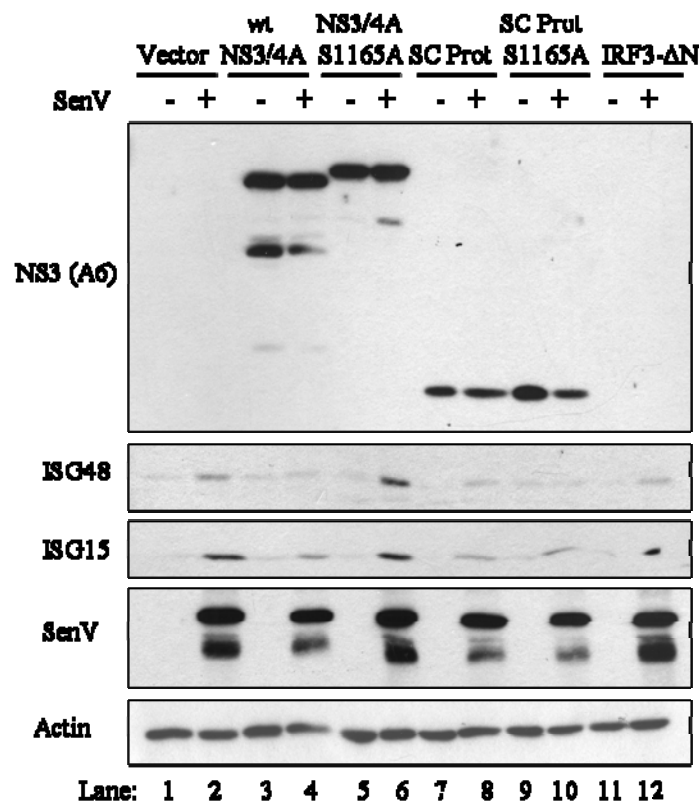


Figure 3-6: Effect of NS3/4A mutants on virus-induced ISG expression. Huh7 cells were transfected with 500ng of the indicated plasmid under control of the pEF promoter. Twenty-four hours later, cells were infected with SenV (+) or mock-infected (-) for 18 hours and samples collected for immunoblot analysis.

The functional NS3/4A protease domain inhibits signaling by RIG-I and MDA5.

NS3/4A suppresses RIG-I signaling of the host response⁴⁴. We verified that our wt NS3/4A construct could suppress RIG-I-enhanced virus signaling as well as constitutive signaling by ectopic N-RIG (encoding the CARDS alone) (**Figure 3-7A**). We then assessed regulation of RIG-I signaling to the IFN- β promoter by a subset of our NS3 constructs. As shown in **Fig. 3-7B**, the SC Protease and Δ Arg constructs suppressed N-RIG signaling of the IFN- β promoter to an extent similar to wt NS3/4A. Expression of NS3 alone, NS4A, NS3/4A S1165A, SC Protease S1165A, or the NS3 helicase domain had no significant effect on promoter activation. Moreover, when expressed in Huh7 cells, wt NS3/4A and the SC Protease suppressed the expression of the IRF-3 target genes, ISG56 and ISG15, but NS3/4A S1165A and the NS3 Protease domain failed to suppress IRF-3 target gene expression (**Fig. 3-8**).

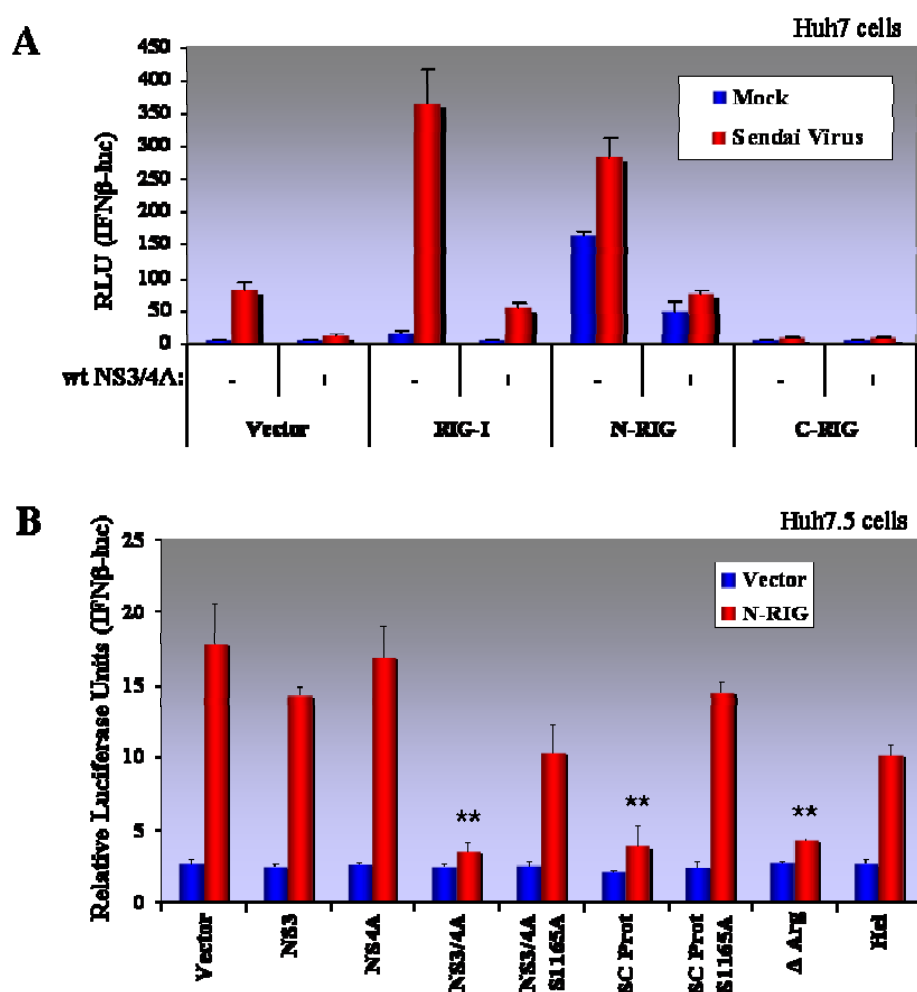


Figure 3-7: Effect of the NS3/4A protease on RIG-I signaling. **A.** Effect of NS3/4A on RIG-I, N-RIG, and C-RIG induction of the IFN- β promoter. Huh7 cells were co-transfected with 20ng of the indicated plasmid, 10 ng CMV-*Renilla*, 35 ng IFN β -luc, and 80 ng wt NS3/4A or pFLAG vector plasmid. Twenty-four hours later, cells were mock (blue bars) or Sendai virus (SenV; red bars) infected, harvested 20 hours later, and luciferase assay conducted. Luciferase results were normalized to *Renilla* values. Bars show the mean relative luciferase units and standard deviation. **B.** Effect of NS3/4A mutant constructs on N-RIG-mediated stimulation of the IFN- β promoter. Huh7.5 cells were transfected with CMV-*Renilla*, IFN β -luc, the pFLAG NS3/4A constructs shown, and vector (blue bars) or N-RIG (red bars), collected, and analyzed as in *A*. Standard deviation is indicated by error bars. Unpaired *t*-test was used to determine statistical significance of results. Asterisks indicate $P < 0.001$. Results are representative of at least three independent experiments.

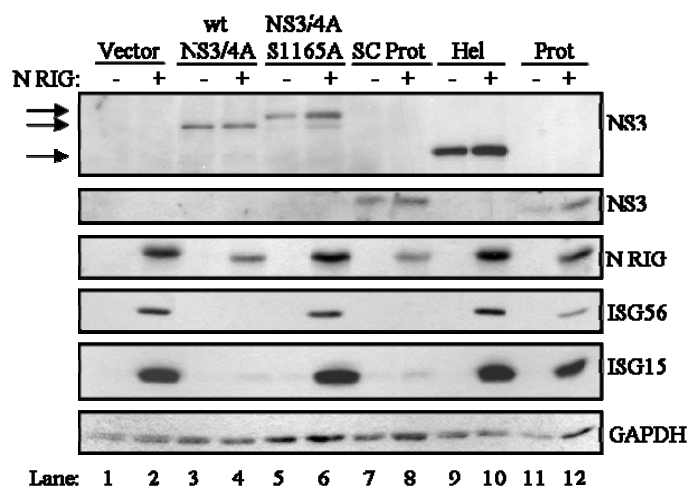


Figure 3-8: Immunoblot analysis of ISG production in response to N-RIG stimulation. Huh7 cells were co-transfected with 400 ng of NS3/4A mutants and 100 ng of vector (-) or N-RIG (+) and production of ISGs examined. Arrows mark the positions of NS3 proteins. Results represent three independent trials.

We also examined NS3 construct regulation of MDA5 signaling. In order to determine the effect of MDA5 regulation in the absence of RIG-I, we utilized Huh7.5 cells lacking RIG-I function¹⁴⁹. As shown in **Figure 3-9A**, Huh7.5 cells failed to activate the IFN- β promoter in response to SenV infection, but ectopic MDA5 complemented this defect. Moreover, we verified that our wt NS3/4A construct could suppress wt MDA5 or N-MDA5 (encoding the CARD domains) signaling to the IFN- β promoter in Huh7.5 cells. Here we can also observe the effect of the repressor domain on differences between RIG-I and MDA5 signaling. Whereas RIG-I did not constitutively activate the IFN- β promoter, MDA5 did (compare **Figures 3-7A and 3-9A**). These data were the first clues that MDA5 lacked a repressor domain¹³⁵.

To determine the minimal domain of NS3/4A necessary to block MDA5 signaling, we evaluated the ability of pEF constructs encoding wt NS3/4A (positive

control), NS3/4A S1165A (negative control), the SC Protease, the SC Protease S1165A, and the Protease domain to regulate signaling to the IFN- β promoter by N-MDA5 (**Figure 3-9B**). The SC Protease and high level expression of the SC Protease S1165A inhibited promoter activation to the same extent as wt NS3/4A and the IRF3- Δ N control, but neither the NS3 protease domain nor NS3/4A S1165A blocked promoter signaling. Additionally, wt pEF NS3/4A, pEF SC Protease, and pEF SC Protease S1165A suppressed ISG15 expression in response to ectopic N-MDA5 (**Figure 3-10**). Taken together, these results demonstrate that the SC Protease is sufficient to block signaling by both RIG-I (**Figures 3-7, 3-8**) and MDA5 (**Figures 3-9, 3-10**) in a process that requires the NS3 protease domain and its NS4A cofactor. The NS3 helicase domain, however, is dispensable for host response regulation.

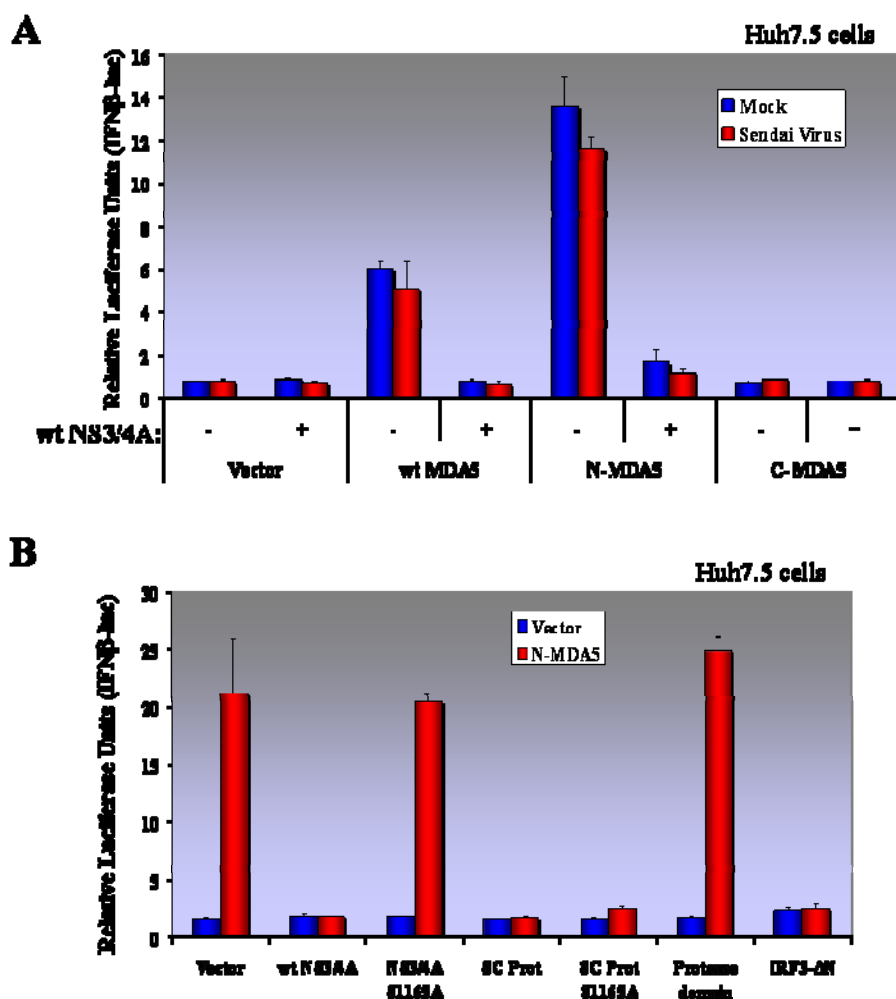


Figure 3-9: NS3/4A protease regulation of MDA5 signaling. **A.** Effect of NS3/4A on MDA5, N-MDA5, and C-MDA5 induction of the IFN- β promoter. Huh7.5 cells, lacking a functional RIG-I, were co-transfected with 20ng of the indicated MDA5 variant, 10ng CMV-*Renilla*, 35ng IFN β -luc, and 80ng wt NS3/4A or vector plasmid. The following day cells were mock (blue bars) or SenV (red bars) infected, harvested 20 hours later, and luciferase assay conducted. Luciferase results were normalized to *Renilla* values. Bars show the mean relative luciferase units and standard deviation. **B.** Effect of NS3/4A mutants on N-MDA5 stimulation of the IFN- β promoter. Seventy-five ng of each pEF-NS3/4A construct were co-transfected into Huh7.5 cells with 25ng vector (blue bars) or N-MDA5 (red bars), CMV-*Renilla*, and IFN β -luciferase plasmids. Cells were harvested 20 hours later and luciferase assay performed. Error bars indicate standard deviation. All data shown represent three experiments performed on different days.

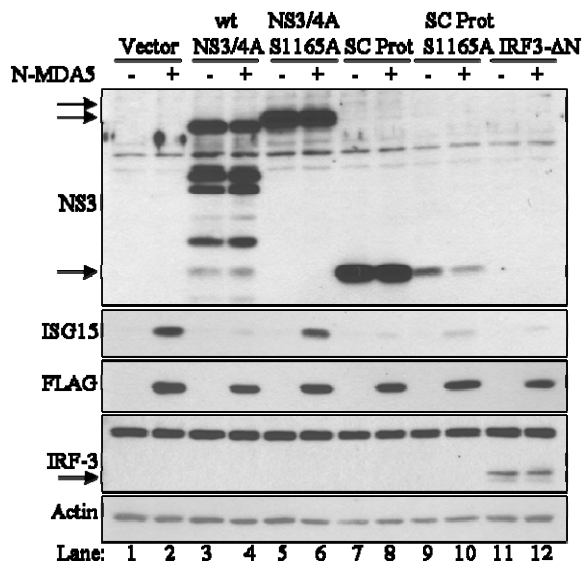


Figure 3-10: NS3/4A protease control of MDA5-induced ISG production. Immunoblot analysis of N-MDA5-induced IRF-3-dependent gene production. Huh7.5 cells were co-transfected with 400 ng of the indicated pEF-NS3/4A mutants and 100ng of vector (-) or N-MDA5 (+), collected 24 hours later, and immunoblot analysis was performed. Data representative of two independent experiments.

The SC Protease blocks activation of IRF-3 and exhibits a subcellular localization pattern similar to wt NS3/4A.

In order to verify that the SC Protease was sufficient for inhibition of IRF-3 activation, we examined IRF-3 and SC Protease distribution in transfected Huh7 cells. SenV infection of cells caused the redistribution of IRF-3 from the cytoplasm to the nucleus⁴⁵, consistent with its virus-induced activation, but this response was blocked in control cells expressing wt NS3/4A (**Figure 3-11**). Expression of the SC Protease also blocked IRF-3 activation, maintaining it in a cytoplasmic context during SenV infection. Notably, despite the lack of the putative amino-terminal membrane anchoring motif of NS4A¹⁶⁶, the SC Protease localized to a subcellular compartment similar to wt NS3/4A.

Thus, the NS3 protease domain and a minimal NS4A cofactor are sufficient to confer proper localization and inhibition of IRF-3 activation.

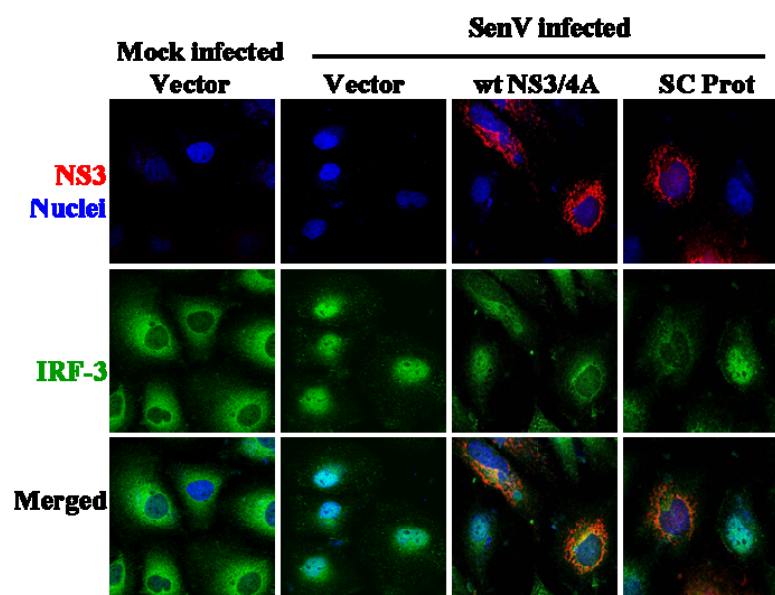


Figure 3-11: Effect of the NS3/4A protease domain on the subcellular distribution of IRF-3. Huh7 cells were transfected with 200 ng of the indicated NS3/4A construct for 24 hours followed by mock or SenV infection for 18 hours. Cells were then fixed, permeabilized, and stained with NS3 (NS3/4A) or FLAG (SC Prot; red), nuclei (blue), and IRF-3 (green). Images were taken using a Zeiss Laser scanning confocal microscope and analyzed using Zeiss LSM image software. Results are representative of three independent experiments.

Regulation of NF- κ B by NS3/4A.

RIG-I and MDA5 signal the parallel activation of IRF-3 and NF- κ B¹⁷⁴, and we sought to examine the effect of NS3/4A protease activity on regulation of NF- κ B function. We performed EMSA to measure NF- κ B binding to a target probe in nuclear extracts of cells treated with tumor necrosis factor- α (TNF- α ; positive control) or infected with SenV. TNF- α or SenV infection triggered NF- κ B binding (**Figure 3-12A**, lanes 1 and 5, respectively). Expression of NS3/4A (lane 11) but not NS3 alone (lane

17) blocked SenV-induced NF- κ B binding. The NS3/4A blockade of NF- κ B binding was relieved when cells were treated with SCH6 or ITMN-C peptidomimetic active site inhibitors of the NS3/4A protease (*lanes 13 and 15*, respectively). These results were verified by luciferase reporter assay, in which wt NS3/4A suppressed SenV induction of an NF- κ B-dependent PRDII-luciferase promoter and its enhancement by ectopic RIG-I or MDA5 (**Figure 3-12B**).

To determine the domain of NS3/4A necessary for this effect, HEK 293 cells were transiently transfected with the indicated NS3/4A construct followed by SenV infection (**Figure 3-13A**), or were cotransfected with a plasmid encoding constitutively active N-RIG to trigger PRDII promoter signaling (**Figure 3-13B**). The SC Protease inhibited activation of the PRDII promoter element in response to both SenV infection and ectopic N-RIG. Similar results were observed when the PRDII promoter element was stimulated by ectopic N-MDA5 (**Figure 3-21**). We also examined the influence of NS3/4A upon virus-induced phosphorylation of the NF- κ B inhibitor, I κ B α . As shown in **Figure 3-14**, SenV infection of HEK 293 cells induced the phosphorylation of I κ B α within 20 hours of infection, but expression of either wt NS3/4A or the SC Protease but not NS3/4A S1165A prevented virus-induced I κ B α phosphorylation (compare *lanes 2, 4, 8, and 6*, respectively). These results link HCV control of NF- κ B function with NS3/4A protease domain regulation of RIG-I and MDA5.

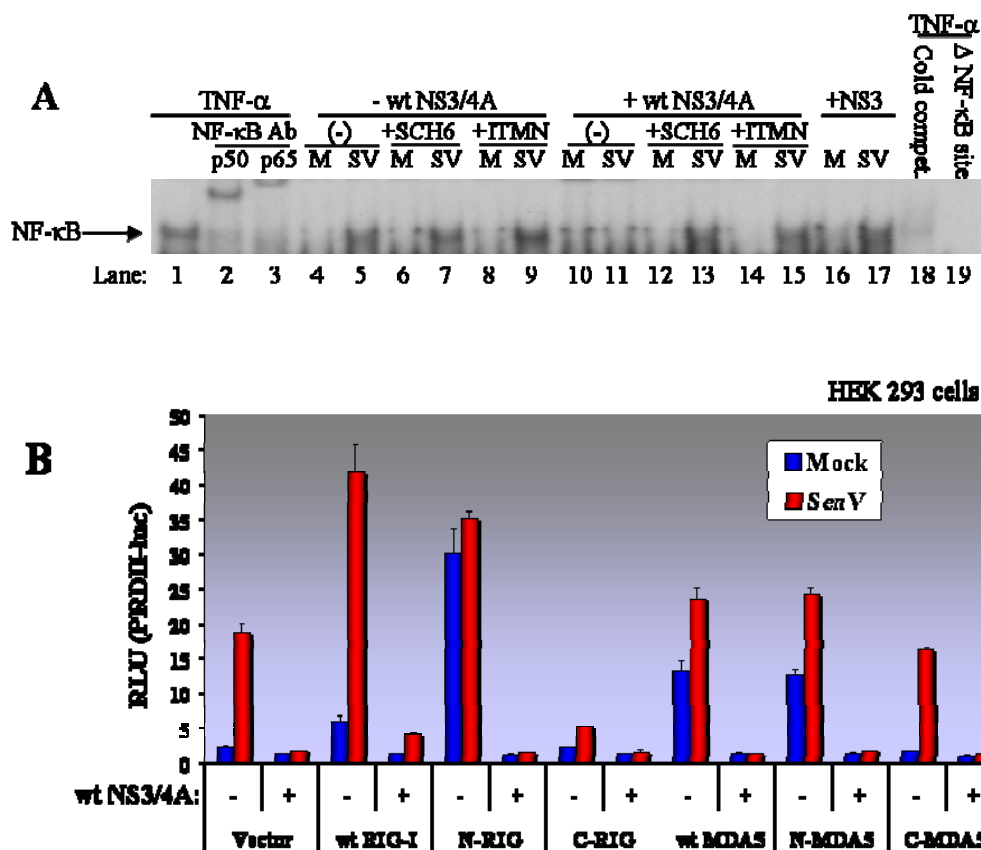


Figure 3-12: NS3/4A regulation of NF- κ B signaling. **A.** Effect of NS3/4A and protease inhibitor therapy on SenV-induced activation of NF- κ B. UNS3/4A and UNS3 cells were cultured to suppress (-NS3/4A) or induce NS3/4A (+ wt NS3/4A) or NS3 (+NS3) expression, alone or in the presence of 20 μ M SCH6 or 10 μ M ITMN-C, HCV NS3/4A peptidomimetic protease active site inhibitors. Twenty-four hours later, cells were either mock (M) or SenV (SV) infected for 18 hours, and nuclear fractions collected and analyzed by electrophoretic mobility shift assay (EMSA). As a positive control, cells were treated with 20 ng/mL TNF- α for 30 minutes. Antibody supershifts using antibodies to the p50 and p65 subunit of NF- κ B, incubation with cold competitor (*lane 18*), or mutated binding site control DNA probe (Δ NF- κ B site; *lane 19*) confirm the specificity of binding. **B.** Effect of NS3/4A on activation of an NF- κ B-dependent promoter element. HEK 293 cells were transfected with 25ng of a PRDII-luciferase reporter construct, 10ng CMV-*Renilla*, 80ng vector or NS3/4A wt, and 20ng of the constructs shown. The next day, cells were mock (blue bars) or SenV infected (red bars) for 20 hours, then collected and analyzed by luciferase assay. Bars show the mean relative luciferase units and standard deviation. Experiments were replicated twice.

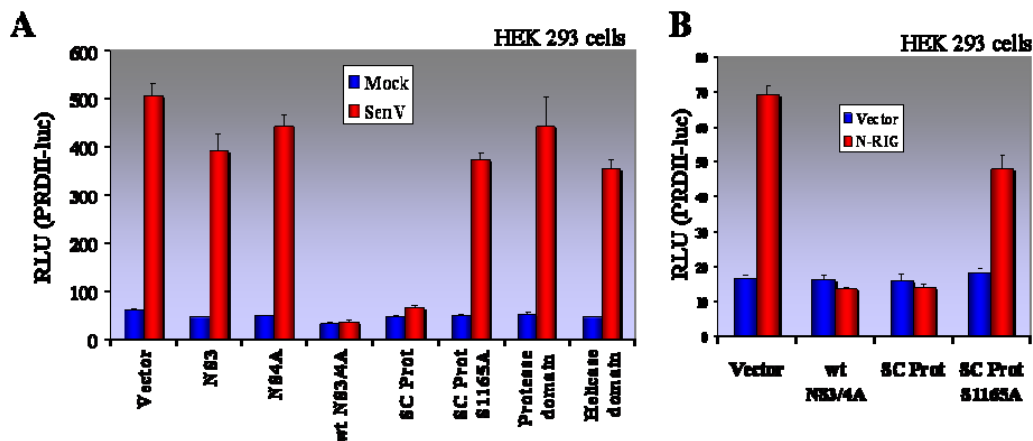


Figure 3-13: Effect of the SC Protease on SenV- and N-RIG-mediated activation of an NF- κ B-dependent promoter. HEK 293 cells were transfected with vector or the indicated pFLAG NS3/4A construct, PRDII-luciferase reporter, and CMV-*Renilla* for 24 hours followed by mock (blue bars) or SenV (red bars) infection for 20 hours (A), or co-transfection with vector (blue bars) or N-RIG (red bars) for 16 hours (B). Results were analyzed by luciferase assay. Bars denote mean relative luciferase units and standard deviation. Data shown represent three separate experiments.

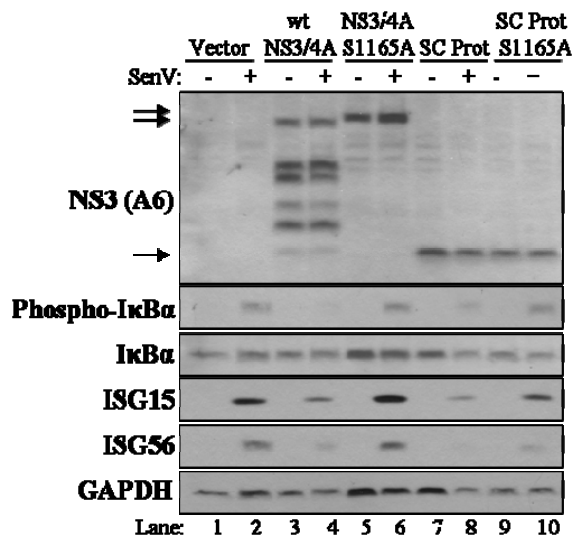


Figure 3-14: Effect of NS3/4A constructs on phosphorylation of I κ B α , the inhibitor of NF- κ B. HEK293 cells were transfected with 500ng of the indicated constructs for 24 hours, then infected with Sendai virus for 20 hours. Cell lysates were collected and analyzed by immunoblotting. Arrows indicate the positions of the various NS3 proteins. Results were repeated twice.

The protease domain of NS3/4A is sufficient to target and cleave IPS-1.

RIG-I and MDA5 signal IRF-3 and NF- κ B activation through the IPS-1 adaptor protein⁸⁰, which is targeted and cleaved by NS3/4A to inactivate signaling^{98,109}. To determine if the functional NS3/4A protease domain was sufficient to physically target and cleave IPS-1, we examined complex formation between IPS-1 and the SC Protease or a protease-defective derivative (**Figure 3-15A**, wt and SA, respectively) in transfected Huh7 cells. Immunoprecipitation studies revealed that the functional SC Protease and the SC Protease S1165A mutant each bound to IPS-1 (**Figure 3-15A lanes 2 and 3**). When compared to the SC Protease, we observed an apparent reduction in the amount of SC Protease S1165A mutant bound to IPS-1 in these experiments. While this could be due to protein expression or stability differences between the SC Protease constructs, it could also be explained by potential changes in the active site conformation caused by the serine to alanine switch, possibly resulting in decreased affinity for cleavage substrates. Importantly, the interaction between IPS-1 and the SC Protease was not disrupted by ITMN-C protease inhibitor treatment, and the SC Protease maintained an interaction with the cleaved form of IPS-1 (**Figure 3-15A, lanes 3 and 4**).

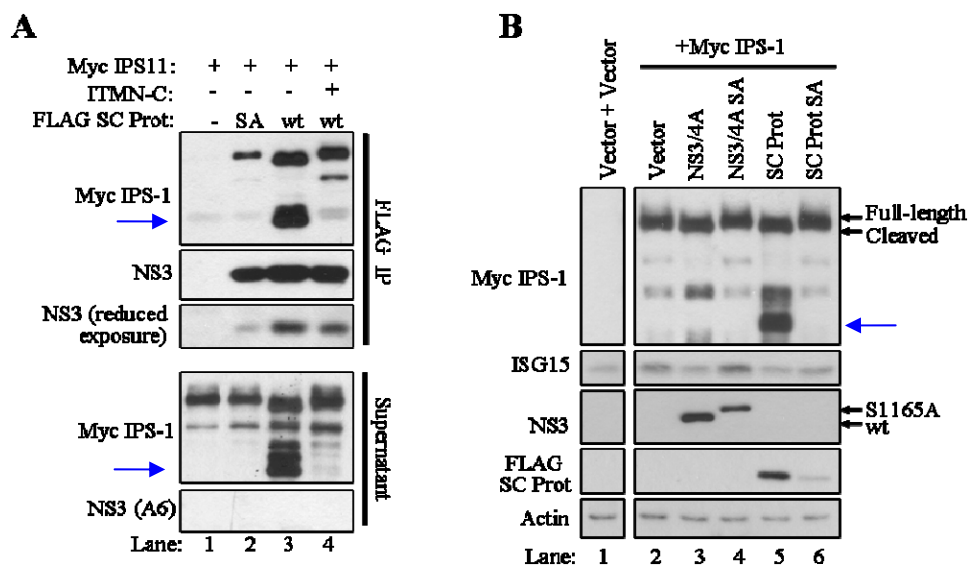


Figure 3-15: Targeting and cleavage of IPS-1 by the SC Protease. **A.** Co-immunoprecipitation analysis of the SC Protease and IPS-1. Huh7 cells were cotransfected with Myc-IPS1 and vector, FLAG-tagged SC Protease S1165A (SA), or wt SC Protease (wt) in the presence (+) or absence (-) of 1 μ M ITMN-C protease inhibitor for 24 hours. Cell lysates were collected and immunoprecipitated using FLAG-conjugated beads followed by immunoblot analysis of supernatant and pellet fractions. The cleaved form of IPS-1 is visible as a faster migrating species (*lane 3*). Reduced exposure of the NS3 panel demonstrates that a lower amount of the SC Protease S1165A mutant was expressed in the corresponding cells as compared to the SC Protease wt construct. **B.** Cleavage of overexpressed IPS-1 and inhibition of downstream signaling by the SC Protease. Huh7 cells were cotransfected with 125ng vector or Myc-IPS1 and 375ng of the pEF NS3/4A constructs indicated for 24 hours, cell lysates collected, and subjected to immunoblotting. The positions of full-length and cleaved forms of IPS-1, or S1165A and wild type forms of NS3, are indicated by black arrows. Blue arrows mark a secondary cleavage product.

Ectopic IPS-1 is a potent trigger of the host response⁸⁰, and we found that it upregulated endogenous ISG15 expression in Huh7 cells (**Figure 3-15B**). This reaction was blocked by pEF SC Protease, pEF SC Protease S1165A, and wt NS3/4A, concomitant with IPS-1 cleavage. Thus, the SC Protease is sufficient to target and cleave IPS-1. Of note, the SC Protease also appeared to cleave IPS-1 at a secondary site, which does not occur with the wt NS3/4A (**Figure 3-15B**, compare *lane 5* versus *3*, respectively).

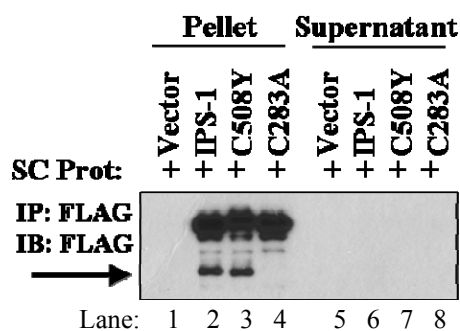


Figure 3-16: The SC Protease cleaves IPS-1 at cysteines 283 and 508. Huh7 cells were transfected with FLAG-tagged IPS-1 constructs shown and untagged SC Protease. Proteins were immunoprecipitated with FLAG bead, immunoblotted, and probed for FLAG. Arrow indicates second cleavage product that disappears with mutation of cysteine 283 to alanine.

In order to determine the secondary SC Protease cleavage location in IPS-1, we examined other possible sites of cleavage within IPS-1. One of those was located at cysteine 283, and when mutated to an alanine, IPS-1 is no longer cleaved at this accessory site by the SC Protease (**Figure 3-16**, compare *lanes 2* and *4*). This cleavage site, similar to the site at IPS-1 a.a. 508, differed from the consensus by one a.a. (**Figure 3-17**).

Cleavage		
↓		
NS3/4A	CMSADLEVVT	STWVLVGGVL
NS4A/B	YQEFDEMEEC	ASHLPYIEQG
NS4B/5A	WINEDCSTPC	SGSWLRDVWD
NS5A/B	EEASEDVVCC	SMSYTWGTAL
Consensus	DXXXXC	SXXX
	E T	A
Position	P6 P1	P1'
IPS-1 508	RKFQEREVOC	HRPSPGALWL
IPS-1 283	ESDQAEPIIC	SSGAEAPANS

Figure 3-17: NS3/4A consensus and IPS-1 cleavage sites. Shown are the a.a. sequences for NS3/4A cleavage sites within the HCV polyprotein and the consensus NS3/4A cleavage sequence. Note that the conserved P1 position contains cysteines (Cys) at all cleavage sites save the NS3-4A junction, which is the only site cleaved in *cis*, thus the Cys residue in the P1 position is required for all *trans*-cleavage events. Negatively charged residues (D, E) are conserved at the P6 position, while serine or alanine occurs at the P1' site as shown. NS3/4A cleaves IPS-1 after Cys 508, and SC Protease additionally cleaves IPS-1 between Cys 283 and Ser 284. Note that both IPS-1 cleavage sequences differ from the conserved sequence at one a.a. Modified from³².

We also found that the SC Protease suppressed IFN- β promoter induction by ectopic IPS-1 to the same extent as wt NS3/4A (**Figure 3-18A**). Further, the SC Protease blocked NF- κ B-dependent induction of the PRDII promoter element by ectopic IPS-1, but neither NS3 nor the protease or helicase domains affected promoter induction (**Figure 3-18B**). Thus, the targeted cleavage of IPS-1 by the NS3/4A protease domain inhibits downstream signaling to IRF-3 and NF- κ B.

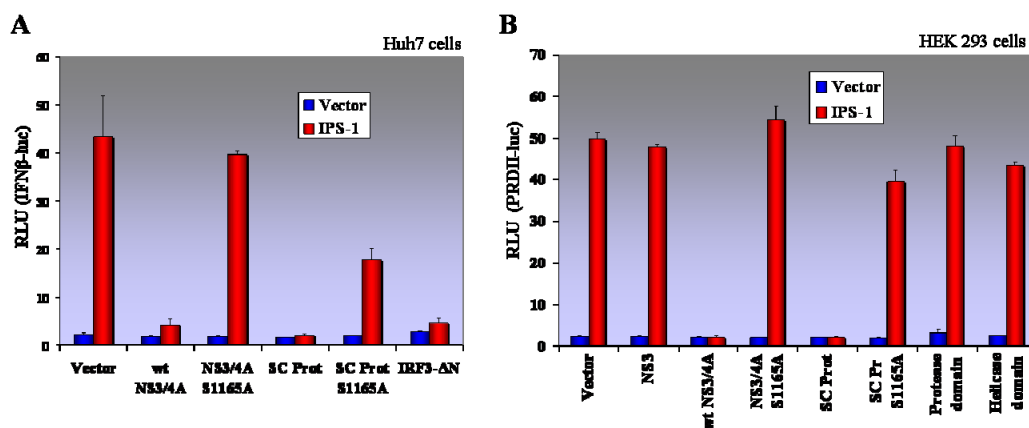


Figure 3-18: Inhibition of IPS-1 signaling by the SC Protease. Huh7 (A) or HEK 293 (B) cells were transfected with IFN- β -luc or PRDII-luc, respectively, plus CMV-*Renilla*, 80ng (A) or 95ng (B) of the NS3/4A mutants shown and 20ng (A) or 5ng (B) of vector (empty bars) or IPS-1 (black bars). Panel A includes cells transfected with dominant-negative IRF-3 (IRF3- Δ N) as a control. Cells were collected 20 hours later and luciferase reporter assay performed. Error bars indicate standard deviation.

However, the SC Protease SA was able to inhibit antiviral signaling promoted by SenV (Figure 3-6), N-MDA5 (Figures 3-9, 3-10), and IPS-1 (Figures 3-15B; 3-19), and furthermore this occurred without cleavage of IPS-1 (Figures 3-15B, 3-19). This might be due to high expression levels achieved with expression from the EF1 promoter. To further examine the blockade engendered by the pEF SC Protease S1165A construct, the pEF NS3/4A mutants, which express to much higher levels than the pFLAG NS3/4A constructs, were used to repeat previous experiments where the pFLAG SC Protease S1165A did not inhibit signaling (Figures 3-4, 3-13B). Figure 3-20A shows pEF SC Protease S1165A effectively blocking SenV-induced activation of the IFN- β promoter, and Figure 3-20B demonstrates that the pEF SC Protease S1165A construct was able to inhibit activation of a NF- κ B-dependent promoter by N-RIG. This verifies that

differences in SC Protease S1165A expression levels accounts for differences in its ability to inhibit host innate immune signaling.

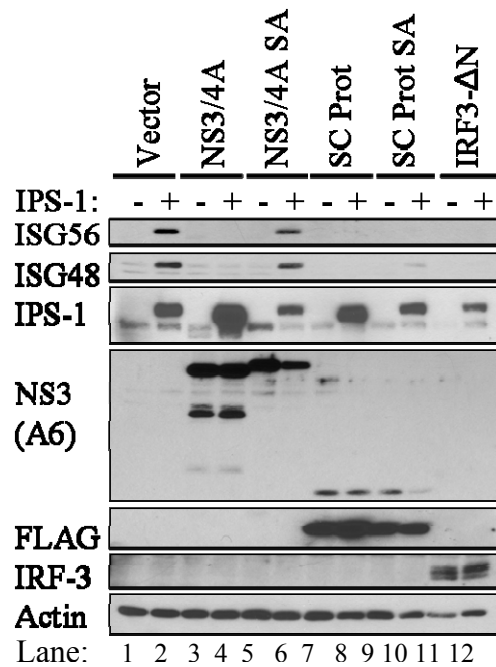


Figure 3-19: The SC Protease active site mutant effectively blocks ISG production by ectopic IPS-1. Huh7 cells were co-transfected with 375ng of the indicated pEF NS3/4A construct and 125ng vector (-) or IPS-1 (+) for 25 hours, collected, and subjected to immunoblotting. IPS-1 cleavage can be seen as a slight decrease in size (*lanes 4 and 8*). Results were repeated twice.

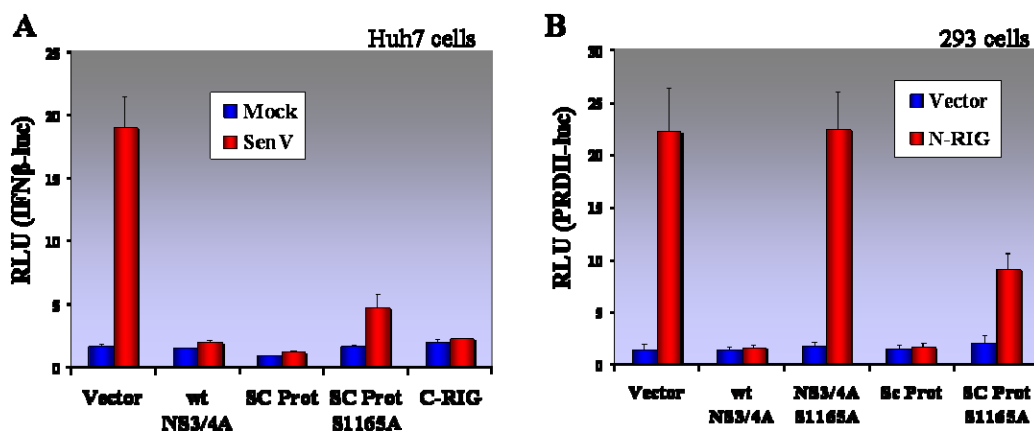


Figure 3-20: The SC Protease S1165A blocks SenV and N-RIG downstream signaling. **A.** Huh7 cells were transfected with 10ng CMV-*Renilla*, 30ng of IFN β -luc, and 100ng of the indicated pEF NS3/4A mutant. The following day, cells were mock treated (blue bars) or infected with 100 HAU/mL SenV (red bars) and collected for luciferase assay 20 hours later. **B.** HEK293 cells were transfected with 5ng CMV-*Renilla*, 30ng PRDII-luc, 25ng vector (blue bars) or N-RIG (red bars), and 75ng of pEF NS3/4A constructs as shown. Cells were collected for luciferase assay 20 hours later. Error bars represent standard deviation.

During the course of our investigations, we noticed differences in the degree of inhibition by the various NS3/4A mutants. Wt NS3/4A potentially ablated the pathways regardless of stimulus, whereas the SC Protease mediated weaker, but significant, inhibition when confronted with a strong stimulus (see **Figure 3-21A**). Furthermore, the SC Protease S1165A mutant was also able to abrogate antiviral signaling, but high expression levels were required. **Figure 3-21** shows one example. Both panels depict activation of an NF- κ B-dependent promoter by N-MDA5 in the presence or absence of various NS3/4A constructs. pFLAG mutants are used in panel **A**, whereas pEF mutants are used in panel **B**. Despite more N-MDA5 transfected and therefore higher levels of stimulus in panel **B**, we see that all three of the constructs mentioned above blocked signaling in panel **B**; however, in panel **A** only wt NS3/4A ablated the pathway to the same degree as if there was no stimulus [compare wt NS3/4A vector transfection (blue

bar) versus N-MDA5 transfected (red bar)]. This suggests that either NS3/4A is expressed to a higher degree than the other mutants, or that NS3/4A is more effective at inhibiting innate immune signaling than the synthetic SC Protease variants.

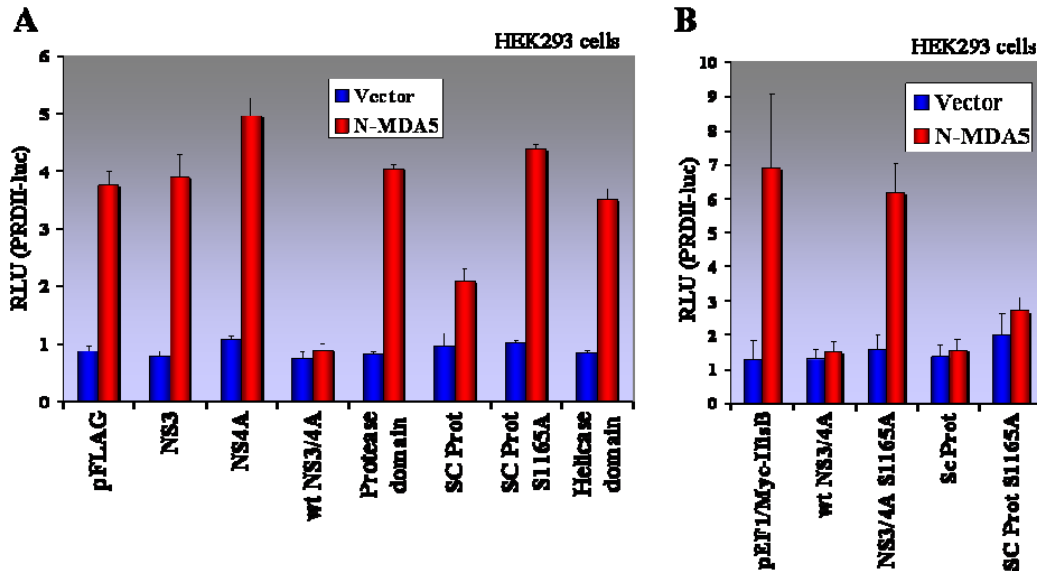


Figure 3-21: Effect of NS3/4A mutants on activation of an NF- κ B promoter element in response to N-MDA5 stimulation. **A.** HEK293 cells were transfected with 10ng CMV-*Renilla*, 35ng PRDII-luc, 80ng of the indicated pFLAG NS3/4A mutant plasmids, and 20ng vector (blue bars) or N-MDA5 (red bars). Cells were collected the following day for luciferase assay. **B.** Experiment was performed as in **A**, except using 75ng pEF-NS3/4A constructs and 25ng vector (blue bars) or N-MDA5 (red bars).

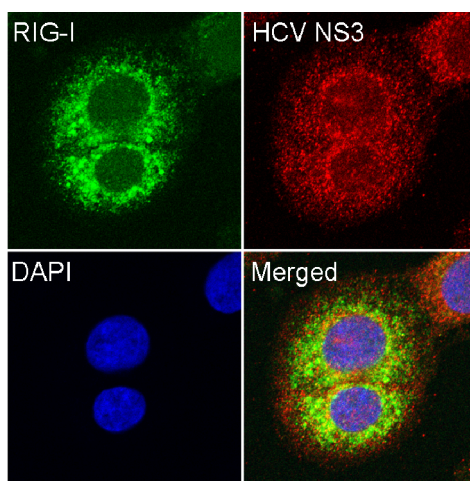


Figure 3-22: Colocalization of endogenous RIG-I and NS3/4A in SenV-infected HCV replicon cells. HP cells harboring a subgenomic HCV replicon were infected with SenV for 18 hours and stained for NS3 (red), endogenous RIG-I (green), and nuclei (DAPI, blue). Images were taken on a Zeiss laser scanning confocal microscope using Zeiss Pascal LSM software. The image shown is a ≥ 7 micron optical slice.

NS3/4A protease inhibitor treatment prevents cleavage and restores localization of IPS-1

NS3/4A distribution matched with RIG-I upon SenV infection in HP replicon cells (**Figure 3-22**), indicating that NS3/4A targets a virus-activated complex⁴⁴. To determine the influence of the NS3/4A protease and protease inhibitor treatment on IPS-1 localization and function, we examined the subcellular distribution of IPS-1 in the presence of NS3/4A alone and in the context of HCV RNA replication when cells were treated with ITMN-C. As shown in **Figure 3-23**, IPS-1 showed a characteristic thread-like appearance in the cell cytoplasm, consistent with its mitochondrial membrane localization⁹⁸. In the presence of NS3/4A, this localization was disrupted, and IPS-1 exhibited the diffuse cytoplasmic staining pattern previously described^{91,98}. However,

when the cells were exposed to the ITMN-C protease inhibitor for 24 hours, IPS-1 was restored to its proper localization in the presence of NS3/4A (**Figure 3-23**).

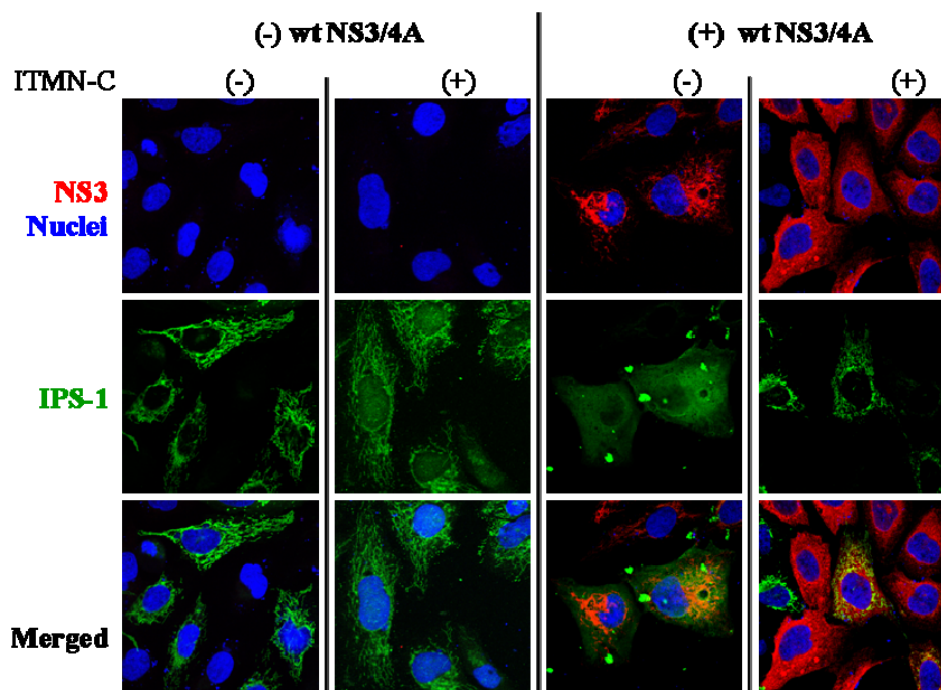


Figure 3-23: IPS-1 localization is disrupted by NS3/4A. UNS3/4A cells cultured to induce (+NS3/4A) or repress (-NS3/4A) NS3/4A expression were transfected with 200ng IPS-1 with (+) or without (-) 10 μ M ITMN-C protease inhibitor for 24 hours. Cells were then fixed and stained for IPS-1 (green), NS3 production (red), and nuclei (blue), and images from <0.7 μ m sections were collected using a Zeiss laser scanning confocal microscope.

We further examined this regulation in the context of HCV RNA replication in two cell lines harboring genetically distinct HCV replicons that are differentially resistant (HP replicon) and sensitive (K2040 replicon) to the antiviral actions of IFN therapy^{150,164}. In the presence of NS3/4A, IPS-1 membrane localization was disrupted, whereas K2040 cells with no visible NS3/4A staining typically retained a normal pattern of IPS-1 localization (**Figure 3-24**, *right panel*, mock treated). When the cells were treated with

ITMN-C, IPS-1 returned to a native distribution within a 24 hour time course even in the presence of NS3/4A (**Figure 3-24**, +ITMN-C). Moreover, during ITMN-C treatment the colocalization of NS3/4A with IPS-1 became apparent, suggesting they are initially present in the same subcellular milieu and that NS3/4A cleavage of IPS-1 disperses it from this environment (**Figures 3-23**, **3-24**).

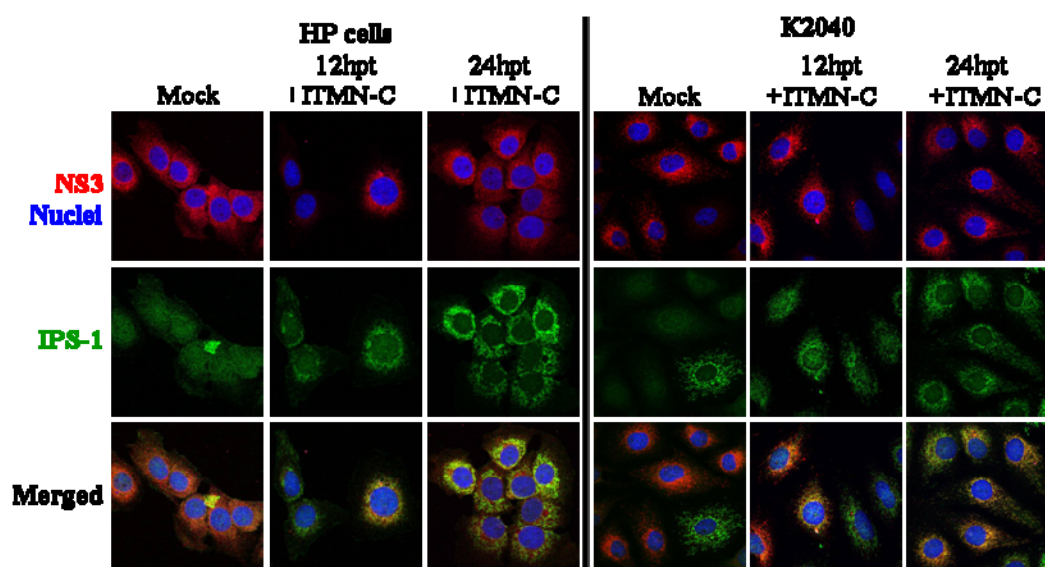


Figure 3-24: Effect of protease inhibitor treatment on subgenomic HCV replicon dispersion of IPS-1. Replicon cells resistant (HP) or sensitive (K2040) to IFN- α treatment were cultured in the presence or absence of 1 μ M ITMN-C protease inhibitor for 12 or 24 hours and processed for confocal microscopy as in *Figure 3-18*. Areas of IPS-1 and NS3/4A colocalization are shown by yellow staining. NS3 was undetectable in approximately 25% of K2040 cells, and these cells exhibited a normal IPS-1 mitochondrial distribution pattern. These data are representative of two independent experiments. Images represent <0.7 μ m sections and were collected using a Zeiss Laser Scanning confocal microscope.

ITMN-C restores the endogenous host response triggered by HCV RNA replication and HCV infection.

To study the effect of protease inhibitor treatment on IPS-1 and the host response to HCV, we examined ITMN-C treatment of Huh7 cells harboring a HCV 2a replicon or infected with the JFH1 strain of HCV 2a. Treatment of HCV 2a replicon cells resulted in alteration of endogenous IPS-1 from a predominantly cleaved form to its native, full-length form concomitant with induction of ISG56 expression over a 48 hour time course (**Figure 3-25A, B**). To verify these results in the context of an actual HCV infection, Huh7 cells were infected with JFH1¹⁶² at an MOI of 1 for 48 hours followed by 24, 36, or 48 hours ITMN-C treatment (**Figure 3-25C**). After 48 hours of HCV infection, endogenous IPS-1 levels were reduced with a large portion of the remaining protein present as the cleaved form, consistent with previously published data⁹⁸. Within 24 hours of ITMN-C treatment and throughout the time course, we observed a recovery of full-length IPS-1 levels with corresponding induction of ISG56 expression and reduction in viral protein abundance (**Figure 3-25C**).

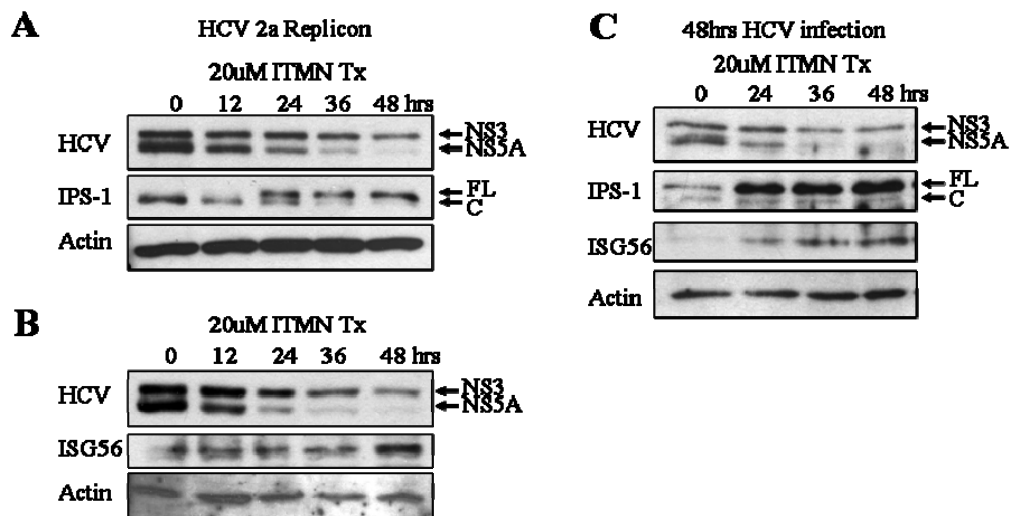


Figure 3-25: Characterization of NS3/4A protease inhibitor treatment on the host response to HCV. Huh7 cells harboring a HCV genotype 2a JFH replicon (A and B) or infected with HCV 2a (MOI=1.0) for 48 hours (C) were treated with 20 μM ITMN-C protease inhibitor for an additional 0, 12, 24, 36, or 48 hours as indicated. Cell lysates were collected and analyzed by immunoblot assay using HCV patient serum (HCV) or antibodies against IPS-1, ISG56, or actin as shown. The positions of NS3, NS5A, full-length IPS-1 (FL), and cleaved IPS-1 (C) are marked by arrows. Data courtesy of David Owen.

DISCUSSION

Our results show that the NS3 protease domain and minimal NS4A cofactor are sufficient to inhibit antiviral signaling through RIG-I and MDA5, and block activation of the downstream transcription factors IRF-3 and NF-κB. This is accomplished by protease domain targeting and cleavage of IPS-1. These data indicate that the NS3 helicase domain does not play a role in host response regulation and inactivation of IPS-1. Moreover, infection studies demonstrated for the first time that NS3/4A protease

inhibitor therapy of HCV infection can effectively remove the NS3/4A blockade to the host response, restoring RIG-I signaling to IPS-1 and activation of ISG expression in infected cells.

The protease domain of NS3 has been shown to mediate internal interactions with the carboxyl terminal helicase domain, in which the latter has been suggested to potentiate protease activity^{49,118,173}. We found that the helicase domain was dispensable for NS3/4A control of the host response and signaling by RIG-I and MDA5. That the helicase domain is not involved in host response control is further supported by the observations that the SC Protease, lacking the complete helicase domain of NS3, mediated binding and cleavage of IPS-1 similar to wt NS3/4A. Taken together, these results imply that the NS3 helicase domain does not play a role in directing NS3/4A interactions with IPS-1. Importantly, our results show that neither full-length NS3 nor the NS3 protease domain alone could block signaling by RIG-I or MDA5 when expressed in the absence of NS4A; however, NS4A does not regulate the host response. In contrast, each NS3 construct efficiently suppressed signaling when expressed as a SC construct with a.a. 21-32 of NS4A, encoding the NS4A central core region integral to NS3 protease activity³¹. Previous work has associated NS4A a.a. 2-19 with localizing NS3 to intracellular membranes¹⁶⁶. Despite lacking this domain of NS4A, our SC constructs effectively cleaved NS5AB and blocked host response signaling. Moreover, when expressed in Huh7 cells, the SC Protease construct demonstrated a subcellular distribution pattern equivalent to wt NS3/4A that similarly supported IPS-1 targeting. We conclude that while NS4A is required for full proteolytic action of NS3, localization and IPS-1 targeting by NS3/4A are controlled by residues located within the NS3

protease domain and/or the NS4A central core. The amino-terminal 21 a.a. of NS3 consist of several highly hydrophobic residues, and crystal structure analysis showed that this region extends away from the rest of the protease⁹⁹, suggesting it may be involved in membrane tethering. Additionally, a recent study demonstrated a mitochondrial membrane localization of NS4A in the context of HCV RNA replication¹¹⁹, implicating NS4A in directing NS3 to the mitochondria and site of interaction with IPS-1. These possibilities are presently being examined.

Intriguingly, the SC Protease active site mutant was able to target IPS-1 and block antiviral signaling without a cleavage event. This suggests that it may interact with a site on IPS-1 essential for downstream signaling, perhaps disrupting binding of an effector molecule or destabilizing a structural motif within IPS-1. Furthermore, we found that the SC Protease mediated cleavage of IPS-1 at two sites: cysteine 508 and a novel cysteine 283 site. Interaction with either of these two cleavage sites could potentiate the SC Protease S1165A signal blockade. It is important to note that wt NS3/4A does not cleave at cysteine 283⁹⁸, probably due to steric hindrance from the helicase domain. This brings into question the many studies that use a similar SC Protease construct for evaluating effectiveness of NS3/4A protease inhibitors, since the SC Protease clearly does not completely mimic wt NS3/4A actions.

It is interesting to speculate on the evolutionary advantage of encoding the essential viral protease and helicase in the same protein, while one of the β -strands necessary for full proteolytic activity of the viral protease is contained within an entirely different protein. During our studies we uncovered evidence that the artificial SC Protease construct, containing the minimal amino acids essential for complete proteolytic

activity, did not inhibit the host innate immune response pathways as well as wt NS3/4A. This is probably not due to a direct effect of the helicase domain, as the SC NS3 construct, containing the full-length NS3 protein, did not block as well as the SC Protease. More, we suspect one or more of three possibilities. Perhaps subtle changes in the conformation of the protease domain occur in the presence of the helicase and/or wt NS4A molecule, enabling it to more effectively target IPS-1. Crystallization studies on the full-length NS3 complexed with truncated NS4A have shown extensive interactions between the helicase and protease domains around the protease active site¹⁷³, and co-immunoprecipitation of NS4A with NS3 is impaired without the amino-terminal residues of NS4A. Alternatively, studies examining the stability of the SC Protease versus wt NS3/4A have suggested that the truncated proteins are significantly less stable than the wt protein complex³². Finally, another group found that the NS3 helicase domain bound directly to TBK1 and inhibited activation of IRF-3¹²¹. Therefore wt NS3/4A may act in other ways downstream of IPS-1 to block antiviral immunity.

We also found that the SC Protease could bind IPS-1 and that this interaction was maintained in the presence of the peptidomimetic protease active site inhibitor ITMN-C, which abrogated IPS-1 proteolysis. Under these conditions ITMN-C is expected to occupy the protease active site and catalytic residues¹¹⁷. Thus, the SC Protease may bind IPS-1 independently of substrate occupancy in the protease active site. This suggests a model in which NS3/4A may first interact with IPS-1 through protease domain residues outside the catalytic pocket, thereby positioning it for subsequent proteolysis. NS3/4A exhibits a shallow substrate binding cleft that might accommodate other protein substrates^{81,100,173}. Indeed, the TRIF adaptor protein has been identified as an *in vitro*

substrate of NS3/4A proteolysis⁹⁰. In this case residues within the 3/10 helix of NS3 located adjacent to the protease active site bind to a region of TRIF near the cleavage site⁴¹. This shared relationship between protein interaction and cleavage could indicate that NS3/4A may target and interact with TRIF and IPS-1 through similar processes. The mechanics of the NS3/4A-IPS-1 interaction are currently under investigation.

Our study demonstrates that NS3/4A proteolysis of IPS-1 blocks signaling by both RIG-I and MDA5, and ablates virus activation of downstream IRF-3 and NF- κ B, thus confirming that IPS-1 serves as the essential adaptor for RIG-I and MDA5 signaling. In the case of NF- κ B, we found that the NS3/4A or SC Protease blockade of NF- κ B activation was concomitant with suppression of I κ B- α phosphorylation, and that NF- κ B activation could be fully restored when cells were treated with a NS3/4A protease inhibitor. Thus, the RIG-I/MDA5 axis may signal NF- κ B activation through a canonical process of kinase phosphorylation of I κ B and unmasking of NF- κ B DNA-binding activity¹⁴⁵. Similar to the control of IRF-3 signaling^{44,45,98}, these processes of NF- κ B signaling are disrupted by IPS-1 proteolysis. As a signaling adaptor protein, IPS-1 may serve to recruit factors of IRF-3 and/or NF- κ B activation. This idea is supported by studies that have demonstrated IPS-1 interactions with various signaling components, including the IKK ϵ protein kinase⁹³, TRAF3¹³³, and FADD⁸⁰ into a complex with IPS-1. In the context of HCV infection, an IPS-1 signaling complex would possibly be disrupted through the targeted proteolysis of IPS-1 by NS3/4A to ablate a wide range of immune signaling action.

NS3/4A protease inhibitors are being developed for use as future HCV therapeutics¹⁵⁴ and our studies define a novel role for these compounds as immunomodulatory agents. NS3/4A cleavage of IPS-1 during HCV RNA replication and infection results in IPS-1 release from the mitochondrial membrane and diffuse redistribution throughout the cytoplasm with associated loss of host immune signaling⁹⁸. We found that ITMN-C treatment of cells harboring distinct HCV 1b replicons mediated a potent inhibition of NS3/4A, restoring the native distribution of endogenous IPS-1 as early as 12 hours after treatment, regardless of the differential sensitivities of each HCV replicon to IFN- α therapy^{150,164}. Moreover, protease inhibitor treatment of Huh7 cells harboring an HCV 2a replicon or infected with the HCV 2a JFH1 clone caused the accumulation of IPS-1 from a NS3/4A-cleaved form to a full-length form and related induction of ISG56 expression. These results indicate that 1) ITMN-C treatment and inhibition of NS3/4A protease function permits a rapid restoration of IPS-1 function, host response signaling, and immune action directly within HCV-infected cells; 2) endogenous HCV RNA is a potent trigger of RIG-I signaling in infected cells¹³⁵; and 3) RIG-I-responsive genes, including ISG56¹⁶⁴, may directly suppress HCV replication. We conclude that NS3/4A protease inhibitors possess immunomodulatory activity through prevention of IPS-1 proteolysis and restoration of RIG-I signaling.

CHAPTER FOUR

Localization and Membrane Targeting by NS3/4A

INTRODUCTION

NS4A

NS4A is a 54 a.a. protein that can be subdivided into three sections by hydrophobicity and secondary structure predictions (**Figure 4-1**). The first twenty and last twenty residues are predicted to form α -helices, while residues 21-34 form a β -strand that intercalates into the NS3 protease to activate full proteolytic processing (**Figure 4-2**). The amino-terminal 34 residues of NS4A are highly hydrophobic (**Figure 4-1**, bolded letters), while the remainder of the molecule is hydrophilic³². Residues 2-19 are hypothesized to form a membrane anchor that serves to hold the NS3/4A holocomplex within ER membranes, and were found to direct membrane targeting of a heterologous protein¹⁶⁶. NS4A is essential for cleavage at the NS3-4A junction, and NS3 complex formation with NS4A significantly increased the stability of NS3 in cell cultures^{8,32}.

NS3 Serine Protease

The NS3 serine protease domain comprises residues 1-180, with the catalytic triad residues at His 57, Asp 81, and Ser 139^{8,32}. Structurally, the serine protease contains two β -barrels with the protease active site sandwiched in between. The amino-terminal β -barrel, when complexed with the NS4A cofactor, consists of eight β -strands, while the carboxy-terminal β -barrel contains six (**Figure 4-2**). In the absence of NS4A the NS3 amino-terminus extends away from the rest of the molecule; however, NS4A

intercalation changes the conformation of this region, forming the β -strand A₀ and the α -helix α_0 ^{81,99}.

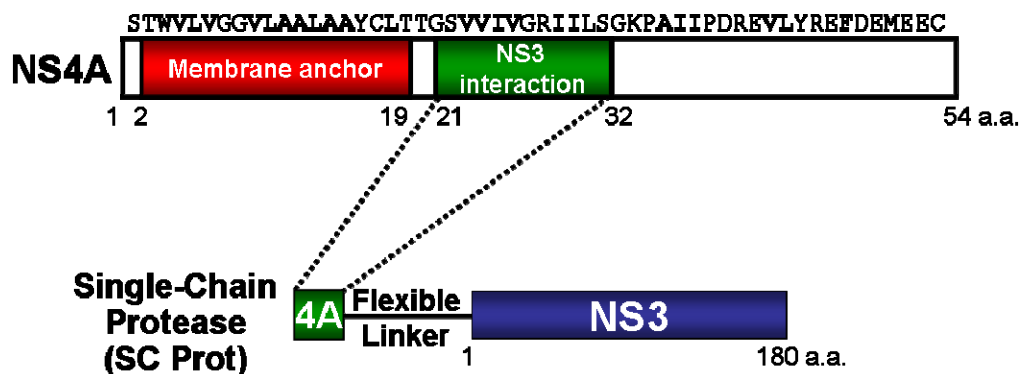


Figure 4-1: Schematic of NS4A and the SC Protease. NS4A contains a putative amino-terminal membrane anchor followed by the β -strand which intercalates into the NS3 protease. The SC Protease contains the NS4A β -strand attached to the NS3 protease domain via a flexible linker. NS4A amino acid (a.a.) sequence is shown, with bolded letters representing hydrophobic residues. Numbers below the bars denote amino acid position.

Carboxy-terminal truncations of the protease domain ablated proteolytic activity; however, deletion of the amino-terminal 29 a.a. of NS3 resulted in greatly diminished, basal serine protease activity. Truncations beyond this point completely abrogated proteolytic processing (**Figure 4-3**)³². Deletion of the first 14 residues, encompassing the A₀ β -strand (**Figure 4-2**), yielded normal processing and activation by NS4A but slight impairment of complex formation¹⁵⁸. NS3 constructs lacking residues 15-22, corresponding to α -helix α_0 , lose the ability to be activated by NS4A and are less stable. The region from a.a. 22-29 was not found to be involved in either complex formation with NS4A or basal NS3 protease activity³².

The SC Protease contains the NS3 serine protease domain linked to the residues of NS4A (a.a, 21-32) that intercalate into the protease domain ³²; it lacks the putative NS4A membrane anchoring region (**Figure 4-1**) ¹⁶⁶, which would predict a diffuse cytoplasmic localization. Despite this fact, localization studies demonstrated that the SC Protease gathered on intracellular membranes, suggesting that residues within the NS3 protease domain or the NS4A intercalation region are responsible for targeting NS3 to membranes. These findings challenge the dogma that NS4A is responsible for NS3 membrane localization.

NS3/4A has been thought to associate with ER membranes almost exclusively ^{113,166}, where it interacts with the HCV replication complex ^{37,56,112}. Our studies have found significant colocalization of NS3/4A with mitochondrial membranes, where it targets and cleaves IPS-1, an adapter molecule intricately involved in innate immune signaling. The current study was aimed at determining the region(s) responsible for targeting NS3/4A to mitochondrial membranes.

EXPERIMENTAL PROCEDURES

Expression cloning and site-directed mutagenesis

Cloning from PCR products

NS4A was amplified using the primers indicated **Table 4-1** by PCR and cloned into the KpnI and AgeI sites of pEGFP-N1 and pdsRED-N1.

Table 4-1: Primers used for PCR

Construct name	Primer name	Primer sequence
NS4A EGFP/dsRED	NS4A KpnI start s	ACTGAC GGTACC ATG AGCACCTGGGTGCTG
	NS4A AgeI (no stop) as	ACTGAC ACCGGT AT GCACTCTCCATCTCATC

Primer subcloning

NS3 amino-terminal residues and NS4A regions were inserted into the pEGFP-N1 and pdsRED-N1 vectors in the KpnI and AgeI sites as follows. Equimolar amounts of sense and antisense primers with phosphorylated 5' ends (**Table 4-2**) were resuspended to 200uM in annealing buffer (10mM Tris pH 8.0, 50mM NaCl, 1mM EDTA), heated to 95°C, and allowed to gradually cool to RT (to maintain dsDNA structure). The pEGFP-N1 and pdsRED-N1 vectors were digested with KpnI and AgeI, followed by calf intestinal alkaline phosphatase (CIP; New England Biolabs) treatment as per manufacturer's protocol. Annealed primers were ligated into the CIP-treated vectors to create the desired carboxy-terminal fluorescently-tagged constructs. The same strategy was utilized to insert NS4A a.a. 21-32 with either an amino-terminal or carboxy-terminal FLAG-tag into the XbaI and Not I sites of the pEF1-Myc/HisB vector.

Table 4-2: Primers for direct subcloning

Construct	Primer name	Primer sequence
NS3 1-20 EGFP/dsRED	KpnI start NS3 1-20 AgeI S	*P C ATG GCGCCTATTACGGCCTACTCCCAACAGACG CGAGGCCTACTTGGCTGCATCATACTAGC AT A
	KpnI start NS3 1-20 AgeI AS	*P CCGGTAT GCTAGTGATGATGCAGCCAAGTAGGCCTCG CGTCTGTTGGGAGTAGGCCGTAATAGGCCG CAT GGTAC
NS3 11-20 EGFP/dsRED	KpnI start NS3 11-20 AgeI S	*P CATGCGAGGCCTACTTGGCTGCATCATACTAGC ATA
	KpnI start NS3 11-20 AgeI AS	*P CCGGT AT GCTAGTGATGATGCAGCCAAGTAGGCC TCG CAT GGTAC
NS3 1-10 EGFP/dsRED	KpnI start NS3 1-10 AgeI S	*P CATGGCGCCTATTACGGCCTACTCCCAACAGACG ATA
	KpnI start NS3 1-10 AgeI AS	*P CCGGT AT CGTCTGTTGGGAGTAGGCCGTAATAGG CGC CAT GGTAC
NS4A 1-20 EGFP/dsRED	KpnI Start NS4A 1- 20 AgeI S	*P C ATG AGCACCTGGGTGCTGGTAGGCGGAGTCCTA GCAGCTCTGGCCGCGTATTGCCTGACAACA AT A
	KpnI Start NS4A 1- 20 AgeI AS	*P CCGGT AT TGTTGTCAGGCAATACGCGGCCAGAGCTGC TAGGACTCCGCTACCAGCACCCAGGTGCT CAT GGTAC
NS4A 21-32 EGFP/dsRED	KpnI Start NS4A 21- 32 AgeI S	*P C ATG GGCAGCGTGGTCATTGTGGGCAGGATCATCT TGTC AT A
	KpnI Start NS4A 21- 32 AgeI AS	*P CCGGT AT GGACAAGATGATCCTGCCCAATG ACCACGCTGCC CAT GGTAC
NS4A 33-54 EGFP/dsRED	KpnI Start NS4A 33- 54 AgeI S	*P C ATG GGAAAGCCGGCCATCATTCCCGACAGGGAAGTC CTTTACCGGGAGTTTCGATGAGATGGAAGAGTGC AT A
	KpnI Start NS4A 33- 54 AgeI AS	*P CCGGT AT GCACTCTCCATCTCATCGAACTCCCGGTA AAGGACTTCCCTGTCCGGAATGATGGCCGGCTTTCC CAT GGTAC
pEF-FLAG NS4A 21-32	NS4A Sense [NotI Flag HindIII NS4A XbaI]	*P GGC CGC ATG GACTACAAAGACGATGACGAC AAGCTT GGCAGCGTGGTCATTGTGGGCAGGATCATCTTGTCTTA GT
	NS4A AS [XbaI NS4A HindIII Flag NotI]	*P CT AGA CTA GGACAAGATGATCCTGCCCAATGAC CACGCTGCCAAGCTT GTCGTCATCGTCTTTGTAGTCCAT GC
pEF-NS4A 21- 32 FLAG [C- term]	NS4A C term Flag sense	*P GGCCGC ATG GGCAGCGTGGTCATTGTGGGCAGGAT CATCTTGTCCGACTACAAAAGACGATGACGACAAGTAGT
	NS4A C term Flag AS	*P CTACTTGTGTCATCGTCTTTGTAGTC GGACAAGAT GATCCTGCCCAATGACCACGCTGCC CAT GC

*P denotes 5' phosphorylation

Site-directed mutagenesis

Amino-terminal NS3 truncation mutations (Δ 1-10, Δ 11-20, Δ 1-20) were constructed in the pEF-NS3/4A, pEF-NS3/4A S1165A, pEF-SC Protease, and pEF-SC Protease S1165A using QuickChange XL site-directed mutagenesis kit (Stratagene) as per manufacturer's protocol. Primer sequences for site-directed mutants are available in **Table 4-3**.

Transmission Electron Microscopy (TEM)

Huh7 cells were grown in 15 cm plates to confluency. Cells were briefly (<5 min) exposed to fixative (2.5% glutaraldehyde in 0.1M cacodylate), mixed in a 1:1 ratio with complete media, gently scraped from the plates, pelleted at low speed (<900xg), and immersed in fixative alone for several hours at 4°C. Cell pellets were embedded, stained with osmium tetroxide, sectioned, and added to formvar-coated grids by Tom Januszewski. Grids were viewed using the TEM2 Technai transmission electron microscope at the Molecular and Cellular Imaging Facility of the University of Texas Southwestern Medical Center.

Table 4-3: Site-directed mutagenesis primers

Construct	Primer name	Primer sequence
pEF1-NS3/4A R117A R118A	NS3/4A R117A R118A s	CGATGTCATTCCGGTG GCGGCG CGGGGCGAC AGCAGGG
	NS3/4A R117A R118A as	CCCTGCTGTCGCCCG GCGCGC CACCGGAAT GACATCG
pEF1-NS3/4A Q80L	NS3/4A D80L s	GTACACCAATGTGGAC CTG GACCTCGTCGGC TGGC
	NS3/4A D80L as	GCCAGCCGACGAGGTCC CAGG TCCACATTGGT GTAC
pEF1-NS3/4A R109K	NS3/4A R109K s	CCTTTACTTGGTCACG AAG CATGCCGATGTCA TTC
	NS3/4A R109K as	GAATGACATCGGCATG CTT CGTGACCAAGTA AAGG
pEF1-NS3/4A L106A	NS3/4A L106A s	CAGCTCGGACCTTAC GCG GTCACGAGGCAT GCCG
	NS3/4A L106A as	CGGCATGCCTCGTGAC CGC GTAAGGTCCGA GCTG
pEF1-NS3/4A D168A	NS3/4A D168A s	GTTGCGAAGGCGGT GCCTT TGTACCCGTCG AG
	NS3/4A D168A as	CTCGACGGGTACAA AGGC CACCGCCTTCGCA AC
pEF SC Protease Δ 1-10	Protease delta 1-10 s	TCCGGTAGTGGTAGTAAGCTT CGAGGCCTACTGGCTGCATC
	Protease delta 1-10 as	GATGCAGCCAAGTAGGCCTCG AAGCTTACTACCACTACCGGAC
pEF SC Protease Δ 1-20	Protease delta 1-20 s	G TCCGGTAGTGGTAGTAAGCTT CTCACAGGCCGGGACAGGAAC
	Protease delta 1-20 as	GTTCTGTCCCGCCTGTGAG AAGCTTACTACCACTACCGGAC
pEF NS3/4A Δ 1-10	WT delta 1-10 s	GAATTCTGCAGATAGCTTATG CGAGGCCTACTGGCTGCATC
	WT delta 1-10 as	GATGCAGCCAAGTAGGCCTCG CATAAGCTATCTGCAGAATTC
pEF NS3/4A Δ 1-20	WT delta 1-20 s	GAATTCTGCAGATAGCTTATG CTCACAGGCCGGGACAGG AAC
	WT delta 1-20 as	GTTCTGTCCCGCCTGTGAG CATAAGCTATCTGCAGAATTC
pEF1-NS3/4A & SC Prot Δ 11-20	Delta 11-20 S	CCTATTACGGCCTACTCCCAACAGACG CTCACAGGCCGGGACAGGAACCAGGTC
	Delta 11-20 AS	GACCTGGTTCTGTCCCGCCTGTGAG CGTCTGTTGGGAGTAGGCCGTAATAGG

RESULTS

NS4A is necessary for NS3-dependent inhibition of IRF-3 activation and for targeting NS3 to the mitochondrial membrane

Since the SC Protease, which lacks two-thirds of the NS4A sequence, was sufficient to inhibit activation of the innate antiviral response, we wanted to determine if NS4A was truly necessary for full-length NS3 to inhibit activation of these pathways. Therefore, UNS3/4A and UNS3 cells were grown under conditions to express NS3/4A and NS3, respectively, or suppress their expression, and infected with SenV for 18 hours. **Figure 4-4** shows that in the absence of NS4A expression, NS3 is unable to block virus-mediated nuclear translocation of IRF-3 (*right panel set*), while the NS3/4A holocomplex effectively blocks this response. These data suggest that NS4A-mediated activation of the NS3 protease is required to block immune recognition of viruses.

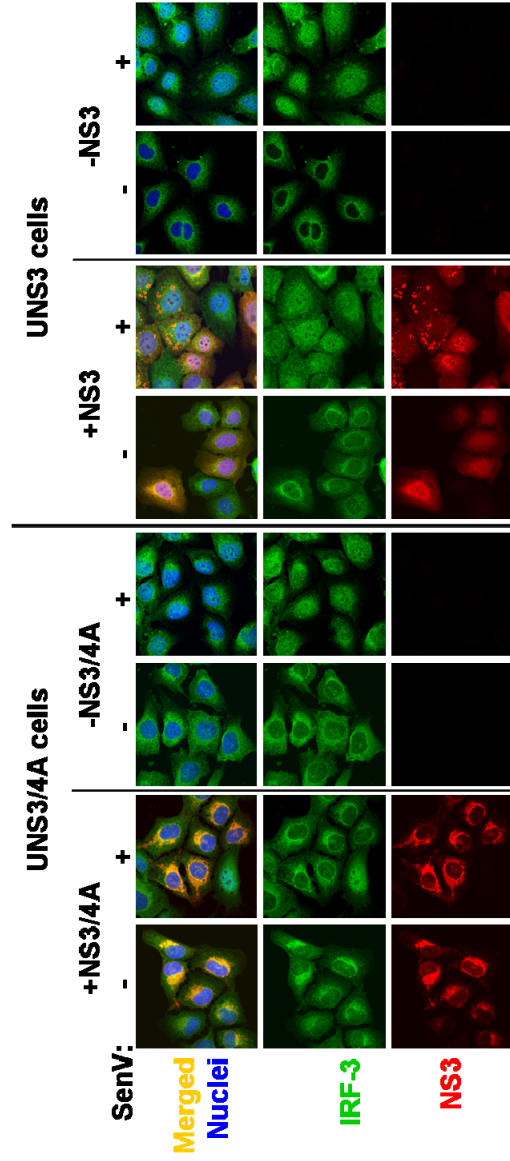


Figure 4-4: NS4A is required for NS3 to inhibit IRF-3 activation in response to virus infection. UNS3/4A and UNS3 cells were cultured to induce (+) or repress (-) expression of NS3/4A or NS3, respectively. The following day, cells were mock (- SenV) or infected with 100 HAU/mL SenV (+ SenV), collected 18 hours later, and processed for laser scanning confocal microscopy. Data were analyzed using Zeiss Pascal imaging software and are <0.7µm sections representative of three independent experiments.

The SC Protease construct localized to intracellular membranes (**Figures 3-5, 3-11**), a surprising discovery since this construct does not contain the amino-terminal membrane targeting region of NS4A (**Figure 4-1**)¹⁶⁶. Additionally, when treated with protease inhibitor, NS3/4A colocalized with IPS-1 (**Figures 3-22, 3-23**), a mitochondrial membrane protein¹⁴³, an unexpected result since NS3/4A was previously shown to be expressed exclusively on ER membranes¹⁶⁶. Therefore in order to determine if NS3/4A was targeted to mitochondrial membranes along with IPS-1, and if NS4A was indeed necessary for membrane targeting, human osteosarcoma cells expressing NS3 or NS3/4A were transfected with IPS-1 to activate the innate antiviral pathways, and stained for mitochondrial localization (**Figure 4-5**). NS3/4A, but not NS3, colocalized with mitochondria, and further co-distributed with IPS-1 when treated with the protease inhibitor ITMN-C. This indicates that NS3/4A exactly colocalizes to mitochondrial membranes and that full-length NS3 requires NS4A in order to be targeted to mitochondria. However, these results did not explain how the SC Protease localized to membranous structures in the cell.

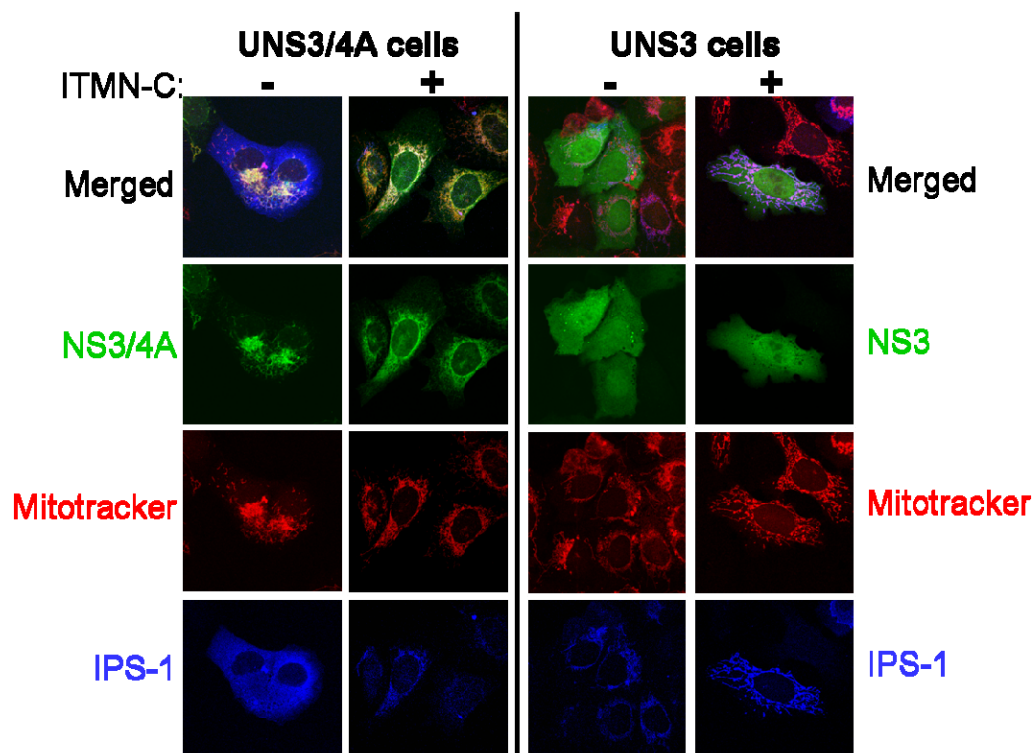


Figure 4-5: Colocalization of NS3/4A, mitochondria, and IPS-1 in cells treated with protease inhibitor. UNS3/4A and UNS3 cells were cultured to express NS3/4A or NS3, respectively. The next day cells were transfected with IPS-1 for 25 hours, then treated with **concentration** Mitotracker Red for 30 min at 37°C. Cells were processed for Zeiss laser scanning confocal microscopy and stained for NS3 or NS3/4A (green) and IPS-1 (blue). Images shown are <math><0.7\mu\text{m}</math> optical slices. Results were replicated in three independent trials.

The SC Protease colocalizes with IPS-1

To further examine SC Protease localization, Huh7 cells were transfected with the SC Protease or the SC Protease active site mutant and observed by confocal microscopy. The SC Protease cleaved IPS-1, dispersing it throughout the cytoplasm (**Figure 4-6**), but the SC Protease S1165A colocalized with IPS-1, indicating that it was targeted to mitochondrial membranes similar to wt NS3/4A, even without the NS4A membrane targeting motif.

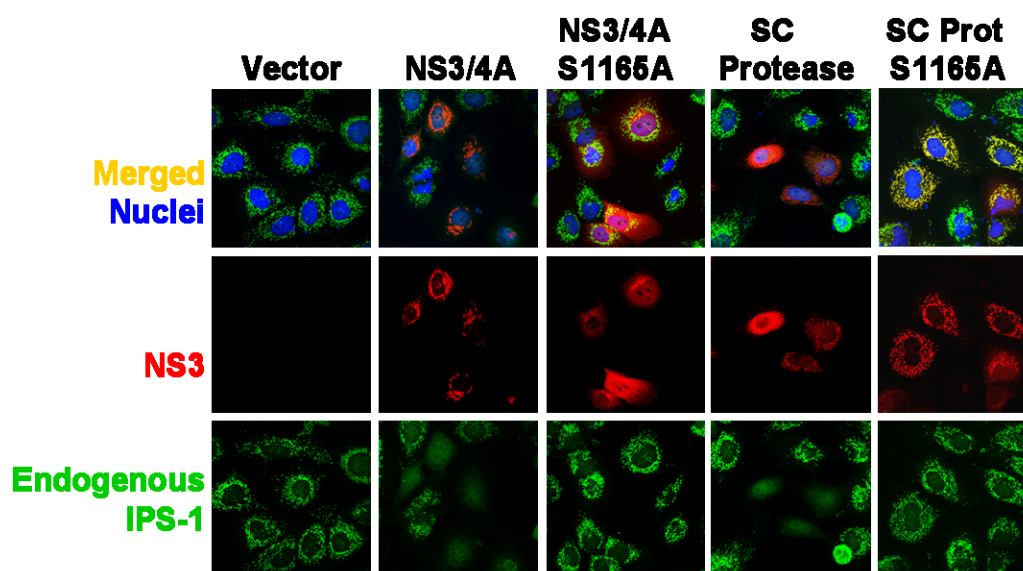


Figure 4-6: Effect of NS3/4A and the SC Protease on IPS-1 localization. Huh7 cells were transfected with 200ng of the indicated NS3/4A constructs, collected the following day, and analyzed by confocal microscopy for NS3 (red), endogenous IPS-1 (green), and nuclear (blue) staining. Images were taken with a Zeiss laser scanning microscope and represent less than 0.7 μ m sections. The experiment was replicated multiple times.

In order to verify that this result was not an artifact of the active site mutation, cells were transfected as before, and then additionally treated with ITMN-C, a peptidomimetic NS3/4A protease inhibitor. Protease inhibitor treatment prevented SC Protease cleavage of IPS-1, revealing their underlying colocalization. Taken together, these data suggest that residues within the NS3 protease domain or the central β -strand of NS4A are responsible for mitochondrial targeting of the SC Protease. Since crystal structure analysis of a similar SC Protease has shown that NS4A residues 21-32 are completely buried within the NS3 protease domain¹⁰⁵, it is unlikely that these residues are responsible for mitochondrial targeting.

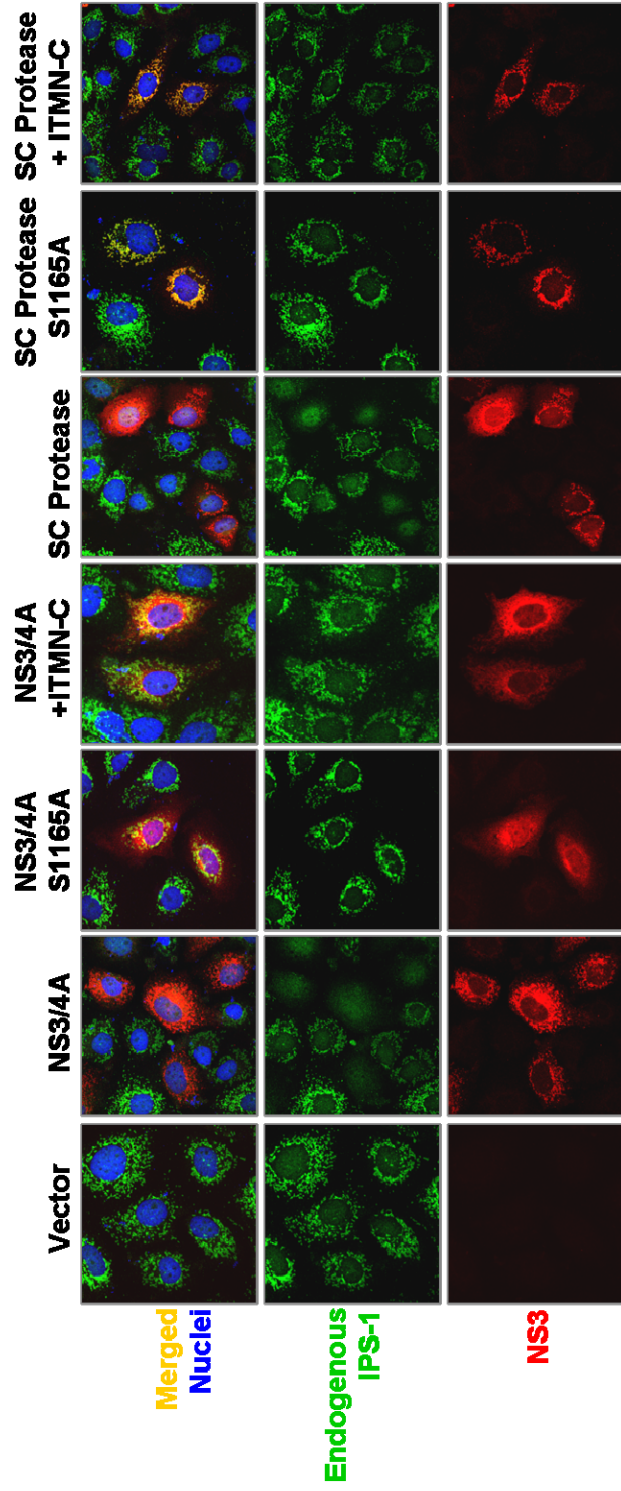


Figure 4-7: Effect of protease inhibitor treatment on localization of the SC Protease. Huh7 cells were treated with 1 μ M of ITMN-C and one hour later transfected with the indicated NS3/4A constructs. Cells were fixed 25 hours later, stained for NS3 (red), IPS-1 (green) and nuclei (blue), and observed on a Zeiss laser scanning confocal microscope. Images taken were <0.7 μ m optical slices and represent two independent experiments.

The amino-terminus of NS3 encodes a potential transmembrane motif

In order to determine if the NS3 protease domain contains a putative transmembrane domain, we analyzed the first 180 residues on the DAS transmembrane prediction server (**Figure 4-8**)²⁹. This program predicted a potential transmembrane motif between residues 13-21 of the NS3 protease domain. These residues are highly hydrophobic (**Figure 4-3**, bolded letters) and, upon crystallization with a synthetic NS4A peptide, form a surface exposed α -helix that sits atop the NS4A β -strand^{81,172}. Moreover, the structural equivalent of this region does not exist in any other member of the chymotrypsin family of serine proteases, suggesting a function removed from proteolytic activity. Additionally, the α_0 helix hydrophobic residues all faced outward, away from the protease core, creating a hydrophobic patch on the surface of the molecule that was speculated to have an accessory membrane attachment role, aiding NS4A in localizing to the ER¹⁷². However, the region immediately following the α_0 helix conforms to the consensus mitochondrial targeting motif of transmembrane domain (TM)- x_0-1 B x_0-6 B, where x is any amino acid and B refers to basic amino acids (usually arginine or lysine). As shown in **Figure 4-3**, residues 23-28, which have no previously identified function, contain two arginine residues (*underlined*) that fit the profile. Moreover, this pattern appears to be conserved among HCV genotypes 1-5, with a lysine replacing the second arginine in most sequences²¹. Therefore, these residues may be critical in mitochondrial targeting and membrane tethering of the SC Protease and wt NS3/4A.

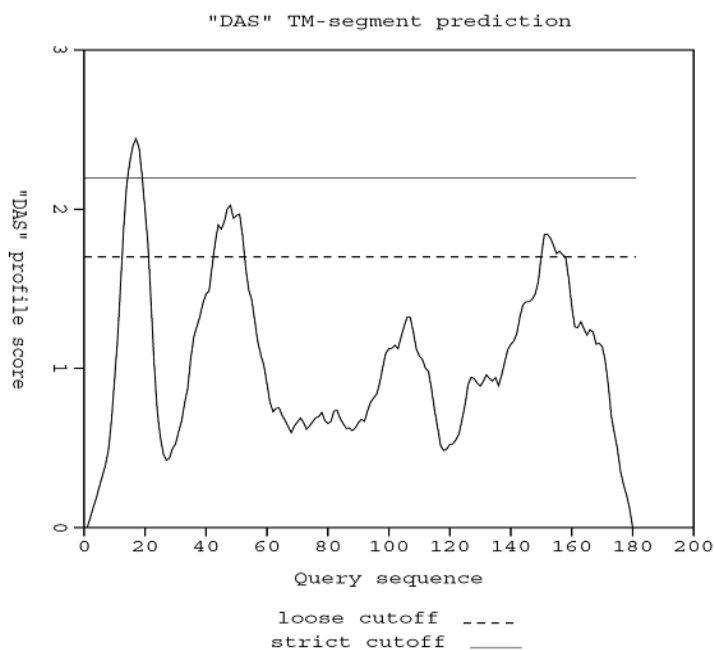


Figure 4-8: Hydrophobicity plot of the NS3 protease domain (a.a. 1-180). Hydrophobicity analysis of the NS3 serine protease (residues 1-180) was carried out using the DAS transmembrane domain prediction server at <http://www.sbc.su.se/~miklos/DAS/tmdas.cgi> according to the method outlined by Cserzo et al.²⁹. This predicted a potential transmembrane segment between a.a. 13-21 with high likelihood, and two others of lower probability between a.a. 43-52 and 150-157.

To examine the function of these residues, we created amino-terminal mutants of wt NS3/4A and the SC Protease lacking residues 1-10, 11-20, or 1-20 of NS3 and assessed their ability to ablate activation of an IRF-3-dependent promoter following SenV infection (**Figure 4-9**). Deletion of the first 10 amino acids had little if any effect on the ability of NS3/4A or the SC Protease to block activation of antiviral pathways. Truncation of the next ten amino acids (Δ 11-20 or Δ 1-20) of NS3 greatly reduced the ability of wt NS3/4A to inhibit IFN- β promoter induction, consistent with the previously described role of these residues in complex formation and activation by NS4A. This

suggested that the *cis* proteolytic activity of NS3/4A lacking amino acids 11-20 was compromised. Deletion of the amino-terminal twenty residues of the SC Protease had no appreciable effect on its ability to inhibit activation of an IFN- β -dependent promoter, suggesting these residues are not involved in *trans* protease activity of the SC Protease. Interestingly, amino-terminal truncation of the SC Protease SA ablated its ability to block IFN- β promoter activation by virus. Note that in **Figure 4-9**, the SC Protease SA did not have any effect on activation of the IFN- β promoter, as is typical with low-level expression of this construct (see **Figure 3-21** for further evidence of this observation).

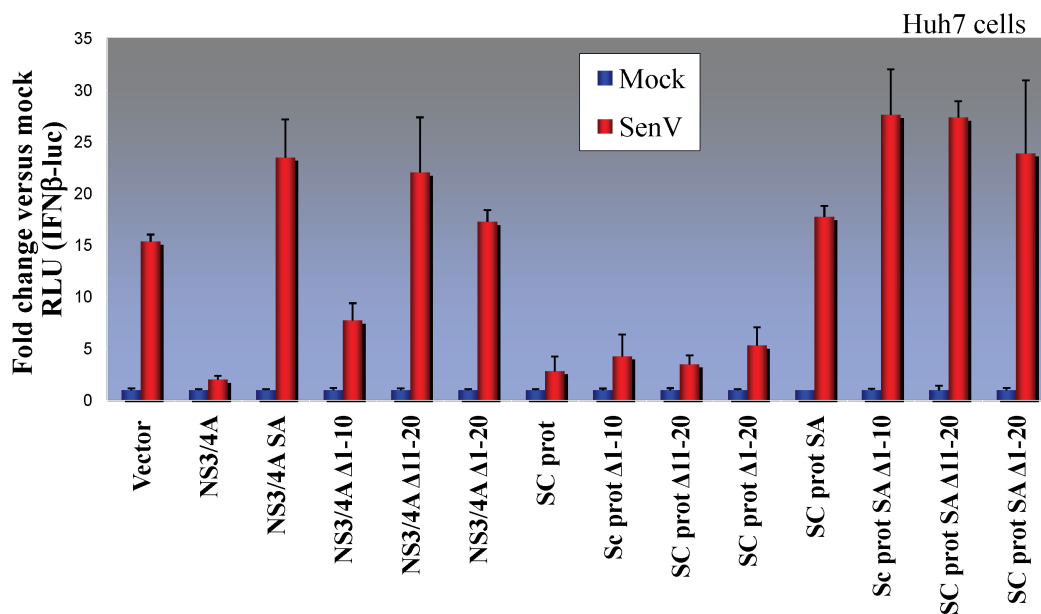


Figure 4-9: Effect of amino-terminal NS3 truncations on virus-mediated activation of the IFN- β promoter. Huh7 cells were transfected with IFN β -luc reporter, CMV-*Renilla*, and the indicated NS3/4A mutants for 24 hours, followed by mock treatment (blue bars) or infection with 100 HAU/mL SenV (red bars) for 20 hours. Cells were then collected and processed for luciferase reporter assay and analyzed relative to *Renilla* values and mock-infection. Results representative of three independent trials and are courtesy of Stacy Horner.

Confocal analysis of truncation mutant localization and cleavage of IPS-1 confirmed the above results (**Figure 4-10**). Amino-terminal NS3 truncation mutants exhibited impaired localization capability, indicating the importance of this region in membrane targeting. Deletion of the first 10 amino acids from NS3/4A had no effect on the ability of NS3/4A or the SC Protease to cleave IPS-1 and only minimal effect on mitochondrial localization. However, selective deletion of amino acids 11-20 ablated mitochondrial targeting of all mutants, while only slightly impairing the ability of the SC Protease to cleave IPS-1 and block signaling. NS3/4A Δ 11-20 and Δ 1-20 failed to remove IPS-1 from mitochondrial membranes, consistent with its inability to block viral activation of IRF-3, likely due to incorrect conformation of the protein or incomplete interaction with NS4A. These results are summarized in **Table 4-4**.

By comparing the SC Protease S1165A mutants, it becomes apparent that complete mitochondrial localization of the SC Protease SA is required for it to have any effect on signaling downstream of IPS-1, but this is not the case for the SC Protease. The differences between the SC Protease and wt NS3/4A suggests that impaired NS3/4A Δ 1-20 regulation of the innate immune response may be affecting its *cis* cleavage competence, and thence ability to cleave NS4A from NS3, a process essential for NS4A intercalation-dependent activation of protease activity. Since the SC Protease Δ 1-20 cleaves IPS-1, it may indicate: 1) that NS4A, when permanently attached to the amino-terminus of NS3, is still able to properly fold and intercalate into the NS3 protease domain; or 2) that cleavage of IPS-1 is, at least to some degree, NS4A-independent.

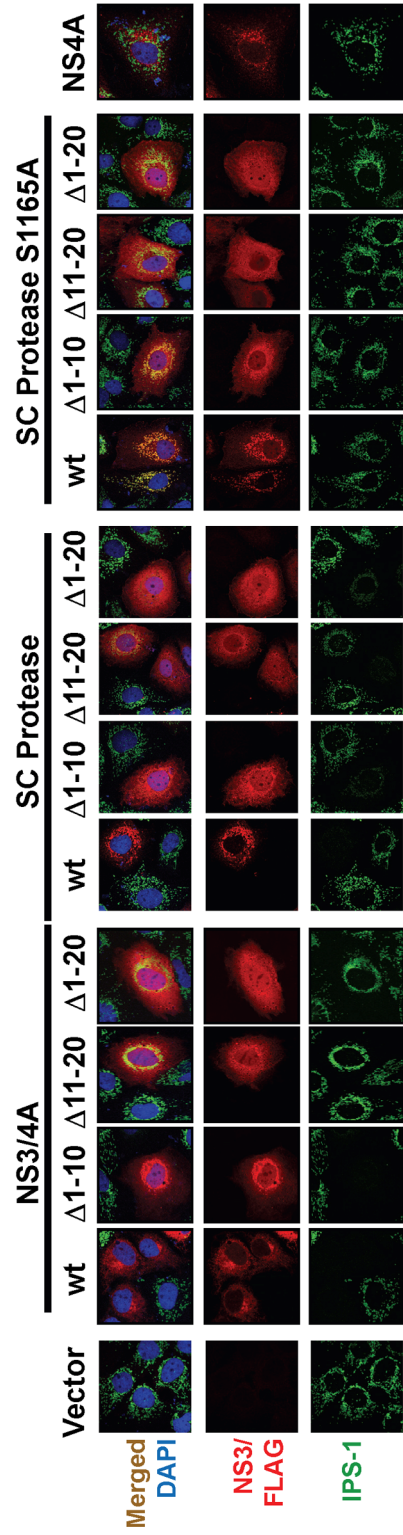


Figure 4-10: Effect of amino-terminal NS3 deletion mutants on localization and cleavage of IPS-1. Huh7 cells were transfected with the indicated constructs, fixed 24 hours later, and stained for NS3 or FLAG (red), IPS-1 (green), and nuclei (blue). Slides were examined using the Zeiss LSM confocal microscope and represent $<0.7\mu\text{M}$ sections. Data shown represent two experiments performed on different days.

Construct	<u>Blocks signaling (luciferase)</u>	<u>Mitochondrial localization (confocal)</u>	<u>IPS-1 cleavage (confocal)</u>
NS3/4A (WT)	+	+	+
WT Δ 1-10	+	-/+	+
WT Δ 11-20	-	-	-
WT Δ 1-20	-	-	-
SC Protease	+	+	+
SC Protease Δ 1-10	+	-/+	+
SC Protease Δ 11-20	+	-	-/+
SC Protease Δ 1-20	+	-	-/+
SC Protease S1165A	-/+	+	-
SC Protease S1165A Δ 1-10	-	-/+	-
SC Protease S1165A Δ 11-20	-	-	-
SC Protease S1165A Δ 1-20	-	-	-

Table 4-4: Summary of NS3/4A and SC Protease deletion construct activity.

Potential ER to mitochondria transport mechanism

Mitochondria-associated ER membranes (MAMs) consist of specialized regions of contact between the mitochondria and ER that direct the transient formation of membrane bridges to facilitate lipid and protein movement between the ER and mitochondria^{139,161}. To explain HCV core protein localization on mitochondrial and ER membranes, Schwer et al. proposed a model in which the core protein utilized these MAM bridges to transfer to the mitochondria¹³⁹. In order to determine if MAMs could form in human hepatocytes such that this sort of transport could occur, we performed TEM on human hepatoma cells (**Figure 4-11**). In Huh7 cells, the mitochondria lay in close apposition to rER, demonstrating that MAM formation could occur in hepatocytes.

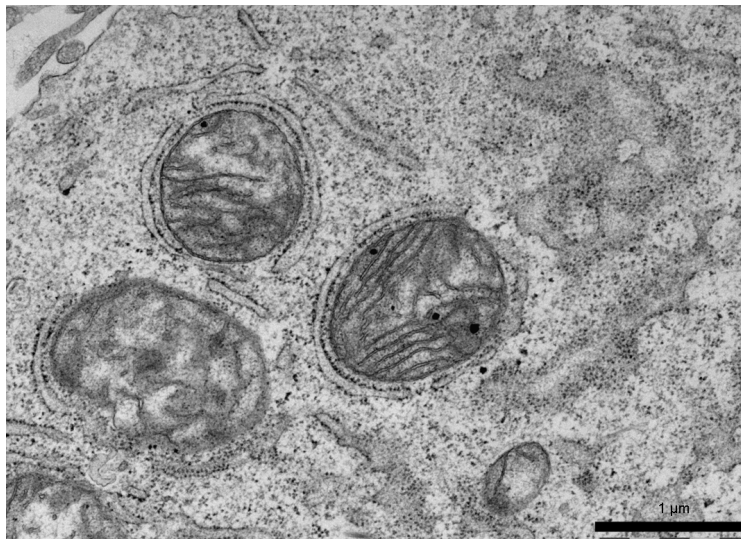


Figure 4-11: Electron micrograph of Huh7 cells. Huh7 human hepatoma cells were fixed, processed for TEM, and viewed using the TEM2 Technai electron microscope. Images were taken using a Gatan CCD camera. Depicted is typical mitochondria wrapped by rough ER. Smaller, highly-prevalent dots in the cytoplasm are polyribosomes. Bar is 1 μ m.

DISCUSSION

Our data show that HCV NS4A is necessary but not sufficient to target wt NS3 to mitochondrial membranes and inhibit activation of the innate immune response through cleavage of the adapter protein IPS-1. Previously, the amino-terminus of NS4A was proposed to serve as a transmembrane α -helix.^{166,172} However, NS4A alone does not localize to mitochondrial membranes. Moreover, its sequence does not contain any surrounding basic residues required for localizing proteins to mitochondrial membranes,⁷⁹ suggesting it most likely is not directly responsible for mitochondrial outer membrane targeting. Additionally, the SC Protease, containing only the minimal NS4A activator,

localized to mitochondrial membranes in the absence of the NS4A membrane anchoring region, suggesting other residues within the NS3 protease domain may contribute to mitochondrial accumulation and thereby affect regulation of host antiviral signaling pathways. Our data combined with NS3 crystalization studies^{81,99} suggests that NS4A imparts a conformation change the amino-terminus of the NS3 protease that allows formation of the mitochondrial membrane targeting helix.

Hydrophobicity analysis revealed a potential transmembrane domain hidden within the amino-terminus of the NS3 protease, and moreover, these residues contained a conserved mitochondrial signal sequence. Mutational analysis of this region (**Figures 4-9 and 4-10**) revealed that amino acids 11-20 of the NS3 protease were critical in determining mitochondrial membrane localization (as seen with the SC Protease mutants) and *cis* cleavage competence (as shown by the lack of correct localization of wt NS3/4A Δ 11-20), while only minimally effecting proteolytic processing of IPS-1 in *trans*. Interestingly, the SC Protease Δ 1-20 was still able to ablate innate immune signaling despite its diffuse, unrestricted localization. This likely represents cleavage by a small number of the SC Protease Δ 1-20 molecules interacting with IPS-1 randomly, without mitochondrial targeting. Since cleavage at NS4A-independent sites, such as NS5AB, are not affected by deletion of the first 20 residues of NS3³², it would be of interest to perform a protease assay on NS5AB as well as an NS4A-depedent cleavage site such as NS4AB to determine if it is possible to uncouple polyprotein processing from IPS-1 cleavage.

Two specific amino acid residues, Arg 24 and Arg 26, of the putative NS3/4A mitochondrial signal sequence at residues 23-28, are similar to conserved basic amino

acid residues critical in this motif. Future experiments could examine site-directed mutation of NS3 Arg 24 and Arg 26 to determine if these residues are responsible for specific targeting of NS3/4A to mitochondrial membranes. Alternatively, the putative signal sequence could be attached to a heterologous protein such as eGFP and localization of this protein determined.

The putative membrane-association domain is encoded within residues 13-21 and contains an α -helix found to have hydrophobic residues clustered on the side facing the surface, an unusual location for hydrophobic amino acids¹⁷². The surface hydrophobicity suggests a potential peripheral membrane association, rather than a transmembrane helix. To determine if the SC Protease localizes to mitochondrial membranes as a peripheral membrane protein, isolated mitochondrial fractions taken from cells expressing the SC Protease could be digested with proteinase K, which would remove outer membrane-associated proteins. Alkaline extraction experiments on mitochondrial fractions could then determine if it is an integral membrane protein or peripherally attached. While the combination of a putative membrane domain coupled with nearby mitochondrial signal sequence points to this region directly targeting NS3 to mitochondrial membranes, it is also possible that NS3 is interacting with another cellular factor that targets it to the mitochondria.

The majority of mitochondrial proteins are synthesized from nascent mRNA by ribosomes in the cytosol or attached to the mitochondrial surface¹⁴. This is likely the mechanism behind IPS-1 arrival at the mitochondrial outer membrane. However, the HCV replication complex is thought to sequester RNA within modified ER vesicles⁵⁶, bringing into question how a significant number of nascent transcripts could escape the

replication complex and still evade the host immune response. Additionally, the translation of the HCV genome as a single polyprotein further complicates the matter of specifically targeting NS3/4A to mitochondria. Bridging of the mitochondrial and ER membranes by the MAM complex could explain how NS3/4A translocates to mitochondrial membranes.

Based on these results, we modified the predicted domain structure of NS3 provided in Chapter Three to reflect this potential membrane targeting region (Figure 4-12).

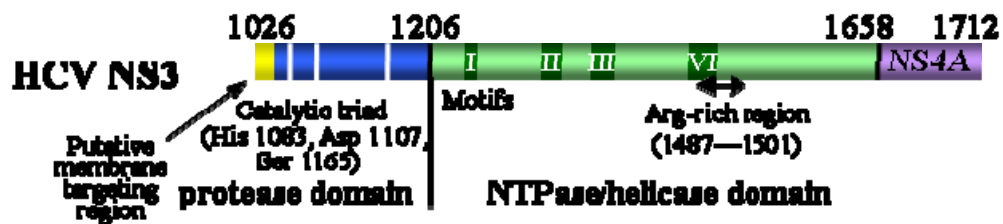


Figure 4-12: Structure of HCV NS3/4A including the putative membrane targeting region. The NS3/4A diagram introduced earlier was updated to include the putative membrane targeting domain (yellow).

CHAPTER FIVE
**Structure/Function Analysis of Interferon- β Promoter Stimulator-1, a Key
Modulator of Innate Antiviral Immunity**

INTRODUCTION

Viral dsRNA intermediates are recognized by RIG-I, promoting a conformation change that potentiates signaling by the RIG-I CARDs^{135,150} to the CARD-containing adaptor protein IPS-1⁷⁴. These CARD-CARD interactions facilitate recruitment of effector proteins that activate the latent cytoplasmic transcription factors IRF-3 and NF- κ B^{80,109,143,170}.

Structurally, the amino terminus of IPS-1 harbors a CARD (Figure 1), a proline-rich region of unknown significance, and multiple TRAF-interaction motifs (TIMs). The CARD alone is insufficient for induction of IFN- β in response to Sendai virus infection^{143,170}. The carboxy-terminal transmembrane (TM) motif (**Figure 5-1, upper panel**) anchors IPS-1 in the outer mitochondrial membrane. Deletion of the TM abrogated the ability of ectopic IPS-1 expression to induce the IFN- β promoter and prevented its localization to mitochondria¹⁴³.

Mutational analysis of IPS-1 has yielded conflicting data. One group indicated that the amino-terminal CARD was essential in signaling IRF3 and NF- κ B¹⁴³, while another reported that the carboxy-terminal one third of IPS-1 was able to activate both NF- κ B and the ISRE¹⁷⁰. A mutant lacking the CARD was found to exhibit a dominant-negative phenotype¹⁴³, suggesting oligomerization of IPS-1. Many other members of this pathway act as multimers, including RIG-I¹³⁵, IRF-3⁹⁴, NEMO⁴³, and the TRAFs⁸⁹,

suggesting a common activation motif. However, another group reported that IRF-3 and NF- κ B signaling by IPS-1 did not involve the oligomerization of IPS-1 ¹⁰⁹.

IPS-1 is a mitochondrial membrane protein and an essential adaptor of RIG-I signaling. A detailed structural analysis of IPS-1 has not been performed to elucidate the regions necessary for this activation of the host innate immune response. We conducted biochemical and molecular analysis of IPS-1 in a structure-function study that revealed distinct processes of IRF-3 and NF- κ B activation. Mutational analyses further identified amino acids of IPS-1 critical for mitochondrial localization, dimerization, and specific signaling domains that uncoupled IRF-3 and NF- κ B signaling.

EXPERIMENTAL PROCEDURES

Plasmids

pEFTak-IPS-1, pMyc-IPS-1, and pEFTak C283A were previously described ⁹⁸. pEFBos IPS-1 444-540, pEFBos IPS-1 1-443, and pEFBos IPS-1 C508Y were kind gifts from Takashi Fujita.

Expression Cloning and Site-directed Mutagenesis

Truncation mutations in IPS-1 (**Figure 5-1**) were made by designing primers containing the desired IPS-1 start/end site attached to the restriction sites NotI and BstEII sites for subcloning into pEFTak or the AgeI and PmeI sites for ligation into pcDNA Myc-His (**Table 5-1**). Vectors were digested with their respective enzymes, CIP treated (New England Biolabs) as per manufacturer's protocol. The pEFTak truncations were

cloned using the TA cloning kit (Invitrogen) according to the manufacturer's instructions, and then subcloned into the NotI and BstEII sites of pEFTak, yielding IPS-1 truncation mutants with amino-terminal FLAG tags. ExTaq polymerase (Takara) was used as per manufacturer's protocol to amplify IPS-1 residues 1-152, which then were directly digested with AgeI and PmeI. Both the digested insert PCR product and vector were then gel extracted using Qiagen's Qiaquick Gel Extraction Kit, eluted into 50 μ l dH₂O, and ligated into the AgeI and PmeI sites of pcDNA Myc-His, creating an amino-terminally myc-tagged IPS-1 1-152. Sequences were verified using Applied Biosystems Inc. (ABI) Big Dye Terminator 3.1 chemistry and ABI capillary instruments at the DNA Sequencing Core Facility in the UT Southwestern McDermott Center for Human Growth and Development.

Table 5-1: Primers for Expression Cloning of IPS-1

Construct	Primer name	Primer sequence
pcDNA Myc IPS-1 1-152	AgeI 1 S	CTCTA ACCGGT CCGTTTGCTGAAGACAAG
	152 stop PmeI as	CTATCG GTTTAAAC TA GGACTCTGGCGCCTGGGTCTCC
pEFTak IPS-1 1-153	NotI-ISP1 [s]	GCGGCCGCTCCGTTTGCTGAAGACAAGA
	IPS 153stop BstEII [as]	GGTCACCCTATGGGGACTCTGGCG
pEFTak IPS-1 1-261	NotI-ISP1 [s]	GCGGCCGCTCCGTTTGCTGAAGACAAGA
	IPS1(261)-BstEII [as]	GGTCACCCTACAAGCCAGGGGATGAGGA
pEFTak IPS-1 154-540	NotI IPS 154 [s]	GCGGCCGCTGGAGAGAATTCAGA
	ISP1-BstEII [as]	GGTGACCTAGTGCAGACGCCGCCGGTAC
pEFTak IPS-1 384-540	NotI-IPS1(384) [s]	GCGGCCGCTAGAAATGAGGAGACCCCA
	ISP1-BstEII [as]	GGTGACCTAGTGCAGACGCCGCCGGTAC
pEFTak IPS-1 468-540	NotI-IPS1(468) [s]	GCGGCCGCTATCCACGTGGCTGAG
	ISP1-BstEII [as]	GGTGACCTAGTGCAGACGCCGCCGGTAC

Site mutants and deletion constructs (**Figure 5-1**) were constructed using QuickChange XL site-directed mutagenesis kit (Stratagene) according to manufacturer's

instructions. Primers used are available in **Table 5-2**. The UT Southwestern Medical Center DNA sequencing core facility verified the DNA sequence of the resulting expression construct.

Cells

MEFs were cultured in complete DMEM supplemented with conditioned media from previous passages. IPS-1 wt and -/- MEFs were a kind gift of Dr. Shizuo Akira. MAVS wt and null MEFs were generously provided by Dr. Zhijian “James” Chen.

Statistical Analysis

Differences among multiple treatments were tested using one-way analysis of variance (ANOVA), and were considered statistically significant when $P < 0.05$ and marked with an asterisk. In cases where significant differences were detected, comparisons between treatment groups and vector control were examined using Dunnett’s multiple comparisons post-test; determinations of linear trend among means of different concentrations of the same treatment group were examined using the post-test for linear trends.

Table 5-2: Primers for site-directed and deletion mutagenesis of IPS-1

Construct name	Primer name	Primer sequence
pEFTak/ pcDNA Myc IPS-1 Δ461-512	IPS-1 delta 461-512s	GGCCCAGAGGAGAATGAGTAT CCTGGGGCTCTGTGGCTCCAG
	IPS-1 delta 461-512as	CTGGAGCCACAGAGC CCCAGG ATACTCATTCTCCTCTGGGCC
pEFTak/ pcDNA Myc IPS-1 Δ144-383	IPS-1 delta CT s	GAAGGAGCCAAGTTACCCCATGCCT AGAAATGAGGAGACCCCAGCAGCTC
	IPS-1 delta CT as	GAGCTGCTGGGGTCTCCTCATTTCT AGGCATGGGGTAACTTGGCTCCTC
pEFTak/ pcDNA Myc IPS-1 Δ383-500	IPS-1 delta 383-500 s	CAGTCCCCACTGACGGGAGCAGC TTCCAGGAGAGGGAGGTGCCATG
	IPS-1 delta 383-500 as	CATGGCACCTCCCTCTCCTGGAA GCTGCTCCCGTCAGTGGGGACTG
pcDNA Myc IPS-1 1-535	Delta C myc S	CACACTCCTGGTGGTGCTGTAC TAGGTTTAAACCCGCTGATCAG
	Delta C myc AS	CTGATCAGCGGGTTTAAACCTA GTACAGCACCCAGGAGTGTG
pEFTak IPS-1 1-535	Delta C FLAG S	GTCACACTCCTGGTGGTGCTGTAC TAGGTCACCCATTGCAACAAAAC
	Delta C FLAG AS	GTTTTGTTCGAATGGGTGACCTA GTACAGCACCCAGGAGTGTGAC
pEFTak/ pcDNA Myc IPS-1 ΔTM	Delta TM S	CCATGCCACAGGCCCTCA CGGGCGTCTGCACTAG
	Delta TM AS	CTAGTCAGACGCCGCCG TGAGGGCCTGTGGCATGG
pEFTak/ pcDNA Myc IPS-1 ΔCARD	Delta 10-77 S	CCGTTTGCTGAAGACAAGACCTAT GGCTGTGAGCTAGTTGATCTCG
	Delta 10-77 AS	CGCGAGATCAACTAGCTCACAGCC ATAGGTCTTGTCTTCAGCAAACGG
pEFTak/ pcDNA Myc IPS-1 Δ103-512	Delta 103-512 S	CCTCGGACCTCGGACCGT CCTGGGGCTCTGTGGCTC
	Delta 103-512 AS	GAGCCACAGAGCCCCAGG ACGGTCCGAGGTCCGAGG
pEFTak/ pcDNA Myc IPS-1 Δ444-467	Delta 444-467 S	GAGGATCTTGCCATCAGTGCC ATCCACGTGGCTGAGAACCCC
	Delta 444-467 AS	GGGGTCTCAGCCACGTGGAT GGCACTGATGGCAAGATCCTC
pEFTak/ pcDNA Myc IPS-1 Δ150-383	IPS1del(150-383)-fwd	CCTGTCCAGGAGACCCAGGC GAGAAATGAGGAGACCCCAGC
	IPS1del(150-383)-rev	GCTGGGGTCTCCTCATTTCTCG CCTGGGTCTCCTGGACAGG
pEFTak/ pcDNA Myc IPS-1 Δ150-467	IPS1del(150-467)-fwd	CCTGTCCAGGAGACCCAGGC GATCCACGTGGCTGAGAACC
	IPS1del(150-467)-rev	GGTCTCAGCCACGTGGATCG CCTGGGTCTCCTGGACAGG
pEFTak/ pcDNA Myc IPS-1 T54I	IPS1-T54I-fwd	CACTCTCAGGGAACCGGGACA TCCTCTGGCATCTCTTCAATACC
	IPS1-T54I-rev	GGGTATTGAAGAGATGCCAGAG GATGTCCCGTCCCTGAGAGTG
pEFTak/pcDNA Myc IPS-1 Δ103-467	IPS1del(103-467)-fwd	CAGCCTCGGACCTCGGACCGTA TCCACGTGGCTGAGAACC
	IPS1del(103-467)-rev	GGTCTCAGCCACGTGGATAC GGTCCGAGGTCCGAGGCTG
pEFTak IPS-1 1-508	IPS 509stop sense	GGAGAGGGAGGTGCCATGC TAGAGGCCCTCACCTGGG
	IPS 509stop anti	CCCAGGTGAGGGCCTCTAG CATGGCACCTCCCTCTCC

RESULTS

Creation of IPS-1 mutation constructs

IPS-1 is a mitochondrial membrane protein with an amino-terminal CARD, proline-rich region, and two TIMS; the carboxy-terminus houses a transmembrane domain and a third TIM (**Figure 5-1, upper panel**). In order to determine the important structural regions of IPS-1, various truncation, deletion, and site-directed mutations were created (**Figure 5-1**). Amino-terminal and carboxy-terminal truncations were made; the CARD and/or TM were deleted; and the residues between the CARD and TM were progressively removed until only the CARD and TM remained.

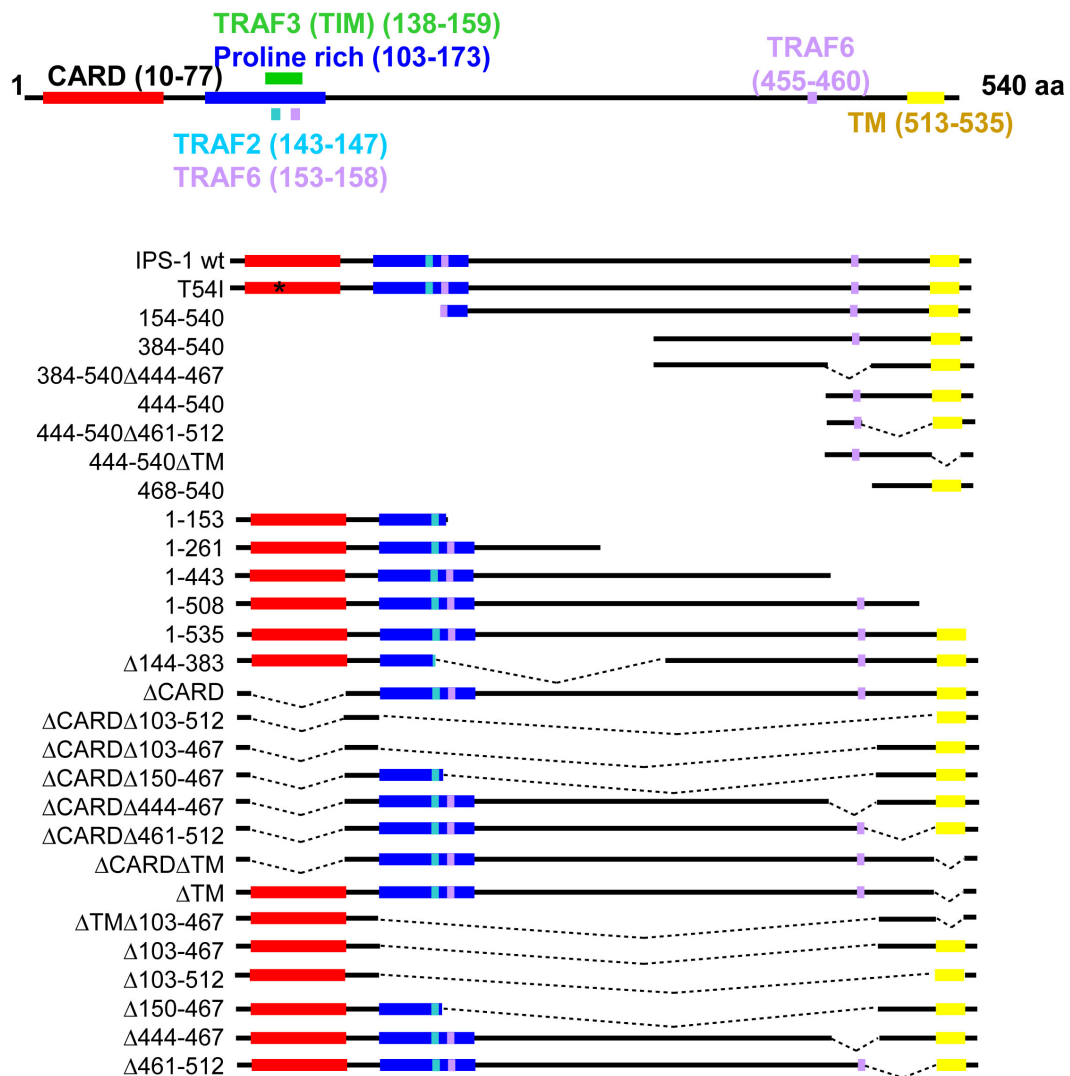


Figure 5-1: Diagram of IPS-1 constructs. *Upper:* Schematic of IPS-1. IPS-1 contains amino-terminal CARD (shown in red), proline rich region (blue), and TRAF interacting motifs (green, lavender, and turquoise). It contains a carboxy terminal transmembrane (TM; yellow) domain that anchors it in the outer mitochondrial membrane and a TRAF6 binding motif (lavender). *Lower:* A variety of deletion and truncation mutants were constructed in order to determine the structural regions required for IPS-1 downstream signaling. Dotted v-shaped lines represent the area deleted from the construct.

Deletion of the IPS-1 CARD domain confers a dominant-negative phenotype

Previous reports suggested that removal of the CARD rendered IPS-1 slightly inhibitory toward RIG-I-dependent antiviral activation¹⁴³, therefore we screened constructs for dose-dependent blockade of virus signaling by reporter luciferase assay. The ability of mutants to block SenV-induced activation of the IFN- β promoter was examined in Huh7 cells, which have a defective NF- κ B response (unpublished observations), making the IFN- β promoter induction primarily IRF-3-dependent (**Figure 5-2**); activation of the PRDII promoter, an NF- κ B dependent promoter, was tested in HEK 293 cells (**Figure 5-3**). At the highest dose the Δ CARD construct as well as all the truncation mutants lacking the CARD but retaining the TM exhibited a dominant-negative phenotype, significantly inhibiting IRF-3 signaling to the IFN- β promoter (**Figure 5-2**). Of note, the T54I mutation, homologous to the RIG-I T55I mutation in Huh7.5 cells that ablates RIG-I mediated signaling, acted in a dominant-negative manner toward IRF-3 activation, suggesting that this residue is important in CARD signaling to IRF-3. The Δ CARD dominant-negative phenotype was relieved upon double deletion of the CARD and TM, indicating that the TM played a role in inhibition by Δ CARD, whether through membrane localization or involvement in signaling events.

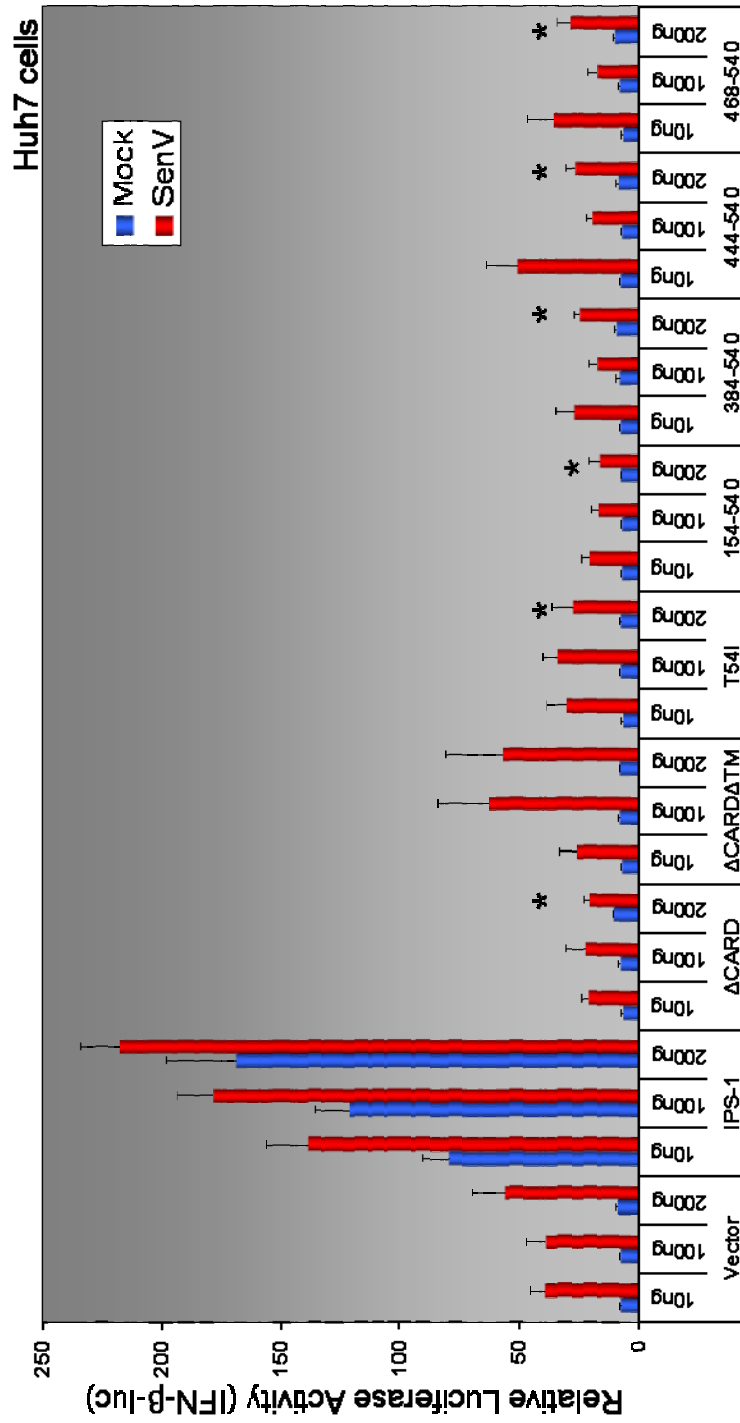


Figure 5-2: Dominant-negative IPS-1 constructs inhibit IFN- β promoter induction. Huh7 cells were transfected with the indicated amounts of IPS-1 constructs, 2.5ng IFN- β promoter luciferase construct, and 5ng CMV-*Renilla* luciferase as a transfection control. After 24 hours, cells were mock treated (blue bars) or infected with SenV (red bars), a potent agonist of these antiviral pathways, for 20 hours and collected for luciferase reporter assay. T54I is a single site mutation in the CARD domain of IPS-1 analogous to the RIG-I mutation in Huh7.5 cells that ablates RIG-I signaling. Asterisks denote significant difference ($p < 0.05$) compared to vector.

Similarly, PRDII promoter activation by virus was significantly inhibited in a dose-dependent manner by ectopic expression of the Δ CARD mutation ($p < 0.001$; **Figure 5-3**). Comparing amino-terminal truncations, IPS-1 444-540 basally activated the PRDII promoter while 468-540 did not, suggesting that the region between amino acids 444 and 468 is important for NF- κ B signaling. Interestingly, increasing concentrations of 468-540 exhibited a significant linear trend ($p = 0.0058$) of inhibiting virus signaling, while the 444-540 mutant did not, further suggesting important differences between residues 444-468. The presence of dominant-negative IPS-1 mutants implies that IPS-1 might multimerize and that this may occur concomitantly with its innate immune signaling actions.

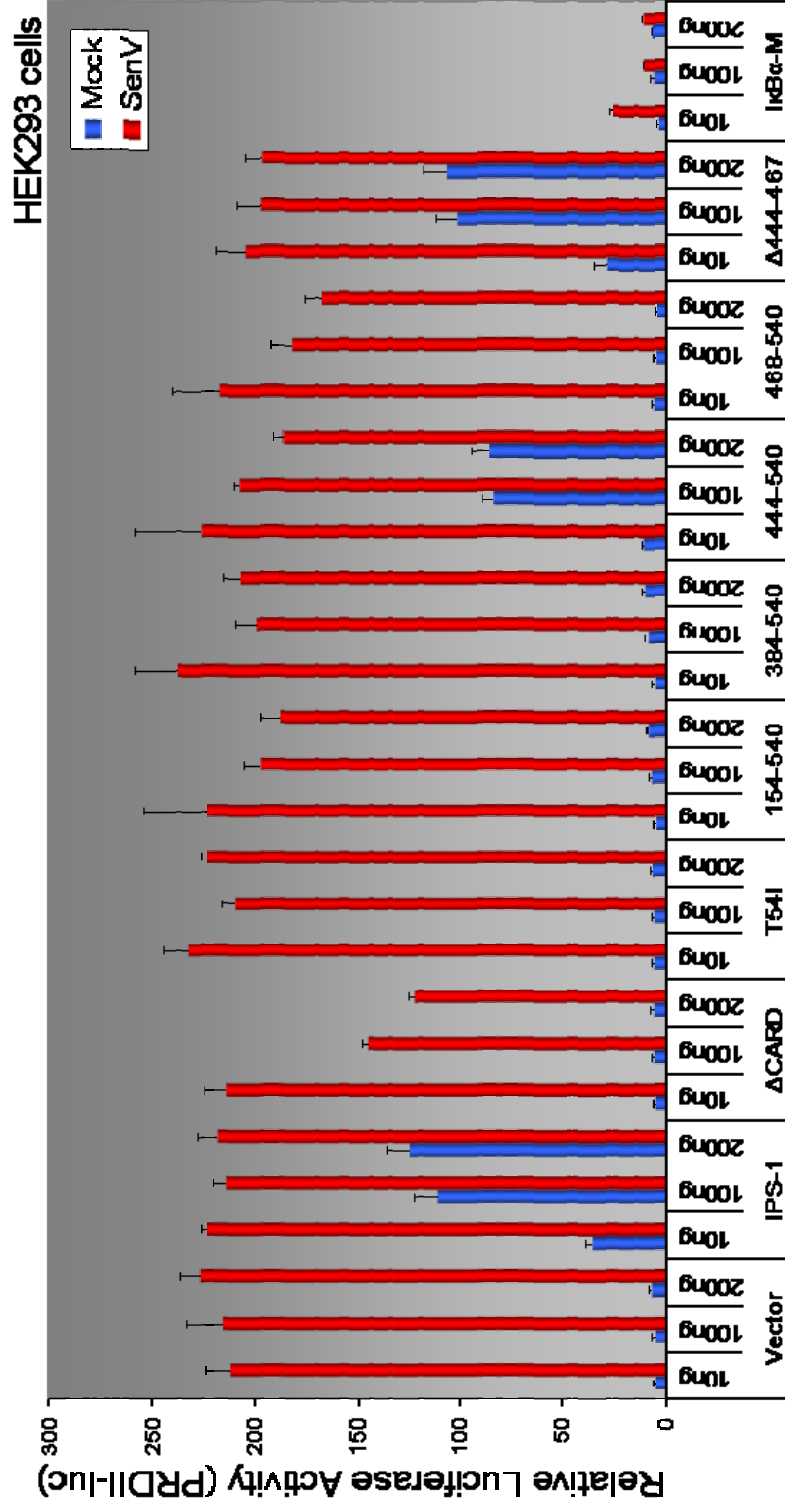


Figure 5-3: Dominant-negative IPS-1 signaling to NF-κB. HEK293 cells were transfected with increasing amounts of IPS-1 mutants, 25ng PRDII-luc, and 5ng CMV-*Renilla*. After 24 hours, cells were mock (blue bars) or SenV (red bars) infected for 20 hours, and analyzed by luciferase assay. Results were normalized to *Renilla* luciferase values. T54I contains a site mutation in the IPS-1 CARD. IκBα-M is a dominant-negative IκBα that prevents NF-κB activation.

IPS-1 oligomerization occurs through two multimerization motifs

To determine if IPS-1 oligomerizes, coimmunoprecipitation studies were carried out (**Figure 5-4**). FLAG-tagged wt IPS-1 associated with myc-tagged wt IPS-1 (*lane 3*), indicating that IPS-1 homo-oligomerizes. Further characterization of potential oligomerization sites using truncation and deletion mutants of IPS-1 revealed an amino-terminal oligomerization motif as well as a separate carboxy-terminal multimerization motif. As shown in **Figure 5-4** (*right panel*), the carboxy-terminal construct 444-540 co-immunoprecipitated wt IPS-1 (*lane 6*), but deletion of the TM ablated this interaction (*lane 8*), intimating that the TM is involved in oligomerization. Several proteins have been shown to dimerize or oligomerize through their transmembrane domains, including the eurythropoietin receptor²⁸, the epidermal growth factor receptor family^{36,107}, and the mitochondrial protein BNIP3^{24,148}. However, deletion of the TM in context of the otherwise full-length molecule was insufficient to block oligomerization with wt IPS-1 (*left panel, lane 25*), denoting a second oligomerization motif. Consistent with this idea, the amino-terminal mutant 1-153 interacted with wt IPS-1 (*left panel, lane 10*), implying that residues located within the CARD or proline-rich region were also involved in IPS-1 multimerization. However, the Δ CARD mutant still pulled-down wt IPS-1 (*right panel, lane 18*), which could be interpreted to mean that either the CARD did not contain the second oligomerization motif, or the carboxy-terminal multimerization site compensated for deletion of the amino-terminal site. Since the Δ CARD exhibited a dominant-negative phenotype to IRF-3 signaling that was relieved upon double deletion of the TM (**Figure 5-2**), we tested the Δ CARD Δ TM for oligomerization and found that this construct no

longer associated with wt IPS-1 (*lane 24*). This indicates that IPS-1 contains two homotypic interaction sites: one within the CARD, and the other involving the TM.

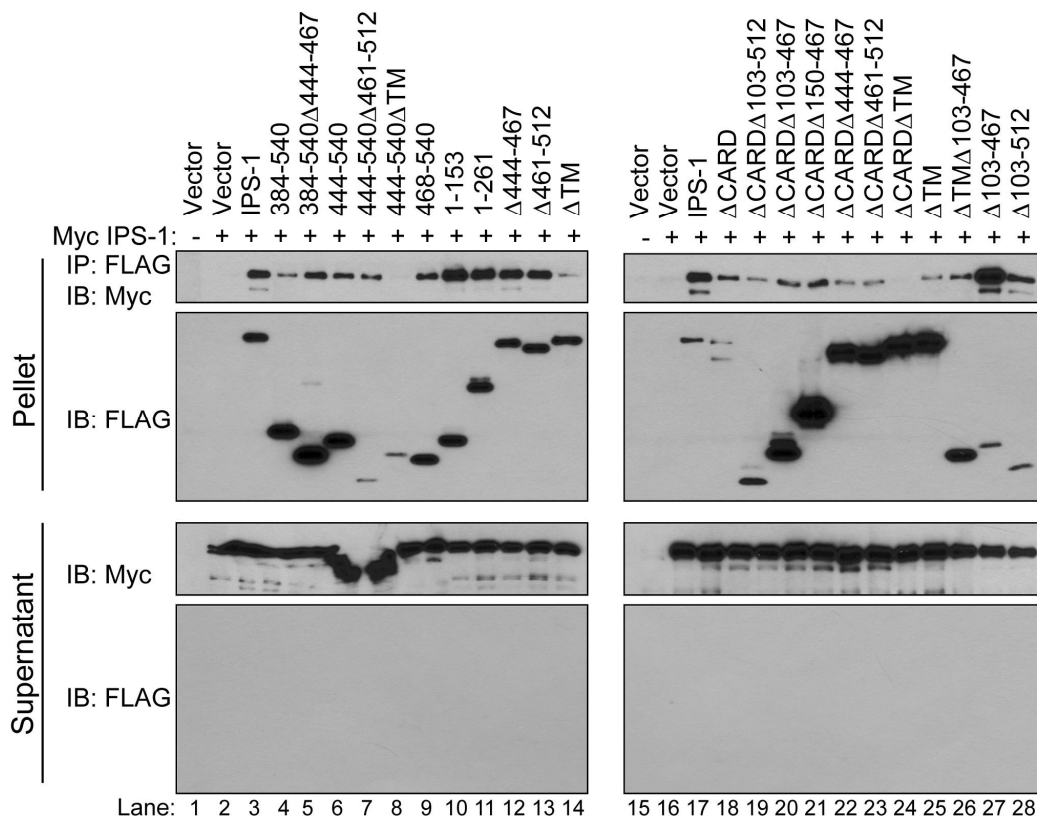


Figure 5-4: Coimmunoprecipitation analysis of IPS-1. In order to determine if IPS-1 oligomerizes, Huh7 cells were co-transfected with 300 ng FLAG-tagged IPS-1 constructs and 50ng of a myc-tagged wt IPS-1 for 24 hours. FLAG IPS-1 constructs were immunoprecipitated using FLAG beads, immunoblotted, and probed with antibodies against Myc and FLAG. Similar results were obtained using HEK293 cells.

Using myc-tagged deletion mutants, we verified the amino-terminal oligomerization domain (**Figure 5-5**). Predictably, Δ CARD interacted with Δ CARD (*lane 7*) consistent with a second multimerization motif, while Δ CARD failed to

coimmunoprecipitate with a carboxy-terminal deletion mutation lacking the TM (FLAG 1-153, *lane 8* or Myc 1-152, *lane 11*). This further validates our results from **Figure 5-4**.

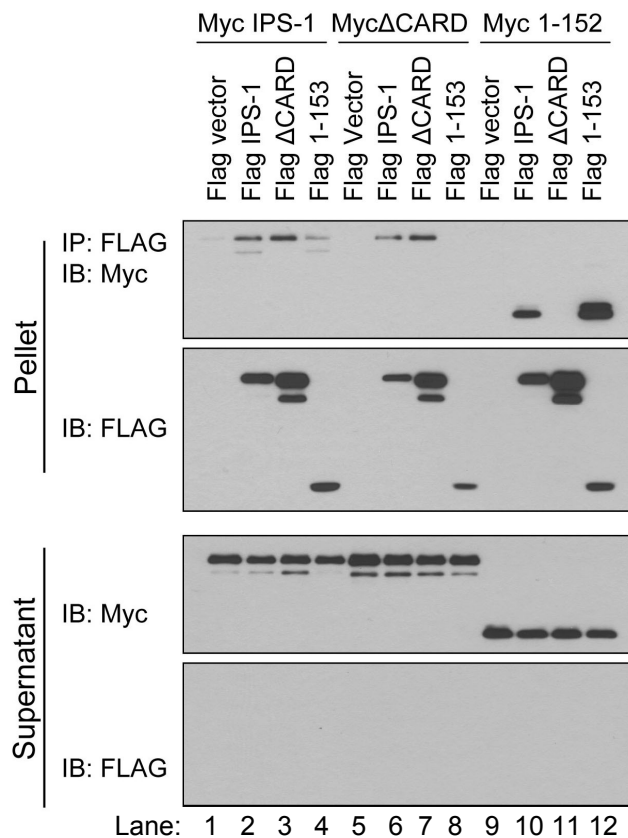


Figure 5-5: Deletion of the CARD ablates amino-terminal oligomerization of IPS-1. To verify that the CARD is responsible for multimerization within the amino-terminus of IPS-1, Huh7 cells were transfected with 400ng of the Flag-tagged IPS-1 constructs shown along with 75ng of the Myc-tagged IPS-1 mutants indicated above the solid line. The following day, cells were harvested by scraping and subjected to immunoprecipitation with FLAG beads and western blotting was performed on pellet and supernatant fractions. Blots were probed against FLAG and Myc as indicated.

NS3/4A inhibits carboxy-terminal multimerization of IPS-1

NS3/4A cleaves IPS-1 off the mitochondrial membrane at Cys 508, immediately upstream of the TM^{98,109}. In order to determine the effect of NS3/4A on IPS-1

oligomerization, Huh7 cells were cotransfected with various FLAG IPS-1 constructs and Myc IPS-1 with or without an NS3/4A expression plasmid (**Figure 5-6**). Association of wt IPS-1, 444-540, and 103-540 with Myc IPS-1 was disrupted in the presence of NS3/4A (compare *lanes 3 and 4, 5 and 6, 9 and 10*, respectively), but interactions involving the amino-terminus of the molecule were unaffected by NS3/4A (*lanes 7 and 8*). This is consistent with NS3/4A cleavage of IPS-1 near the TM, and further suggests that carboxy-terminal oligomerization is dependent on membrane anchoring.

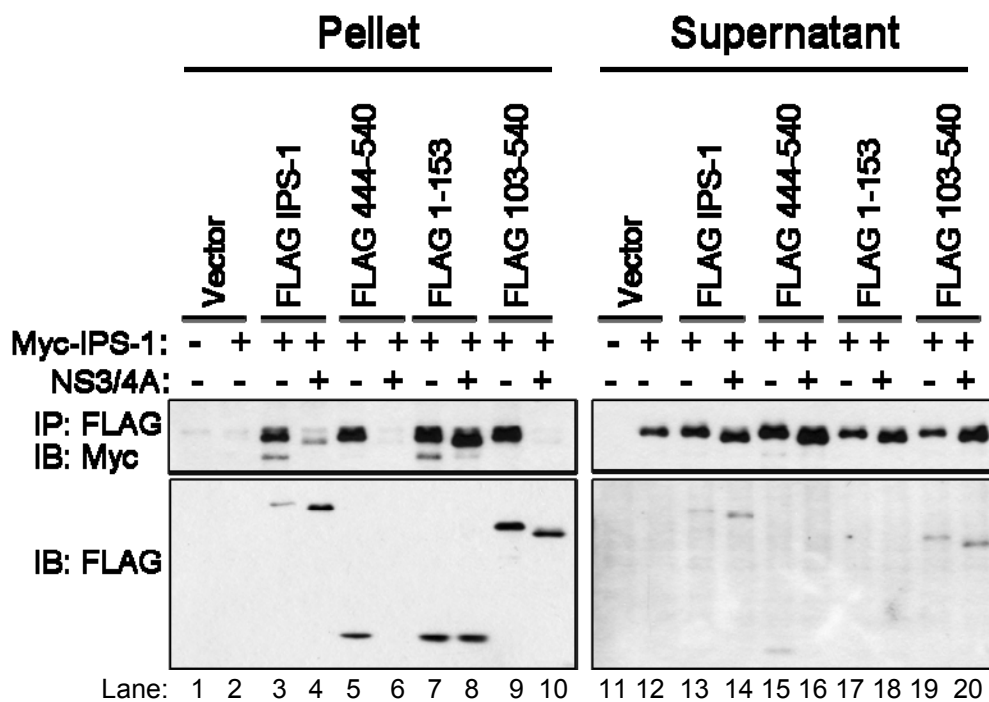


Figure 5-6: NS3/4A inhibits IPS-1 dimerization. Huh7 cells were transfected with 250ng of FLAG-tagged IPS-1 mutants, 50ng Myc-IPS-1, and 700ng vector or untagged pEF NS3/4A for 24 hours. Cells were collected for immunoprecipitation with FLAG beads, and immunoblotted.

Uncoupling IRF-3 and NF- κ B signaling

To determine the structural regions important for IRF-3 and NF- κ B signaling, we screened the IPS-1 mutants by luciferase reporter assay for constitutive signaling to IFN- β promoter (**Figure 5-7**) or PRDII promoter (**Figure 5-8**) elements. As shown previously, ectopic addition of IPS-1 constitutively activates IRF-3 and NF- κ B. Therefore, deletion of key signaling motifs would be predicted to no longer signal these transcription factors. Note the differences in IFN- β and PRDII promoter activation between the amino-terminal and carboxy-terminal truncation mutants. At the higher concentration, amino-terminal IPS-1 constructs constitutively activated an IRF-3 dependent promoter, but not an NF- κ B promoter element (compare constructs 1-153 and 1-261 in **Figures 5-7 and 5-8A**). Conversely, the carboxy terminal truncation mutant 444-540 activated an NF- κ B-dependent promoter at the higher concentration, but had no effect on promoter induction mediated by IRF-3. Interestingly, we once again observed that further amino-terminal truncation of IPS-1 was insufficient to signal NF- κ B (**Figure 5-8B**, 468-540), implicating residues 444-468 in activation of NF- κ B. Deletion of the TM also ablated induction of the PRDII promoter (**Figure 5-8B**, compare 444-540 and 444-540 Δ TM), suggesting either membrane localization or dimerization is necessary to induce NF- κ B signaling.

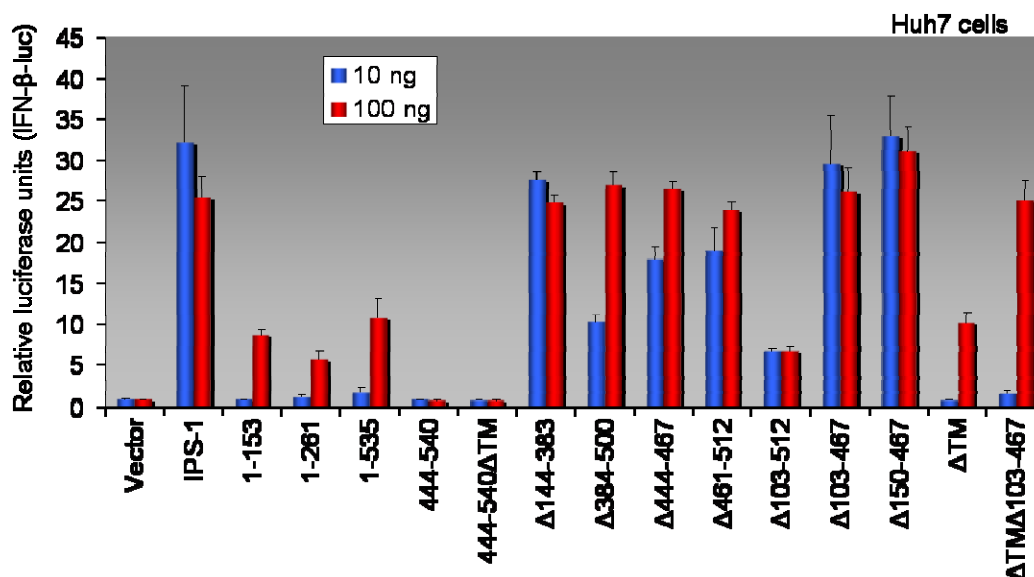


Figure 5-7: Effect of constitutively active IPS-1 constructs on IRF-3 activation. In order to determine the structural requirements for IRF-3 activation, Huh7 cells were transfected for 24 hours with 10ng (blue bars) or 100ng (red bars) of the indicated IPS-1 construct, 25ng IFN β -luc, and 5ng CMV-*Renilla*, and activity of the IFN- β promoter luciferase construct was measured relative to *Renilla* values.

It was previously reported that IPS-1 mutants containing only the CARD and the TM domains (Δ 101-512) retained signaling to the IFN- β promoter in HEK293 cells, albeit not to wt levels¹⁴³; however another group found that deletion of residues 150-502 ablated IFN- β promoter activation in HEK293 cells⁹³. To investigate this discrepancy, IPS-1 constructs with sequential deletions of the residues between the CARD and TM were examined for activation of IRF-3 and NF- κ B. All deletions in this region retained signaling to the IFN- β and PRDII promoter elements to varying degrees (Figures 5-7, 5-8A). NF- κ B activation by these constructs increased in a dose-dependent manner, including a construct lacking almost all residues except the CARD and TM (Figure 5-8A, Δ 103-512). However, Δ 103-512 consistently showed decreased activation of the IFN- β

promoter in all trials, and no increase in signaling with higher concentration plasmid transfected (**Figure 5-7**). These data support a model in which endogenous IPS-1 multimerizes with these deletion constructs, changing the conformation of the endogenous molecule such that it is able to bind downstream effector molecules. Thus the endogenous molecule provides the signaling effector regions, absent in these IPS-1 deletions, that are necessary for activation of the transcription factors IRF-3 and NF- κ B. The Δ 103-512 construct results may indicate that IRF-3 activation is dependent on one or more cellular factors that bind in between the CARD and TM, and once endogenous IPS-1 is saturated with Δ 103-512 molecules in the homo-multimer, no further signaling increase to IRF-3 is possible.

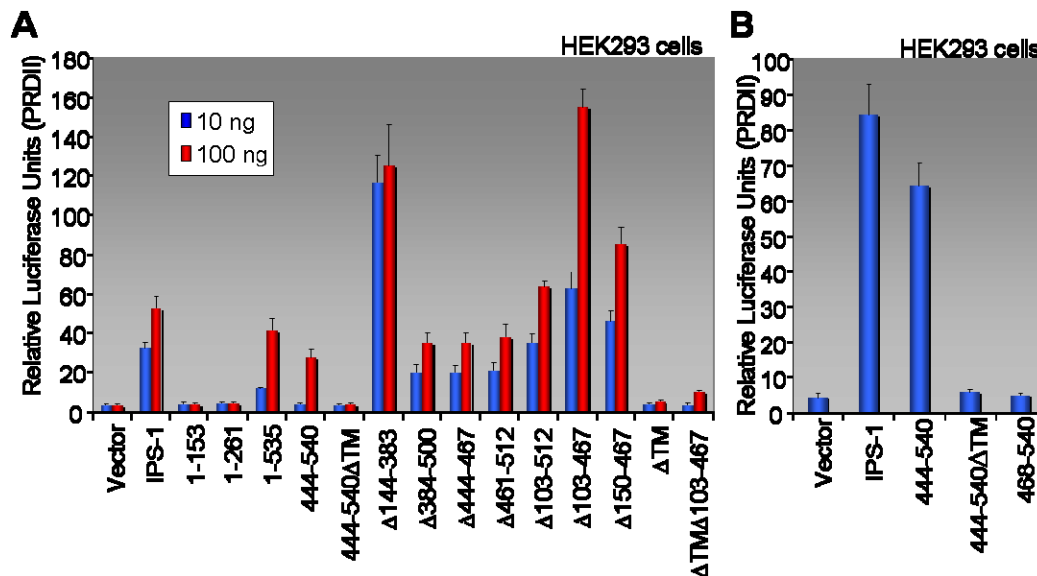


Figure 5-8: Effect of constitutively active IPS-1 constructs on NF- κ B activation. *A.* HEK293 cells were transfected with 10ng (blue columns) or 100ng (red columns) of each IPS-1 mutant as shown, 25ng PRDII-luc, and 5ng CMV-*Renilla*, and collected 24 hours later for luciferase reporter assay. *B.* HEK293 cells were transfected for 24 hours with 100ng of IPS-1 constructs, 25ng PRDII-luc, and 5ng CMV-*Renilla*, and harvested for luciferase assay. Values were normalized to *Renilla* luciferase.

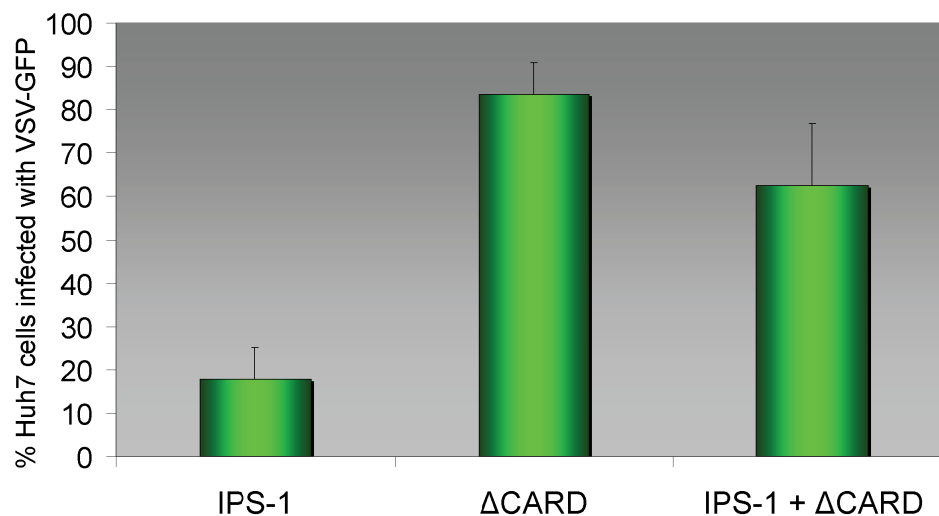


Figure 5-9: Effect of the dominant-negative IPS-1 construct, Δ CARD, on VSV-GFP infectivity. Huh7 human hepatoma cells were transfected with 100ng of the indicated constructs for 24 hours followed by infection with VSV-GFP (MOI=1) for 24 hours. Cells were stained for nuclei and four representative photos taken of each treatment. The number of infected cells (as indicated by GFP) were counted and compared to total number of cells. Bars indicated standard deviation. Data representative of two independent experiments..

Vesicular stomatitis virus (VSV) infectivity is exquisitely sensitive to the effects of interferon. When Huh7 cells are transfected by the constitutively active wt IPS-1, this turns on downstream signaling pathways leading to production of IFN (**Figure 5-9**). If cells are then infected with a GFP-tagged VSV, cells with actively reproducing virus can be visualized by fluorescence microscopy and quantitated. In **Figure 5-9**, IPS-1 overexpression inhibits replication of VSV. However, the Δ CARD construct does not lead to the production of interferon, and therefore virus freely replicates. When we mix the constitutively active IPS-1 with Δ CARD, the dominant-negative nature of this

construct is revealed and VSV replication is restored. These data show that Δ CARD rescues the viral replication blockade imposed by ectopic IPS-1 expression.

Identification of the IPS-1 mitochondrial signal sequence

To verify that IPS-1 mutants were targeted to the mitochondrial membrane to effect their action, selected IPS-1 constructs were observed by confocal microscopy (**Figure 5-10**). Wild-type (wt) IPS-1 colocalizes with mitochondria (yellow staining in the merged images). Constructs lacking the TM predictably show a diffuse localization, consistent with a lack of membrane tethering. All the IPS-1 mutants containing the TM were found on the mitochondria (**Figure 5-10**, wt IPS-1, Δ CARD, 468-540, Δ 103-512, 444-540), with the exception of 1-535, a five amino acid truncation construct. Deletion of these terminal five residues of IPS-1 impairs mitochondrial targeting such that it no longer colocalizes solely to mitochondrial membranes and can be found associated with other intracellular membranes. Thus these residues are essential for mitochondrial membrane anchoring.

Bcl-2 and Bcl-x_L are members of the Bcl-2 family of apoptosis regulating proteins and both contain a carboxy-terminal transmembrane domain. Bcl-2, however, is distributed on several intracellular membranes including the nuclear envelope, ER, and mitochondrial outer membrane (MOM) while Bcl-x_L is targeted specifically to the mitochondrial outer membrane ⁷⁷. Kaufman et al. compared the sequences for transmembrane domains and the surrounding sequence of several MOM proteins as well as other membrane proteins containing a tail-anchored hydrophobic α -helix in order to determine the sequence requirements for targeting proteins to the MOM. They found that

MOM tethering required at least two basic amino acids carboxy-terminal to the TM, and at least two nearby amino-terminal basic residues. Greater numbers of basic residues provided increased targeting stabilization. This gave a consensus sequence of:



where **B** indicates a basic amino acids and x denotes any residue ⁷⁹.

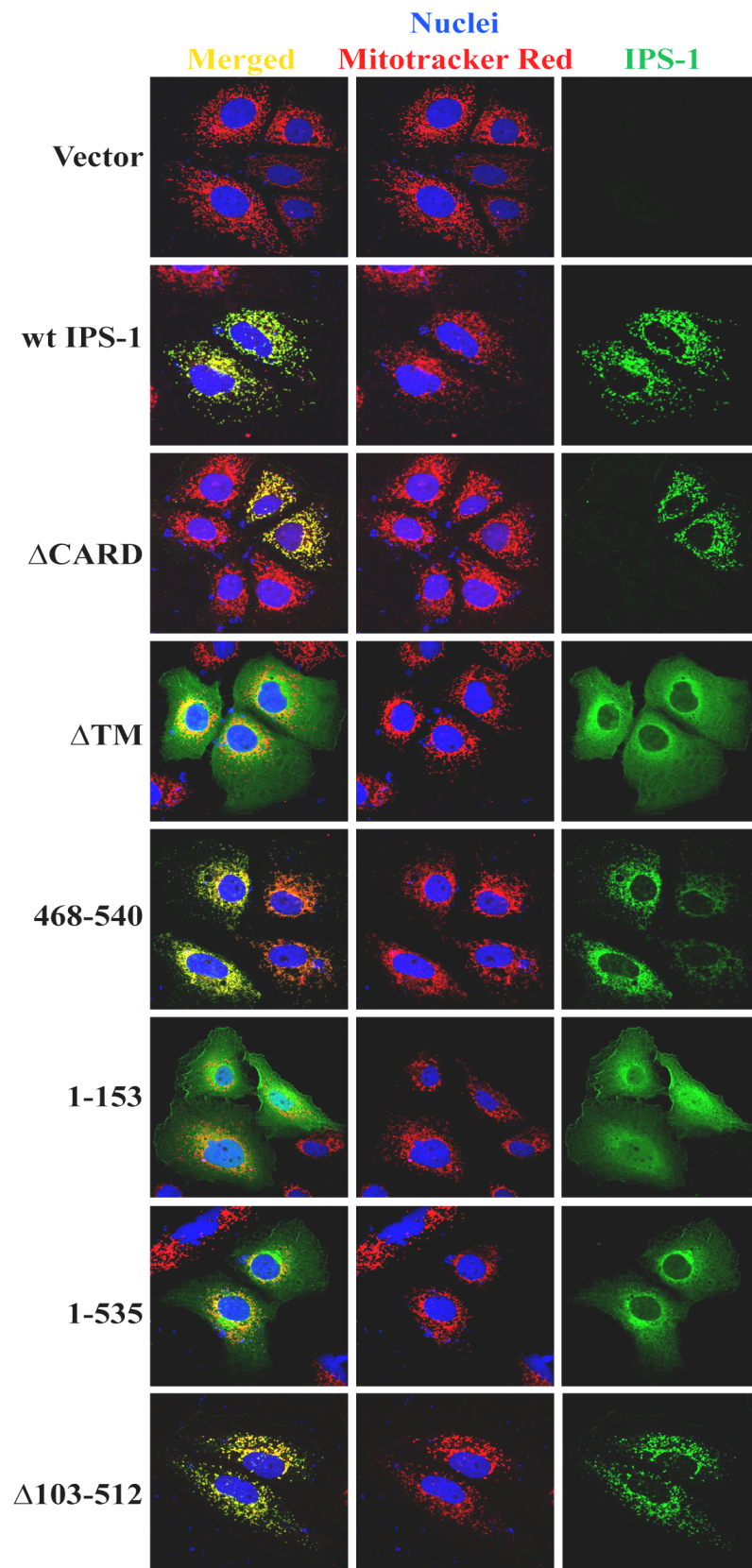


Figure 5-10: Localization of selected IPS-1 mutants. The indicated IPS-1 mutants (100ng) were transfected into Huh7 cells for 24 hours followed by treatment with 300nM Mitotracker Red for 1 hour at 37°C. Cells were then fixed and prepared for confocal microscopy. Cells were examined for colocalization (yellow staining in merged images) of mitochondria (red) and IPS-1 constructs (green). Nuclei are shown in blue.

CARD is involved in downstream signaling events. Furthermore, the identification of dominant-negative mutants suggested oligomerization of IPS-1 occurred and was important for signaling. To investigate this, a series of coimmunoprecipitation experiments revealed that IPS-1 multimerization originated in two regions: the CARD and the TM. Additionally, our results uncouple IRF-3 and NF- κ B regulation, demonstrating that the amino-terminus of IPS-1 is important for IRF-3 signaling while residues 444-467 are involved in NF- κ B activation. Finally, amino acids 535-540 were vital for correct subcellular distribution of IPS-1. Our findings suggest that IPS-1 dimerization may be important for virus signaling.

These data lead us to propose a model for multimerization-dependent activation of IPS-1 (**Figure 5-12**). Endogenous IPS-1 is abundantly expressed on the mitochondrial surface. Upon virus infection, dsRNA intermediates are recognized by RIG-I, enabling its dimerization and subsequent CARD-mediated signaling to IPS-1. RIG-I dimer binding promotes and stabilizes oligomerization of IPS-1 (shown here as a dimer), changing its conformation such that it can bind and signal downstream effector molecules to activate IRF-3 and NF- κ B. Unfortunately, native gel dimerization assays have been unsuccessful at determining if the higher order IPS-1 structure is a dimer or multimer. To preserve protein conformation, the use of denaturing detergents is precluded in these sorts of studies, making extraction of the membrane-bound IPS-1 more difficult. Additionally, upon virus infection, IPS-1 moves to a detergent-insoluble fraction ¹⁴³, further complicating these experiments.

Our results also demonstrated that deletion of the CARD engendered a dominant-negative phenotype while the Δ TM mutant did not (unpublished observations),

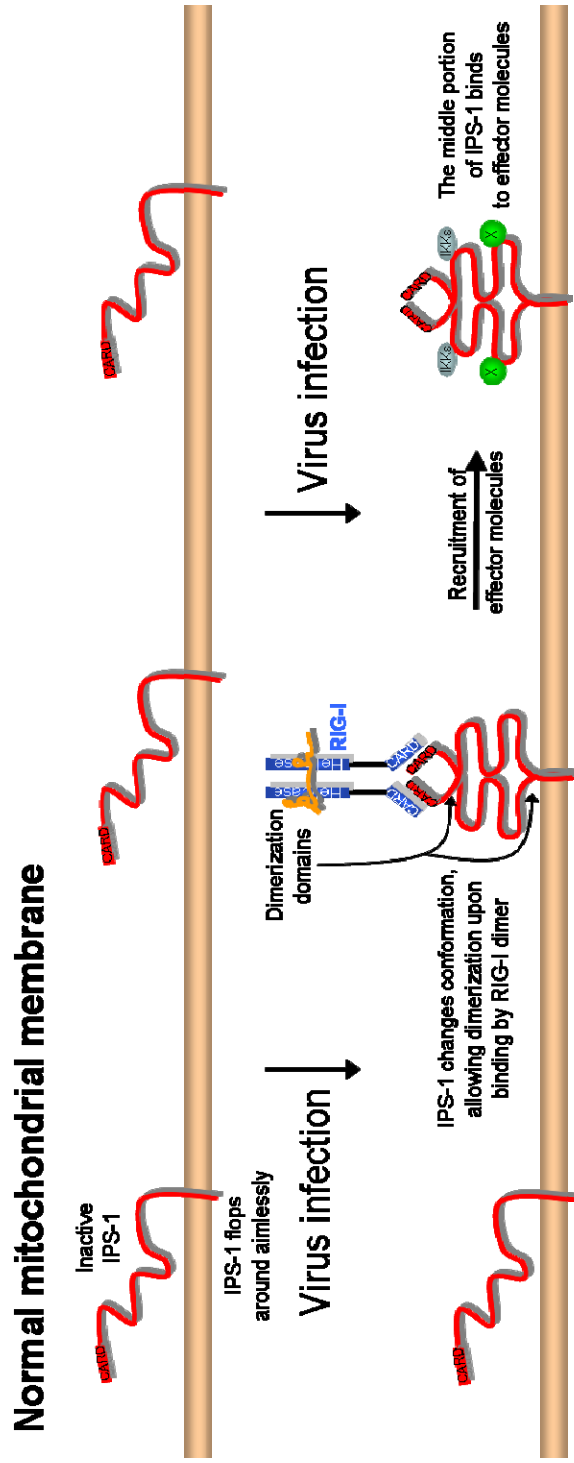


Figure 5-12: Oligomerization-dependent activation of endogenous IPS-1. The mitochondrial membrane in untransfected cells harbors endogenous IPS-1 (shown in red) on its outer membrane. Upon virus infection, dimers of RIG-I (blue) bind to the CARDs of two adjacent IPS-1 molecules, bringing them in close apposition and facilitating dimerization of IPS-1. This changes the conformation of IPS-1, allowing binding of downstream effector molecules and activation of IRF-3 and NF- κ B.

suggesting that the order of oligomerization occurs first at the TM, and secondly at the CARD. It is possible that IPS-1 TM association occurs basally (not pictured), with the amino-terminal CARD oligomerization event alone mediating the conformational change. Trypsin digestion protection experiments using recombinant IPS-1 protein in insect membranes may aid in evaluation of IPS-1 basal oligomerization status.

Ectopic expression of IPS-1 activates innate immune pathways independently of RIG-I. Wt IPS-1 or deletion construct transfection saturates the mitochondrial membrane (**Figure 5-13**) such that random interactions between adjacent molecules occur more frequently, increasing the probability of oligomerization. This enables a conformation change within the endogenous IPS-1 partner, leading to recruitment of effector molecules. Therefore, the ectopically expressed IPS-1 construct need not possess signaling domains so long as it has the CARD and TM to mediate dimerization with endogenous wt IPS-1.

A potential criticism of this work stems from the fact that CARDS are molecular motifs that mediate interactions with other CARDS. Therefore it is possible that the association of the IPS-1 CARD with itself is a non-specific CARD-CARD artifact. However, preliminary coimmunoprecipitation results using the CARDS from NOD2 and other CARD-containing molecules indicate the IPS-1 CARD-CARD interaction is specific. These data will need to be repeated and are therefore not presented here.

Overexpression of deletion IPS-1 constructs

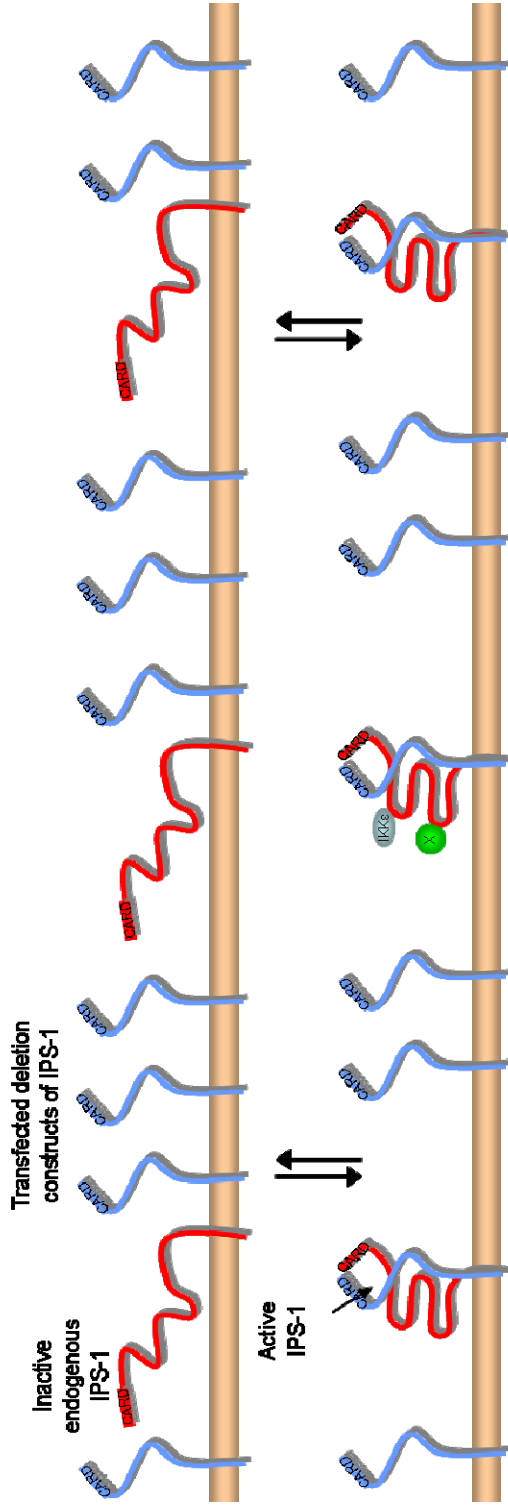


Figure 5-13: IPS-1 activation by deletion constructs. When deletion mutants of IPS-1 that contain both the CARD and TM are ectopically expressed (shown in blue), the increased numbers of IPS-1 molecules on the mitochondrial membrane makes random dimerization events more probable, even in the absence of upstream signaling from RIG-I. Despite lacking the structural requirements for binding to downstream effector molecules, dimerization of the deletion mutants (blue) with endogenous IPS-1 (red) changes the conformation of the endogenous molecule such that it can bind and activate downstream effector molecules, thus the antiviral response is turned on in the absence of viral stimulus.

Dimerization (and recently trimerization) of proteins through carboxy-terminal TM α -helical interactions is well established: SARS coronavirus spike protein trimerizes in its TM⁶; the epidermal growth factor receptor family self-associates through their TM^{36,107}; BNIP3 is a mitochondrial outer membrane protein involved in hypoxia-induced apoptosis that dimerizes through its TM^{24,148}. These α -helical interactions usually occur through specific motifs. A heptad motif of leucine residues with the consensus sequence **LLxxLLxLLxxLLxLL**, where **L** is a leucine and **x** represents any amino acid, was located in several proteins that dimerize through their TMs⁶¹. Another common motif found in TM helices was a [small amino acid]xxx[small amino acid] motif such as GxxxG and AxxxG, since four residues comprise about one helical turn in a regular α -helix conformation^{138,141}. The IPS-1 TM has a VxxxV motif at residues 528-532 which could mediate dimerization; similarly, it contains a large number of leucines which might contribute to a leucine heptad (**Figure 5-11**). Further investigations into these residues could determine the mechanism of TM dimerization.

To better examine domain requirements for signaling, the effect of constitutively active IPS-1 deletion mutants on induction of IRF-3 and NF- κ B could be compared between wt and IPS-1-deficient MEFs. Mutants that lost constitutive activity in IPS-1-null MEFs must signal in wt MEFs via dimerization with endogenous, full-length IPS-1. This would implicate the deleted region as important for effective downstream signaling, and further indicate that dimerization is essential in viral activation of the interferon immune response. These studies are currently underway.

Our data revealed that the area between amino acids 444 and 468 of IPS-1 is important for NF- κ B activation. Encompassed within this region, residues 455-460

encode a TRAF6 binding motif (**Figure 5-1**). TRAF6 is an upstream regulator of NF- κ B activation and acts to ubiquitinate NEMO²⁶. Importantly, deletion of the TM from 444-540 blocked signaling to NF- κ B, suggesting either that localization to the MOM or dimerization at the carboxy terminus is required. We propose that TRAF6 binds IPS-1 via residues 455-460 and acts in *trans*, targeting NEMO bound to the opposite IPS-1 molecule, resulting in the activation of the IKK complex and subsequent induction of the antiviral immune response.

CHAPTER SIX

Discussion and Future Directions

DISCUSSION

Structural analysis of NS3/4A regulation of the host response

The studies in Chapter Three describe efforts aimed at determining the minimal structural requirement for NS3/4A control of the innate antiviral response. A variety of NS3 carboxy-truncation mutants were constructed, culminating in the deletion of the entire helicase domain. These truncated NS3 segments were attached to the region of NS4A necessary for complete proteolytic activation of NS3 via a flexible linker, creating single-chain constructs that did not require a *cis* cleavage event for activity. The NS3/4A protease domain alone was found to be the minimal effector region necessary for cleavage of IPS-1.

Surprisingly, while protease activity was required to inhibit the RIG-I pathway in the context of wt NS3/4A, this was not the case for the single-chain protease. Active site serine mutation to alanine mutation in the SC Protease prevented cleavage of NS5AB, the natural substrate of NS3/4A, as well as IPS-1; however the SC Protease S1165A still inhibited antiviral signaling when expressed at high levels. This was unexpected, but seemed to indicate that the SC Protease SA binding to IPS-1 may prevent dimerization of IPS-1 or block binding of an essential downstream factor. This would not be unprecedented. IKK ϵ has been reported to bind IPS-1, causing IKK ϵ activation and the subsequent phosphorylation of IRF-3⁹³. LGP2, a RNA helicase in the same family as RIG-I and MDA5, was found to bind directly to IPS-1 at the IKK ϵ binding site,

preventing IKK ϵ interaction with IPS-1, thus inhibiting IRF-3 activation ⁸⁴. The SC Protease S1165A mutations could be acting in a similar manner. Alternatively, the SC Protease S1165A could be preventing oligomerization of the IPS-1 TM. The NS3/4A cleavage site on IPS-1, Cys 508, is located near the TM. It is possible that SC Protease S1165A binding to this region may disrupt interactions between adjacent IPS-1 TMs, preventing the conformation change that is necessary for downstream signaling.

Also of note was the discovery that the SC Protease cleaves IPS-1 at a second site, Cys 283. Mutation of the Cys 283 residue to alanine had no effect on signaling ⁹⁸, but prevented the SC Protease cleavage event. Increased promiscuity of the SC Protease is not entirely unpredictable: deletion of the helicase domain removes a significant steric hindrance to the protease active site, potentially allowing access to more substrates.

Interestingly, the SC Protease localized to intracellular membranes. In constructing this molecule, we discarded the NS4A membrane targeting region. The amino-terminus of NS4A was found to localize the NS3/4A holocomplex to ER membranes ¹⁶⁶, and this region was lacking in the SC Protease. This suggested that another membrane anchoring motif may exist within the NS3 protease domain, perhaps one specific for mitochondrial membranes. Alternatively, the NS3 protease domain may interact with another protein which shuttles it to a membrane compartment. This was explored further in Chapter Four.

Finally, use of pharmacological inhibitors of NS3/4A protease activity inhibited NS3/4A cleavage of IPS-1. This showed that NS3/4A normally colocalized with IPS-1. Furthermore, protease inhibitor treatment in HCV-infected cells decreased HCV protein production and restored the interferon antiviral response. These data indicate the power

of protease inhibitor therapy. Protease inhibitors not only block viral replication, but also inhibit the ability of the virus to regulate host defenses. These drugs hold great promise for the future.

Mitochondrial localization and targeting by NS3/4A

The goal of Chapter Four was to follow up on observations from Chapter Three suggesting that the NS3 protease domain might be responsible for mitochondrial, and hence IPS-1, targeting. In order to determine if NS4A was required for NS3 membrane localization and IPS-1 targeting, we used cell lines conditionally expressing NS3 or NS3/4A. NS3-dependent blockade of IRF-3 activation and mitochondrial membrane targeting were indeed dependent on NS4A expression. However, targeting of the SC Protease to IPS-1 and the MOM did not require the NS4A membrane anchoring domain, suggesting that the role of NS4A involved conformational change of NS3. That NS4A causes specific and distinct rearrangement of the NS3 protease domain is well documented by crystallization studies^{81,99}. Therefore we focused our efforts on the NS3 protease domain.

Hydrophobicity analysis showed that the amino-terminal 20 residues of NS3 contained a putative membrane targeting motif. Previous deletion mapping had identified that for the most part the only residues that could be deleted from the protease domain and retain at least minimal protease activity resided in this region. The first 22 amino acids were determined to be responsible for complex formation with NS4A and subsequent NS4A-dependent protease activation. Cleavage at NS4A-independent sites, such as NS5AB, were not effected by these mutations³². We therefore deleted the first

10 or 20 amino acids in the context of the wt NS3/4A as well as the SC Protease and found that deletion of the first 10 residues had no effect on inhibition of antiviral signaling, but resulted in abnormal localization. A NS3/4A mutant lacking the amino-terminal 20 residues, however, lost the ability to cleave IPS-1 and failed to block IRF-3 activation in response to virus infection. Interestingly, this same deletion within the SC Protease had no effect on its inhibition of virus-mediated signaling to the IFN- β promoter, and still cleaved IPS-1 despite its diffuse cellular localization. The covalent attachment of the NS4A β -strand to the amino-terminal region of the SC Protease might allow direct β -strand intercalation into the protease domain, NS3/4A, on the other hand, contains NS4A attached to the carboxy-terminus, on the far side of the helicase domain. Lacking this pre-positioning near the active site, NS4A from wt NS3/4A may be unable to form a stable complex with the protease domain without additional help from residues that function to hold it close to the active site. Therefore, amino acids 1-20 may serve to arrange NS4A in the proper location for intercalation to occur.

The amino-terminus of NS3 contains an α -helix with hydrophobic residues surface exposed followed by two arginine residues. The arginine residues may represent part of a conserved mitochondrial targeting sequence while the surface exposed residues may allow peripheral attachment of the protease domain to membranes. It remains to be determined if these residues can target a heterologous protein to mitochondrial membranes.

Structural analysis of IPS-1 signaling

Chapter Five was aimed at determining regions of IPS-1 that were important in signaling activation of IRF-3 and NF- κ B. Once again, we relied on extensive mutagenesis in these studies. These constructs were initially screened for activation of these pathways constitutively or in response to virus. Interestingly, deletion of the IPS-1 CARD caused inhibition of virus-mediated signaling to both IRF-3 and NF- κ B, which suggested that IPS-1 acted as an oligomer. To study this further, we looked at interaction of ectopic IPS-1 with itself and found that it did indeed self-associate, and furthermore that this occurred through two domains: the CARD and TM. Deletion of one was insufficient to ablate self-association, while deletion of both domains prevented oligomerization of IPS-1. Moreover, CARD-dependent interaction with wt IPS-1 was unaffected by NS3/4A, however, oligomerization of the TM region was inhibited by NS3/4A.

Additionally, we were able to uncouple IRF-3 from NF- κ B signaling. The amino-terminus of IPS-1 was important for activation of IRF-3, while the carboxy-terminus acted as a dominant-negative for IRF-3 signaling. On the other hand, the carboxy-terminal residues 444-467 were vital in NF- κ B signaling, with the TM playing a role either through membrane localization or dimerization. These residues contained a conserved TRAF6 binding motif, suggesting interaction of TRAF6 may be important in IPS-1 signaling to NF- κ B. This will be discussed in more depth later.

These data led us to propose a model for oligomerization-dependent activation of IPS-1. RIG-I recognition of dsRNA mediates a conformational change leading to its

dimerization and CARD-dependent signaling to IPS-1¹³⁵. Binding of RIG-I dimers brings IPS-1 molecules in close proximity to each other, promoting oligomerization of the IPS-1 CARD and TM. This causes a conformation change, revealing binding sites for downstream adapters. This model explains the observation that a construct lacking all residues between the CARD and TM still constitutively signaled to IRF-3 and NF- κ B. As long as this deletion construct is able to multimerize with endogenous, wt IPS-1, this multimerization changes the conformation of the endogenous IPS-1 allowing it to signal, even in the absence of signaling by the mutant partner.

Amino-terminal IPS-1 truncation mutants lacking the CARD were dominant-negative for IRF-3 activation following virus infection. This is likely due to IPS-1 mutant oligomerization with the TM of endogenous wt IPS-1 in the absence the second CARD-mediated multimerization event, preventing the conformation change necessary to open binding sites for downstream effector proteins. Therefore, not only are these constructs unable to signal constitutively, they prevent the wt partner from doing so. These results raised in an intriguing possibility. Since NS3/4A cleaves the amino-terminus of IPS-1 away from the TM, it is possible that the carboxy-terminal fragments of IPS-1 are retained on the mitochondrial membrane. Immunoblot analysis of HCV-infected cells shows that IPS-1 cleavage by NS3/4A is incomplete, with some wt IPS-1 molecules remaining. The carboxy-terminal cleavage fragments would still be able to associate with uncleaved IPS-1 via the TM, further inhibiting activation of IRF-3 and subsequent production of IFN. Therefore NS3/4A may effect inhibition of antiviral signaling through two mechanisms: direct cleavage of IPS-1 and inhibition of IPS-1 activation by cleavage fragments.

Finally, we identified the carboxy-terminal five amino acids as critical residues for IPS-1 targeting to the mitochondrial membrane. Specific deletion of these residues impaired IPS-1 localization to the mitochondria, instead distributing it nonspecifically on intracellular membranes. This targeting occurred through two conserved basic residues, a motif consistent with other mitochondrial outer membrane proteins.

CURRENT AND FUTURE DIRECTIONS

Involvement of TRAFs in IPS-1 signaling

TRAFs have been found to interact with a variety of cell surface receptors and are critical in the inflammatory response as well as cell survival signaling. Three TRAF interacting motifs (TIMs) were found to be encoded within IPS-1¹⁷⁰, the first and third being highly conserved across species (**see Appendix A**). The first TIM corresponded to a consensus TRAF 2, 3, and 5 binding motif found in cellular receptors such as CD40; the last two TIMs matched the distinct consensus binding motif for TRAF6⁸².

Xu et al. found endogenous TRAF6 immunoprecipitated with endogenous IPS-1, and that this interaction occurred through the second and third TIMs¹⁷⁰. TRAF6 is an upstream regulator of the NF- κ B activation, acting as an ubiquitin ligase for NEMO²⁶. Mutation of the third TIM significantly decreased NF- κ B activation, but had very little effect on ISRE promoter activity¹⁷⁰. These results suggested that TRAF6 binding to the third TIM of IPS-1 is a critical step in NF- κ B activation.

However, Seth et al. did not find any association between TRAF6 and IPS-1, and moreover, production of IFN- β in the supernatants of SenV-infected TRAF6-deficient MEFs was normal ¹⁴³. Conversely, Xu et al. found a significant decrease in NF- κ B promoter activation with ectopic IPS-1 stimulation in TRAF6-null MEFs compared to wt MEFs, but, consistent with Seth et al., ISRE promoter element activation was normal ¹⁷⁰. While these two reports seem to contradict each other on the role of TRAF6 in IPS-1 signaling, the disparities can be explained by previous studies showing that nuclear NF- κ B in the absence of activated IRFs was insufficient to induce the IFN- β promoter ⁷⁰, suggesting that IRF signaling predominates in IFN- β induction. Therefore Seth et al. did not see differences in IFN- β production because IRF-3 activation was normal. Experiments in our hands found that TRAF6 did indeed interact with IPS-1 (unpublished observations), and moreover that an area encompassing the third TIM regulated NF- κ B activation. The conserved nature of the third IPS-1 TIM among diverse species further suggests its importance (**Appendix A**). Studies examining the effects of this region in TRAF6-deficient MEFs are currently planned. Taken together these data suggest that TRAF6 plays a vital role in NF- κ B responses in the RIG-I pathway but not activation of IRF-3, and this occurs through an interaction with the third TIM of IPS-1.

We found that an IPS-1 construct comprising the first 153 residues of IPS-1 was able to constitutively activate IRF-3 but not NF- κ B, suggesting a motif within this region may be important in signaling to IRF-3. The first and second TIMs are encoded within this segment, but only the first TIM is highly conserved among species (**Appendix A**). Xu et al. showed that TRAF2 bound IPS-1 through the first TIM, while TRAF5 failed to

interact with IPS-1¹⁷⁰. TRAF2 is involved in JNK and NF- κ B activation in response to TNF receptor stimulation¹¹⁶, but no function has been described for it in activation of IRF-3. However, as stated earlier, the first TIM contained a consensus TRAF 2, 3, and 5 binding motif⁸². While Xu et al. ruled out the association of TRAF5, they neglected to look for TRAF3 association, probably because it was largely uncharacterized at that time. One year later, TRAF3 was identified as an essential factor in the activation of IRF-3 but not NF- κ B, and was vital in the induction of type I IFN in both TLR and RIG-I-dependent signaling pathways¹²⁰. It was found to bind directly to IPS-1, TBK1, and IKK ϵ ^{120,133}, suggesting it might serve as a bridge between IPS-1 and the IRF-3 kinases. TRAF3 interacted with in the first TIM of IPS-1, and was required for IFN- α production in response to dsRNA or Sendai virus infection¹³³, suggesting it also plays a role in the IFN amplification loop and activation of IRF-7. Preliminary results show that NS3/4A does not seem to affect TRAF3 binding to IPS-1 (unpublished observations), consistent with NS3/4A interacting with IPS-1 near its C-terminus. Interestingly, TRAF3 had limited effect on IFN- β production: its activity was mainly confined to IFN- α ¹³³. Therefore, TRAF3 binding the first TIM may explain activation of the IFN- β promoter in the amino-terminal IPS-1 constructs, but other effectors may be involved.

Downstream effector molecules and their involvement in IPS-1 signaling

The identity of other downstream IPS-1 binding partners responsible for initiating IRF-3 and NF- κ B activation has remained elusive, but current research has shed light in this arena. Initially a dispute arose over whether the essential IRF-3 kinases

TBK1 or IKK ϵ directly bind IPS-1, with several groups on each side of the argument^{80,93,109,133,170}. This debate has yet to be resolved.

NEMO was previously determined to be a critical scaffolding component of NF- κ B activation in response to virus⁵⁴, but also recently was found to be an essential component in RIG-I signaling to IRF-3 and IRF-7. Using NEMO-deficient MEFs, activation of the ISRE and IFN- α production in response to SenV or ectopic IPS-1 absolutely required NEMO¹⁷⁹, suggesting NEMO may be involved in recruitment of effector molecules to IPS-1.

Another report showed that NAK-associate protein 1 (NAP1) was also found to directly bind RIG-I, MDA5, and weakly to IPS-1; colocalize with IPS-1; and be important for RIG-I-dependent IRF-3 activation¹³⁶. TRAF family member-associate NF- κ B activator (TANK) has also been shown to bind to IPS-1, TRAF3, TBK1, IKK ϵ and potentiate signaling by IPS-1⁶⁰. However, these latter two studies were weakened by their lack of genetic deletion data, thus their relative importance has yet to be determined.

Many other proteins have been identified in association with IPS-1, not always consistently. Kawai et al. detected IPS-1 binding Fas-associated death domain (FADD) and receptor-interacting protein 1 (RIP1) by co-immunoprecipitation⁸⁰, while Seth et al. did not¹⁴³. Furthermore, Seth et al. found normal virus-mediated IFN- β production in RIP1-null MEFs¹⁴³. Xu et al. reported that IPS-1 interfaced with IRF-3 and TAK1¹⁷⁰, and Meylan et al. immunoprecipitated IKK α and IKK β with IPS-1¹⁰⁹. It is probable that many of these associations discovered by coimmunoprecipitation are in fact not direct interactions but instead denote the presence of a multicomponent signaling complex of

which IPS-1 is a member. Gene ablation studies will be important in determining the importance of many of these interactions.

LGP2

Another RNA helicase with homology to both MDA5 and RIG-I is LGP2. Lacking the CARD signaling component, LGP2 negatively regulates virus-mediated activation of RIG-I¹⁷⁴ but not MDA5¹³⁵. LGP2 contains a repressor domain that is essential for inhibition of viral activation of the IFN- β promoter¹³⁵, suggesting a model of LGP2 repression of innate signaling via repressor domain interactions with RIG-I. LGP2 also inhibits virus-induced activation of IRF-3 and has been shown to bind pIC as well as the 5' and 3' UTR of the HCV RNA genome, suggesting an additional mechanism of direct competition for RNA ligands^{135,174}. Another study indicated that LGP2 interacts with IPS-1, displacing IKK ϵ , and thus may act directly to prevent IPS-1 activation⁸⁴.

Research using the recently-described LGP2-deficient MEFs has shown that LGP2-deficient mice: 1) produce more IFN- β in response to pIC stimulus than wt; 2) showed enhanced type I IFN mRNA levels with exogenous RIG-I or MDA5 stimulation, but not IPS-1 overexpression, suggesting LGP2 acts as a negative regulator of RIG-I and MDA5; 3) were resistant to VSV infection, suggesting a negative regulatory role with RIG-I; and 4) were sensitive to EMCV infection, suggesting a positive regulatory role in MDA5 signaling¹⁶⁰. These differences between MDA5 and RIG-I signaling are likely due to repressor domain interactions between RIG-I and LGP2 that do not occur between LGP2 and MDA5.

As an ISG itself, LGP2 expression is controlled by RIG-I activation of IFN production¹³⁵. LGP2 may therefore represent an autoregulatory mechanism to stop RIG-I signaling and arrest the IFN amplification loop. However, the exact mechanism of LGP2 action during virus infection remains to be defined.

ISG15 interaction with IPS-1

During these studies, we noted endogenous ISG15 in the pellet fractions of some immunoprecipitations. ISG15 is a small, ubiquitin-like molecule that forms covalent attachments on various cellular proteins. It is a direct target of IRF-3¹³⁷ in addition to being an ISG, and was recently shown to covalently modify IRF-3 and prevent its activation-dependent degradation, prolonging IRF-3 signaling¹⁰¹. A real-time RT-PCR study of percutaneous liver biopsy specimens from HCV-infected patients (taken before combination therapy) compared gene expression levels between fifteen non-responders, sixteen responders, and twenty healthy specimens. They found 18 genes differentially expressed between responders and non-responders, including ISG15²⁵. These data may have uncovered the importance of ISG15 in response to combination therapy during HCV infection. We found that endogenous ISG15 specifically associated with ectopic IPS-1, and this interaction was ablated by NS3/4A. Furthermore, the absence of conjugation products in the pellet fraction implies that this may have been a direct, non-covalent interaction (unpublished observations). While the purpose of this interaction is unknown, these data are intriguing.

The studies presented in this dissertation reveal structural mechanisms of HCV NS3/4A targeting of IPS-1 and inhibition of antiviral signaling. Furthermore, we

determined regions of IPS-1 essential for downstream signaling. This will facilitate identification of effector molecules important in innate immune signaling. Knowledge of the structural regions required for activation and inhibition of IFN production could lead to more effective therapies to treat HCV infection or shut down an overactive immune response during inflammation.

		Section 5					
	(205)	205	210	220	230	240	255
IPS-1 (204)		STHTAGAT	SSLT	PSRGPVSP	SVSFQPLAR	STFRASRLPGPT	GSVVSTGTSF
IPS-1 chimpanzee (204)		STHTAGAT	SSLT	PSRGPVSP	SVSFQPLAR	STFRASRLPGPT	SVVSTGTSF
IPS-1 rhesus macaque (204)		STHTAGAT	SSLIP	PSRGPVSP	SVSFQPLAR	STFRASRLPGPAG	SVVSTGTS
IPS-1 cow (203)		NHTAGV	VSSST	SLRGPVSP	TVSFQPLAR	STFRASRLPGPP	VSAFVSTGTS
IPS-1 pig (202)		SAHTAGT	VSSPT	SPRGPVSP	TVSFQPLAR	STFRASRLPGP	PVSTASSSTGL
IPS-1 dog (202)		GAHTAGT	ASGLT	SARGPVSP	TVSFKPLRS	IFRASRLPAP	SALALSTGTS
IPS-1 mouse (202)		GAHAANV	ASVPI	ATYGPVSP	TVSFQPLPR	TALRTNLL	SGVTVSALSADTSL
IPS-1 rat (202)		GPSTIAN	VDSVPI	ATYGPVSP	TVSFQPLPR	IAFRTNLS	PGVTVSALS
Consensus (205)		STHTAG	SSLTSS	SRGPVSP	TVSFQPLAR	STFRASRLPGPT	VSALSTGTS
		Section 6					
	(256)	256	270	280	290	306	
IPS-1 (255)		SSSS--	PGLASAGA	EEGKQGAES	DQAEPI	ICSSGAEAPANS	LPSKVPPTLM
IPS-1 chimpanzee (255)		SSSS--	PGLASAGA	EEGKQGAES	DQAEPI	ICSSGAEAPANS	LPSKVPPTLM
IPS-1 rhesus macaque (255)		SSSSSS	PGLASAGA	EEGKQGAES	DQAEPI	ICSSGAEAPANS	LPSKVPPTLM
IPS-1 cow (254)		SSSTG	-----	-----	LTSAGGAGDQTE	ETICSSGAGV	PNNP-----
IPS-1 pig (253)		ASAG	-----	-----	GAGDQVEAT	ICSSGAGV	PTTS-----
IPS-1 dog (253)		SSPG	-----	-----	SAAGVAGDH	GEATICSTM	AGVSTGA-----
IPS-1 mouse (253)		SSSS	-----	-----	TGSFAKAGD	QAKAATCF	STTLTNSV
IPS-1 rat (253)		SSSS	-----	-----	TGSFAKAGD	QAKAATCF	VSTKEGVPTN
Consensus (256)		SSSS			A A AGGAGDQAEA	ICSSGAEAPANS	
		Section 7					
	(307)	307	320	330	340	357	
IPS-1 (304)		PVNTVAL	KVPANPA	SVSTVPS	SKLPTSS	SKPPGAVPS	NALTNPA
IPS-1 chimpanzee (304)		PVNTVAL	KVPANPA	SVSTVPS	SKLPTSS	SKPPGAVPS	NVLTNPA
IPS-1 rhesus macaque (306)		PVNTVAP	KVPANPA	SASTVPS	SKLPTSS	SKPPGTVPS	-VFTNPA
IPS-1 cow (285)		AASTVPS	SKVPTNS	AFSSVPS	SKLPTSL	SKPPGAVPT	----NLAPS
IPS-1 pig (279)		TASMVPS	SKVPTNS	AFSTMP	SKLPTSL	SKPPGAMST	NVSPSVA
IPS-1 dog (284)		TTSTAPS	SKVPTH	STFDRMAP	SKLPPASS	SKSGTMPT	---TSLP
IPS-1 mouse (285)		-TSSVPS	P---RLVP	VKTMS	SKLPLSS	SKSTAAMT	STVLTNT
IPS-1 rat (287)		TTSSVPS	IKP---VP	VNTMS	SKLPIST	SKSTAATP	STVPTNL
Consensus (307)		STVPSKVP	N A	VSTVPSKLP	TSSKPPGAVPS	V	TNLAPS
		Section 8					
	(358)	358	370	380	390	408	
IPS-1 (355)		RAGMVPS	SKVPTS	-----	MVLTKVS	ASTVPTD	GSSR--NEET
IPS-1 chimpanzee (355)		RAGMVPS	SKVPTS	-----	MVLTKVS	ASTVPTD	GSSR--NEET
IPS-1 rhesus macaque (356)		RAGMVPS	SKVPAS	-----	MVRTKVS	ASTVPTDR	SSR--TEET
IPS-1 cow (332)		RSGMVPP	PKVPTS	GIPDHRIP	PASTVPS	SKVPANT	RLTIRSS
IPS-1 pig (330)		FPGAMSP	PKVPT	GLLPDHR	KPTSTV	ASKVPANT	GPTIRSS
IPS-1 dog (332)		RAGTVPP	FRVPAG	LVPDHKMS	ASTVPS	SKGPANT	VPSISS
IPS-1 mouse (332)		YAGTVPS	RVVPAS	-----	VAKAPANT	IPPERNS	KQ-AKET
IPS-1 rat (335)		YTGIVPS	SKVTAS	-----	VAKASAST	MPPERNN	KQ-AKET
Consensus (358)		RAGMVPS	SKVPTS		VLSKVS	ASTVPTDR	SSR KETPAAP

		Section 9												
	(409)	409	420	430	440						459			
IPS-1 (394)		PAG	-ATGGSSAWLDSSSE	NRGLGS-	ELSKPGV	LASQVDS	P-	FSGC	FEDLAI					
IPS-1 chimpanzee (394)		PVG	-ATGGSSAWLDSSSE	NRGLGS-	ELSKPGV	LASQVDS	P-	FSGC	FEDLAI					
IPS-1 rhesus macaque (395)		PAG	-ATGGRSAWLDSSSE	NGGFES-	ELSKPGL	LVSQADS	Q-	FSGC	SEDLAI					
IPS-1 cow (383)		PTGT	ATGGTSLWP	DSSSDCCG	SEL-	ELSKPGR	LVS	RMDS	QPF	VS	CASDLAI			
IPS-1 pig (381)		PIGT	AAGGTS	WPDSNSD	RWDSEEP	ELSKPGR	LVS	RMDS	QPF	VS	CSSEDLAI			
IPS-1 dog (382)		PTDI	STRD	SLPGLDRSS	AGWGS	SEL-	ELSKPGR	LASQVDS	EP	FSGC	SADLAL			
IPS-1 mouse (369)		ATKVT	TGGNQ	TGFNS	IRSLHSG	P-	EMSKPGV	LVS	QLDEP	-	FSACSVDLAI			
IPS-1 rat (372)		ATVVT	TGSS	LTRPDIS	RSLSHSG	P-	ELSKPGV	LVS	QVDNE	EP	FSACSMDLAI			
Consensus (409)		PTG	ATGGSS	WPDSSSE	GSG	ELSKPGV	LVS	QVDS	PF	FSGC	SEDLAI			
		Section 10												
	(460)	460	470	480	490	500						510		
IPS-1 (442)		SASTSL	GMG	PCHG	PEENEY	KSE	EGTFG	IHVA	ENPSI	QLLEG	NP	GP	PAD	PDGG
IPS-1 chimpanzee (442)		SASTSL	GMG	PCHG	PEENEY	KSE	EGTFG	IHVA	ENPSI	QLLEG	NP	GP	PAD	PDGG
IPS-1 rhesus macaque (443)		SASTSL	GMG	PCRG	PEENEY	KSE	EGTFG	IHVA	ENPSI	QLMEG	NP	GP	PAD	PQGG
IPS-1 cow (433)		SHSN	SLGMG	PDNA	PEENEY	VSE	DTIRI	HE--	NP	STSL	LG	SP	GT	YTP---
IPS-1 pig (432)		SYSN	PLGSG	PDNT	PEENEY	VSV	DTIRI	Q--	DP	STPP	VG	DS	SP	GLTAS---
IPS-1 dog (432)		SYSR	SLGAG	PDNA	PEENEY	QSV	DIRIQ	VQD	PS	ADLL	EH	NP	GR	ATP---
IPS-1 mouse (418)		SPSS	SLVSE	PNHG	PEENEY	SS---	FRIQ	VDH	SP	SADLL	G-	SE	E	FLATQ---
IPS-1 rat (422)		SPST	SLGSE	PNHG	PEENEY	SS---	FRIQ	VDKS	PS	VDLL	G-	SE	E	FLATQ---
Consensus (460)		S	STSLGMG	P	CHGPEENEY	SE	TFRIQ	V	ENPSI	LLG	SPGP	ATP		
		Section 11												
	(511)	511	520	530	540						559			
IPS-1 (493)		PRPQADRKF	QEREV	PC	HRP	SPGAL	WLQ	VAVT	GV	LVV	TLLV	VLY	RR	RLH-
IPS-1 chimpanzee (493)		PRPQADRKF	QEREV	PC	HRP	SPGAL	WLQ	VAVT	GV	LVV	TLLV	VLY	RR	RLH-
IPS-1 rhesus macaque (494)		PRPHIDQKF	QEREG	PC	HRP	SPGAL	WLQ	AAVAG	V	LVV	TLLV	VLY	RR	RLH-
IPS-1 cow (479)		-----	EDEL	KEL	PVVR	MPWAS	WLGVA	MAGALL	V	LLAS	I	YR	FR	LPQ-
IPS-1 pig (478)		--EFQA	EEEL	EEG	EEV	KT	EARAP	W	GVAV	V	GVLL	AT	LL	AMLYRRRLPQ
IPS-1 dog (480)		-----	QP--	TV	EEEP	VQAS	SWAP	W	LGVA	T	GV	FL	AM	LLAVLYRRRLPQ
IPS-1 mouse (462)		-----	QP-	Q	EEEH	CAS	MPWAK	W	LGATS	A	LLAV	FL	AM	LYRSRRRLAQ
IPS-1 rat (466)		-----	QS-	P	EEEE	PCASS	VSWAK	W	LGATS	A	LLAA	FL	AM	LYRSRHLLAQ
Consensus (511)			Q	QEREL	PC	RSS	PWA	W	LGVA	V	AGV	LVV	TLLV	LLYRRRLQ

BIBLIOGRAPHY

1. **Afdhal, N. H.** 2004. The natural history of hepatitis C. *Semin. Liver Dis.* **24** Suppl 2:3-8.
2. **Alexopoulou, L., A. C. Holt, R. Medzhitov, and R. A. Flavell.** 2001. Recognition of double-stranded RNA and activation of NF-kappaB by Toll-like receptor 3. *Nature* **413**:732-738.
3. **Alter, H. J., P. V. Holland, A. G. Morrow, R. H. Purcell, S. M. Feinstone, and Y. Moritsugu.** 1975. Clinical and serological analysis of transfusion-associated hepatitis. *Lancet* **2**:838-841.
4. **Alter, H. J. and L. B. Seeff.** 2000. Recovery, persistence, and sequelae in hepatitis C virus infection: a perspective on long-term outcome. *Semin. Liver Dis.* **20**:17-35.
5. **Andrejeva, J., K. S. Childs, D. F. Young, T. S. Carlos, N. Stock, S. Goodbourn, and R. E. Randall.** 2004. The V proteins of paramyxoviruses bind the IFN-inducible RNA helicase, mda-5, and inhibit its activation of the IFN-beta promoter. *Proc. Natl. Acad. Sci. U. S. A* **101**:17264-17269.

6. **Arbely, E., Z. Granot, I. Kass, J. Orly, and I. T. Arkin.** 2006. A trimerizing GxxxG motif is uniquely inserted in the severe acute respiratory syndrome (SARS) coronavirus spike protein transmembrane domain. *Biochemistry* **45**:11349-11356.
7. **Asselah, T., I. Bieche, V. Paradis, P. Bedossa, M. Vidaud, and P. Marcellin.** 2007. Genetics, genomics, and proteomics: implications for the diagnosis and the treatment of chronic hepatitis C. *Semin. Liver Dis.* **27**:13-27.
8. **Bartenschlager, R.** 1999. The NS3/4A proteinase of the hepatitis C virus: unravelling structure and function of an unusual enzyme and a prime target for antiviral therapy. *J. Viral Hepat.* **6**:165-181.
9. **Bartenschlager, R., L. Ahlborn-Laake, K. Yasargil, J. Mous, and H. Jacobsen.** 1995. Substrate determinants for cleavage in cis and in trans by the hepatitis C virus NS3 proteinase. *J. Virol.* **69**:198-205.
10. **Bartenschlager, R. and V. Lohmann.** 2000. Replication of hepatitis C virus. *J. Gen. Virol.* **81**:1631-1648.
11. **Bartenschlager, R., V. Lohmann, T. Wilkinson, and J. O. Koch.** 1995. Complex formation between the NS3 serine-type proteinase of the hepatitis C

- virus and NS4A and its importance for polyprotein maturation. *J. Virol.* **69**:7519-7528.
12. **Barth, H., A. Ulsenheimer, G. R. Pape, H. M. Diepolder, M. Hoffmann, C. Neumann-Haefelin, R. Thimme, P. Henneke, R. Klein, G. Paranhos-Baccala, E. Depla, T. J. Liang, H. E. Blum, and T. F. Baumert.** 2005. Uptake and presentation of hepatitis C virus-like particles by human dendritic cells. *Blood.*
 13. **Bassett, S. E., K. M. Brasky, and R. E. Lanford.** 1998. Analysis of hepatitis C virus-inoculated chimpanzees reveals unexpected clinical profiles. *J. Virol.* **72**:2589-2599.
 14. **Beddoe, T. and T. Lithgow.** 2002. Delivery of nascent polypeptides to the mitochondrial surface. *Biochim. Biophys. Acta* **1592**:35-39.
 15. **Bigger, C., B. Guerra, K. Brasky, G. Hubbard, M. R. Beard, B. A. Luxon, S. M. Lemon, and R. Lanford.** 2004. Intrahepatic gene expression during chronic hepatitis C virus infection in chimpanzees. *J. Virol* **78**:xx.
 16. **Bigger, C. B., K. M. Brasky, and R. E. Lanford.** 2001. DNA microarray analysis of chimpanzee liver during acute resolving hepatitis C virus infection. *J. Virol.* **75**:7059-7066.

17. **Borowski, P., K. Oehlmann, M. Heiland, and R. Laufs.** 1997. Nonstructural protein 3 of hepatitis C virus blocks the distribution of free catalytic subunit of cyclic AMP-dependent protein kinase. *J. Virol.* **71**:2838-2843.
18. **Borowski, P., J. S. zur Wiesch, K. Resch, H. Feucht, R. Laufs, and H. Schmitz.** 1999. Protein kinase C recognizes the protein kinase A-binding motif of nonstructural protein 3 of hepatitis C virus. *J. Biol. Chem.* **274**:30722-30728.
19. **Brown, R. S.** 2005. Hepatitis C and liver transplantation. *Nature* **436**:973-978.
20. **Bukh, J.** 2004. A critical role for the chimpanzee model in the study of hepatitis C. *Hepatology* **39**:1469-1475.
21. **Carney, D. S. and M. Gale, Jr.** 2006. Unpublished data.
22. **Centers for Disease Control and Prevention.** 1998. Recommendations for Prevention and Control of Hepatitis C Virus (HCV) Infection and HCV-Related Chronic Disease. *Morbidity and Mortality Weekly Report* **47**:1-40.
23. Centers for Disease Control and Prevention, Division of Viral Hepatitis. *Epidemiology and Prevention of Viral Hepatitis A to E: Hepatitis C Virus.* 1-17-2003.

Ref Type: Slide

24. **Chen, G., R. Ray, D. Dubik, L. Shi, J. Cizeau, R. C. Bleackley, S. Saxena, R. D. Gietz, and A. H. Greenberg.** 1997. The E1B 19K/Bcl-2-binding protein Nip3 is a dimeric mitochondrial protein that activates apoptosis. *J. Exp. Med.* **186**:1975-1983.
25. **Chen, L., I. Borozan, J. Feld, J. Sun, L. L. Tannis, C. Coltescu, J. Heathcote, A. M. Edwards, and I. D. McGilvray.** 2005. Hepatic gene expression discriminates responders and nonresponders in treatment of chronic hepatitis C viral infection. *Gastroenterology* **128**:1437-1444.
26. **Chen, Z. J.** 2005. Ubiquitin signalling in the NF-kappaB pathway. *Nat. Cell Biol.* **7**:758-765.
27. **Choo, Q. L., G. Kuo, A. J. Weiner, L. R. Overby, D. W. Bradley, and M. Houghton.** 1989. Isolation of a cDNA clone derived from a blood-borne non-A, non-B viral hepatitis genome. *Science* **244**:359-362.
28. **Constantinescu, S. N., T. Keren, M. Socolovsky, H. Nam, Y. I. Henis, and H. F. Lodish.** 2001. Ligand-independent oligomerization of cell-surface erythropoietin receptor is mediated by the transmembrane domain. *Proc. Natl. Acad. Sci. U. S. A* **98**:4379-4384.

29. **Cserzo, M., E. Wallin, I. Simon, G. von Heijne, and A. Elofsson.** 1997. Prediction of transmembrane alpha-helices in prokaryotic membrane proteins: the dense alignment surface method. *Protein Eng* **10**:673-676.
30. **De Francesco, R. and G. Migliaccio.** 2005. Challenges and successes in developing new therapies for hepatitis C. *Nature* **436**:953-960.
31. **De Francesco, R., A. Pessi, and C. Steinkuhler.** 1998. The hepatitis C virus NS3 proteinase: structure and function of a zinc-containing serine proteinase. *Antivir. Ther.* **3**:99-109.
32. **De Francesco, R. and C. Steinkuhler.** 2000. Structure and function of the hepatitis C virus NS3-NS4A serine proteinase. *Curr. Top. Microbiol. Immunol.* **242**:149-169.
33. **De Francesco, R., L. Tomei, S. Altamura, V. Summa, and G. Migliaccio.** 2003. Approaching a new era for hepatitis C virus therapy: inhibitors of the NS3-4A serine protease and the NS5B RNA-dependent RNA polymerase. *Antiviral Res.* **58**:1-16.
34. **Diao, F., S. Li, Y. Tian, M. Zhang, L. G. Xu, Y. Zhang, R. P. Wang, D. Chen, Z. Zhai, B. Zhong, P. Tien, and H. B. Shu.** 2007. Negative regulation of

- MDA5- but not RIG-I-mediated innate antiviral signaling by the dihydroxyacetone kinase. *Proc. Natl. Acad. Sci. U. S. A* **104**:11706-11711.
35. **Dumont, S., W. Cheng, V. Serebrov, R. K. Beran, I. Tinoco, Jr., A. M. Pyle, and C. Bustamante.** 2006. RNA translocation and unwinding mechanism of HCV NS3 helicase and its coordination by ATP. *Nature* **439**:105-108.
 36. **Duneau, J. P., A. P. Vegh, and J. N. Sturgis.** 2007. A dimerization hierarchy in the transmembrane domains of the HER receptor family. *Biochemistry* **46**:2010-2019.
 37. **Egger, D., B. Wolk, R. Gosert, L. Bianchi, H. E. Blum, D. Moradpour, and K. Bienz.** 2002. Expression of hepatitis C virus proteins induces distinct membrane alterations including a candidate viral replication complex. *J. Virol.* **76**:5974-5984.
 38. **Feinstone, S. M., A. Z. Kapikian, R. H. Purcell, H. J. Alter, and P. V. Holland.** 1975. Transfusion-associated hepatitis not due to viral hepatitis type A or B. *N. Engl. J. Med.* **292**:767-770.
 39. **Feld, J. J. and J. H. Hoofnagle.** 2005. Mechanism of action of interferon and ribavirin in treatment of hepatitis C. *Nature* **436**:967-972.

40. **Fensterl, V., D. Grotheer, I. Berk, S. Schlemminger, A. Vallbracht, and A. Dotzauer.** 2005. Hepatitis A virus suppresses RIG-I-mediated IRF-3 activation to block induction of beta interferon. *J. Virol.* **79**:10968-10977.
41. **Ferreon, J. C., A. C. Ferreon, K. Li, and S. M. Lemon.** 2005. Molecular determinants of TRIF proteolysis mediated by the hepatitis C virus NS3/4A protease. *J. Biol. Chem.* **280**:20483-20492.
42. **Fitzgerald, K. A., S. M. McWhirter, K. L. Faia, D. C. Rowe, E. Latz, D. T. Golenbock, A. J. Coyle, S. M. Liao, and T. Maniatis.** 2003. IKKepsilon and TBK1 are essential components of the IRF3 signaling pathway. *Nat. Immunol.* **4**:491-496.
43. **Fontan, E., F. Traincard, S. G. Levy, S. Yamaoka, M. Veron, and F. Agou.** 2007. NEMO oligomerization in the dynamic assembly of the IkappaB kinase core complex. *FEBS J.* **274**:2540-2551.
44. **Foy, E., K. Li, R. Sumpter, Jr., Y. M. Loo, C. L. Johnson, C. Wang, P. M. Fish, M. Yoneyama, T. Fujita, S. M. Lemon, and M. Gale, Jr.** 2005. Control of antiviral defenses through hepatitis C virus disruption of retinoic acid-inducible gene-I signaling. *Proc. Natl. Acad. Sci. U. S. A* **102**:2986-2991.

45. **Foy, E., K. Li, C. Wang, R. Sumpter, Jr., M. Ikeda, S. M. Lemon, and M. Gale, Jr.** 2003. Regulation of interferon regulatory factor-3 by the hepatitis C virus serine protease. *Science* **300**:1145-1148.
46. **Fredericksen, B., G. R. Akkaraju, E. Foy, C. Wang, J. Pflugheber, Z. J. Chen, and M. Gale, Jr.** 2002. Activation of the interferon-beta promoter during hepatitis C virus RNA replication. *Viral Immunol.* **15**:29-40.
47. **Frick, D. N., S. Banik, and R. S. Rypma.** 2007. Role of divalent metal cations in ATP hydrolysis catalyzed by the hepatitis C virus NS3 helicase: magnesium provides a bridge for ATP to fuel unwinding. *J. Mol. Biol.* **365**:1017-1032.
48. **Frick, D. N., R. S. Rypma, A. M. Lam, and B. Gu.** 2004. The nonstructural protein 3 protease/helicase requires an intact protease domain to unwind duplex RNA efficiently. *J. Biol. Chem.* **279**:1269-1280.
49. **Fukuda, K., S. Sekiya, K. Kikuchi, K. Funaji, A. Kuno, T. Hasegawa, and S. Nishikawa.** 2001. Construction of the dual-functional RNA ligand against HCV NS3 protease and helicase. *Nucleic Acids Res. Suppl*147-148.
50. **Fukuda, K., T. Umehara, S. Sekiya, K. Kunio, T. Hasegawa, and S. Nishikawa.** 2004. An RNA ligand inhibits hepatitis C virus NS3 protease and helicase activities. *Biochem. Biophys. Res. Commun.* **325**:670-675.

51. **Gale, M., Jr., C. M. Blakely, B. Kwieciszewski, S. L. Tan, M. Dossett, N. M. Tang, M. J. Korth, S. J. Polyak, D. R. Gretch, and M. G. Katze.** 1998. Control of PKR protein kinase by hepatitis C virus nonstructural 5A protein: molecular mechanisms of kinase regulation. *Mol. Cell Biol.* **18**:5208-5218.
52. **Gale, M., Jr. and E. M. Foy.** 2005. Evasion of intracellular host defence by hepatitis C virus. *Nature* **436**:939-945.
53. **Gale, M., Jr. and M. G. Katze.** 1998. Molecular mechanisms of interferon resistance mediated by viral-directed inhibition of PKR, the interferon-induced protein kinase. *Pharmacol. Ther.* **78**:29-46.
54. **Gilmore, T. D.** 2006. Introduction to NF-kappaB: players, pathways, perspectives. *Oncogene* **25**:6680-6684.
55. **Gitlin, L., W. Barchet, S. Gilfillan, M. Cella, B. Beutler, R. A. Flavell, M. S. Diamond, and M. Colonna.** 2006. Essential role of mda-5 in type I IFN responses to polyriboinosinic:polyribocytidylic acid and encephalomyocarditis picornavirus. *Proc. Natl. Acad. Sci. U. S. A* **103**:8459-8464.
56. **Gosert, R., D. Egger, V. Lohmann, R. Bartenschlager, H. E. Blum, K. Bienz, and D. Moradpour.** 2003. Identification of the hepatitis C virus RNA replication complex in Huh-7 cells harboring subgenomic replicons. *J. Virol.* **77**:5487-5492.

57. **Grandvaux, N., M. J. Servant, B. Tenoever, G. C. Sen, S. Balachandran, G. N. Barber, R. Lin, and J. Hiscott.** 2002. Transcriptional profiling of interferon regulatory factor 3 target genes: direct involvement in the regulation of interferon-stimulated genes. *J. Virol.* **76**:5532-5539.
58. **Griffin, S. D., L. P. Beales, D. S. Clarke, O. Worsfold, S. D. Evans, J. Jaeger, M. P. Harris, and D. J. Rowlands.** 2003. The p7 protein of hepatitis C virus forms an ion channel that is blocked by the antiviral drug, Amantadine. *FEBS Lett.* **535**:34-38.
59. **Gu, B., C. M. Pruss, A. T. Gates, and S. S. Khandekar.** 2005. The RNA-unwinding activity of hepatitis C virus non-structural protein 3 (NS3) is positively modulated by its protease domain. *Protein Pept. Lett.* **12**:315-321.
60. **Guo, B. and G. Cheng.** 2007. Modulation of the interferon antiviral response by the TBK1/IKKi adaptor protein TANK. *J. Biol. Chem.* **282**:11817-11826.
61. **Gurezka, R., R. Laage, B. Brosig, and D. Langosch.** 1999. A heptad motif of leucine residues found in membrane proteins can drive self-assembly of artificial transmembrane segments. *J. Biol. Chem.* **274**:9265-9270.
62. **Hayden, M. S. and S. Ghosh.** 2004. Signaling to NF-kappaB. *Genes Dev.* **18**:2195-2224.

63. **Hayden, M. S., A. P. West, and S. Ghosh.** 2006. NF-kappaB and the immune response. *Oncogene* **25**:6758-6780.
64. **Helbig, K. J., D. T. Lau, L. Semendric, H. A. Harley, and M. R. Beard.** 2005. Analysis of ISG expression in chronic hepatitis C identifies viperin as a potential antiviral effector. *Hepatology* **42**:702-710.
65. **Hemmi, H., O. Takeuchi, S. Sato, M. Yamamoto, T. Kaisho, H. Sanjo, T. Kawai, K. Hoshino, K. Takeda, and S. Akira.** 2004. The roles of two IkappaB kinase-related kinases in lipopolysaccharide and double stranded RNA signaling and viral infection. *J. Exp. Med.* **199**:1641-1650.
66. **Hinrichsen, H., Y. Benhamou, H. Wedemeyer, M. Reiser, R. E. Sentjens, J. L. Calleja, X. Forns, A. Erhardt, J. Cronlein, R. L. Chaves, C. L. Yong, G. Nehmiz, and G. G. Steinmann.** 2004. Short-term antiviral efficacy of BILN 2061, a hepatitis C virus serine protease inhibitor, in hepatitis C genotype 1 patients. *Gastroenterology* **127**:1347-1355.
67. **Hiscott, J.** 2007. Triggering the innate antiviral response through IRF-3 activation. *J. Biol. Chem.* **282**:15325-15329.

68. **Hiscott, J., T. L. Nguyen, M. Arguello, P. Nakhaei, and S. Paz.** 2006. Manipulation of the nuclear factor-kappaB pathway and the innate immune response by viruses. *Oncogene* **25**:6844-6867.
69. **Hoffmann, A., G. Natoli, and G. Ghosh.** 2006. Transcriptional regulation via the NF-kappaB signaling module. *Oncogene* **25**:6706-6716.
70. **Honda, K., A. Takaoka, and T. Taniguchi.** 2006. Type I interferon gene induction by the interferon regulatory factor family of transcription factors. *Immunity*. **25**:349-360.
71. **Honda, K., H. Yanai, H. Negishi, M. Asagiri, M. Sato, T. Mizutani, N. Shimada, Y. Ohba, A. Takaoka, N. Yoshida, and T. Taniguchi.** 2005. IRF-7 is the master regulator of type-I interferon-dependent immune responses. *Nature*.
72. **Hoofnagle, J. H.** 1997. Hepatitis C: the clinical spectrum of disease. *Hepatology* **26**:15S-20S.
73. **Hornung, V., J. Ellegast, S. Kim, K. Brzozka, A. Jung, H. Kato, H. Poeck, S. Akira, K. K. Conzelmann, M. Schlee, S. Endres, and G. Hartmann.** 2006. 5'-Triphosphate RNA Is the Ligand for RIG-I. *Science*.

74. **Johnson, C. L. and M. Gale, Jr.** 2006. CARD games between virus and host get a new player. *Trends Immunol.* **27**:1-4.
75. **Johnson, C. L., D. M. Owen, and M. Gale, Jr.** 2007. Functional and therapeutic analysis of hepatitis C virus NS3.4A protease control of antiviral immune defense. *J. Biol. Chem.* **282**:10792-10803.
76. **Jones, C. T., C. L. Murray, D. K. Eastman, J. Tassello, and C. M. Rice.** 2007. Hepatitis C virus p7 and NS2 proteins are essential for infectious virus production. *J. Virol.*
77. **Karbowski, M., K. L. Norris, M. M. Cleland, S. Y. Jeong, and R. J. Youle.** 2006. Role of Bax and Bak in mitochondrial morphogenesis. *Nature* **443**:658-662.
78. **Kato, H., O. Takeuchi, S. Sato, M. Yoneyama, M. Yamamoto, K. Matsui, S. Uematsu, A. Jung, T. Kawai, K. J. Ishii, O. Yamaguchi, K. Otsu, T. Tsujimura, C. S. Koh, Reis e Sousa, Y. Matsuura, T. Fujita, and S. Akira.** 2006. Differential roles of MDA5 and RIG-I helicases in the recognition of RNA viruses. *Nature* **441**:101-105.

79. **Kaufmann, T., S. Schlipf, J. Sanz, K. Neubert, R. Stein, and C. Borner.** 2003. Characterization of the signal that directs Bcl-x(L), but not Bcl-2, to the mitochondrial outer membrane. *J. Cell Biol.* **160**:53-64.
80. **Kawai, T., K. Takahashi, S. Sato, C. Coban, H. Kumar, H. Kato, K. J. Ishii, O. Takeuchi, and S. Akira.** 2005. IPS-1, an adaptor triggering RIG-I- and Mda5-mediated type I interferon induction. *Nat. Immunol.* **6**:981-988.
81. **Kim, J. L., K. A. Morgenstern, C. Lin, T. Fox, M. D. Dwyer, J. A. Landro, S. P. Chambers, W. Markland, C. A. Lepre, E. T. O'Malley, S. L. Harbeson, C. M. Rice, M. A. Murcko, P. R. Caron, and J. A. Thomson.** 1996. Crystal structure of the hepatitis C virus NS3 protease domain complexed with a synthetic NS4A cofactor peptide. *Cell* **87**:343-355.
82. **Kobayashi, T., M. C. Walsh, and Y. Choi.** 2004. The role of TRAF6 in signal transduction and the immune response. *Microbes. Infect.* **6**:1333-1338.
83. **Kolykhalov, A. A., E. V. Agapov, K. J. Blight, K. Mihalik, S. M. Feinstone, and C. M. Rice.** 1997. Transmission of hepatitis C by intrahepatic inoculation with transcribed RNA. *Science* **277**:570-574.
84. **Komuro, A. and C. M. Horvath.** 2006. RNA- and virus-independent inhibition of antiviral signaling by RNA helicase LGP2. *J. Virol.* **80**:12332-12342.

85. **Kuang, W. F., Y. C. Lin, F. Jean, Y. W. Huang, C. L. Tai, D. S. Chen, P. J. Chen, and L. H. Hwang.** 2004. Hepatitis C virus NS3 RNA helicase activity is modulated by the two domains of NS3 and NS4A. *Biochem. Biophys. Res. Commun.* **317**:211-217.
86. **Kumar, H., T. Kawai, H. Kato, S. Sato, K. Takahashi, C. Coban, M. Yamamoto, S. Uematsu, K. J. Ishii, O. Takeuchi, and S. Akira.** 2006. Essential role of IPS-1 in innate immune responses against RNA viruses. *J. Exp. Med.* **203**:1795-1803.
87. **Kwong, A. D., J. L. Kim, and C. Lin.** 2000. Structure and function of hepatitis C virus NS3 helicase. *Curr. Top. Microbiol. Immunol.* **242**:171-196.
88. **Lanford, R. E. and C. Bigger.** 2002. Advances in model systems for hepatitis C virus research. *Virology* **293**:1-9.
89. **Lee, N. K. and S. Y. Lee.** 2002. Modulation of life and death by the tumor necrosis factor receptor-associated factors (TRAFs). *J. Biochem. Mol. Biol.* **35**:61-66.
90. **Li, K., E. Foy, J. C. Ferreon, M. Nakamura, A. C. Ferreon, M. Ikeda, S. C. Ray, M. Gale, Jr., and S. M. Lemon.** 2005. Immune evasion by hepatitis C

virus NS3/4A protease-mediated cleavage of the Toll-like receptor 3 adaptor protein TRIF. *Proc. Natl. Acad. Sci. U. S. A* **102**:2992-2997.

91. **Li, X. D., L. Sun, R. B. Seth, G. Pineda, and Z. J. Chen.** 2005. Hepatitis C virus protease NS3/4A cleaves mitochondrial antiviral signaling protein off the mitochondria to evade innate immunity. *Proc. Natl. Acad. Sci. U. S. A* **102**:17717-17722.
92. **Lin, C., K. Lin, Y. P. Luong, B. G. Rao, Y. Y. Wei, D. L. Brennan, J. R. Fulghum, H. M. Hsiao, S. Ma, J. P. Maxwell, K. M. Cottrell, R. B. Perni, C. A. Gates, and A. D. Kwong.** 2004. In vitro resistance studies of hepatitis C virus serine protease inhibitors, VX-950 and BILN 2061: structural analysis indicates different resistance mechanisms. *J. Biol. Chem.* **279**:17508-17514.
93. **Lin, R., J. Lacoste, P. Nakhaei, Q. Sun, L. Yang, S. Paz, P. Wilkinson, I. Julkunen, D. Vitour, E. Meurs, and J. Hiscott.** 2006. Dissociation of a MAVS/IPS-1/VISA/Cardif-IKKepsilon molecular complex from the mitochondrial outer membrane by hepatitis C virus NS3-4A proteolytic cleavage. *J. Virol.* **80**:6072-6083.
94. **Lin, R., Y. Mamane, and J. Hiscott.** 1999. Structural and functional analysis of interferon regulatory factor 3: localization of the transactivation and autoinhibitory domains. *Mol. Cell Biol.* **19**:2465-2474.

95. **Lindenbach, B. D., M. J. Evans, A. J. Syder, B. Wolk, T. L. Tellinghuisen, C. C. Liu, T. Maruyama, R. O. Hynes, D. R. Burton, J. A. McKeating, and C. M. Rice.** 2005. Complete replication of hepatitis C virus in cell culture. *Science* **309**:623-626.
96. **Lindenbach, B. D. and C. M. Rice.** 2005. Unravelling hepatitis C virus replication from genome to function. *Nature* **436**:933-938.
97. **Lohmann, V., F. Korner, J. Koch, U. Herian, L. Theilmann, and R. Bartenschlager.** 1999. Replication of subgenomic hepatitis C virus RNAs in a hepatoma cell line. *Science* **285**:110-113.
98. **Loo, Y. M., D. M. Owen, K. Li, A. K. Erickson, C. L. Johnson, P. M. Fish, D. S. Carney, T. Wang, H. Ishida, M. Yoneyama, T. Fujita, T. Saito, W. M. Lee, C. H. Hagedorn, D. T. Lau, S. A. Weinman, S. M. Lemon, and M. Gale, Jr.** 2006. Viral and therapeutic control of IFN-beta promoter stimulator 1 during hepatitis C virus infection. *Proc. Natl. Acad. Sci. U. S. A* **103**:6001-6006.
99. **Love, R. A., H. E. Parge, J. A. Wickersham, Z. Hostomsky, N. Habuka, E. W. Moomaw, T. Adachi, and Z. Hostomska.** 1996. The crystal structure of hepatitis C virus NS3 proteinase reveals a trypsin-like fold and a structural zinc binding site. *Cell* **87**:331-342.

100. **Love, R. A., H. E. Parge, J. A. Wickersham, Z. Hostomsky, N. Habuka, E. W. Moomaw, T. Adachi, S. Margosiak, E. Dagostino, and Z. Hostomska.** 1998. The conformation of hepatitis C virus NS3 proteinase with and without NS4A: a structural basis for the activation of the enzyme by its cofactor. *Clin. Diagn. Virol.* **10**:151-156.
101. **Lu, G., J. T. Reinert, I. Pitha-Rowe, A. Okumura, M. Kellum, K. P. Knobeloch, B. Hassel, and P. M. Pitha.** 2006. ISG15 enhances the innate antiviral response by inhibition of IRF-3 degradation. *Cell Mol. Biol. (Noisy-le-grand)* **52**:29-41.
102. **Luedde, T., N. Beraza, V. Kotsikoris, G. van Loo, A. Nenci, R. De Vos, T. Roskams, C. Trautwein, and M. Pasparakis.** 2007. Deletion of NEMO/IKKgamma in liver parenchymal cells causes steatohepatitis and hepatocellular carcinoma. *Cancer Cell* **11**:119-132.
103. **Lyra, A. C., X. Fan, and A. M. Di Bisceglie.** 2004. Molecular biology and clinical implication of hepatitis C virus. *Braz. J. Med. Biol. Res.* **37**:691-695.
104. **Matsuda, A., Y. Suzuki, G. Honda, S. Muramatsu, O. Matsuzaki, Y. Nagano, T. Doi, K. Shimotohno, T. Harada, E. Nishida, H. Hayashi, and S. Sugano.** 2003. Large-scale identification and characterization of human genes that activate NF-kappaB and MAPK signaling pathways. *Oncogene* **22**:3307-3318.

105. **McCoy, M. A., M. M. Senior, J. J. Gesell, L. Ramanathan, and D. F. Wyss.** 2001. Solution structure and dynamics of the single-chain hepatitis C virus NS3 protease NS4A cofactor complex. *J. Mol. Biol.* **305**:1099-1110.
106. **McHutchison, J. G. and B. R. Bacon.** 2005. Chronic hepatitis C: an age wave of disease burden. *Am. J. Manag. Care* **11**:S286-S295.
107. **Mendrola, J. M., M. B. Berger, M. C. King, and M. A. Lemmon.** 2002. The single transmembrane domains of ErbB receptors self-associate in cell membranes. *J. Biol. Chem.* **277**:4704-4712.
108. **Mercer, D. F., D. E. Schiller, J. F. Elliott, D. N. Douglas, C. Hao, A. Rinfret, W. R. Addison, K. P. Fischer, T. A. Churchill, J. R. Lakey, D. L. Tyrrell, and N. M. Kneteman.** 2001. Hepatitis C virus replication in mice with chimeric human livers. *Nat. Med.* **7**:927-933.
109. **Meylan, E., J. Curran, K. Hofmann, D. Moradpour, M. Binder, R. Bartenschlager, and J. Tschopp.** 2005. Cardif is an adaptor protein in the RIG-I antiviral pathway and is targeted by hepatitis C virus. *Nature* **437**:1167-1172.
110. **Mihm, S., M. Frese, V. Meier, P. Wietzke-Braun, J. G. Scharf, R. Bartenschlager, and G. Ramadori.** 2004. Interferon type I gene expression in chronic hepatitis C. *Lab Invest* **84**:1148-1159.

111. **Moradpour, D. and H. E. Blum.** 2004. A primer on the molecular virology of hepatitis C. *Liver Int.* **24**:519-525.
112. **Moradpour, D., R. Gosert, D. Egger, F. Penin, H. E. Blum, and K. Bienz.** 2003. Membrane association of hepatitis C virus nonstructural proteins and identification of the membrane alteration that harbors the viral replication complex. *Antiviral Res.* **60**:103-109.
113. **Moradpour, D., P. Kary, C. M. Rice, and H. E. Blum.** 1998. Continuous human cell lines inducibly expressing hepatitis C virus structural and nonstructural proteins. *Hepatology* **28**:192-201.
114. **Nakabayashi, H., K. Taketa, K. Miyano, T. Yamane, and J. Sato.** 1982. Growth of human hepatoma cell lines with differentiated functions in chemically defined medium. *Cancer Res.* **42**:3858-3863.
115. National Digestive Diseases Information Clearinghouse, National Institute of Diabetes and Digestive and Kidney Diseases, and National Institutes of Health. Chronic Hepatitis C: Current Disease Management. NIH Publication number 07-4230, 1-23. 2007. Bethesda, MD.

Ref Type: Report

116. **Natoli, G., A. Costanzo, A. Ianni, D. J. Templeton, J. R. Woodgett, C. Balsano, and M. Levrero.** 1997. Activation of SAPK/JNK by TNF receptor 1 through a noncytotoxic TRAF2-dependent pathway. *Science* **275**:200-203.
117. **Ni, Z. J. and A. S. Wagman.** 2004. Progress and development of small molecule HCV antivirals. *Curr. Opin. Drug Discov. Devel.* **7**:446-459.
118. **Nishikawa, F., N. Kakiuchi, K. Funaji, K. Fukuda, S. Sekiya, and S. Nishikawa.** 2003. Inhibition of HCV NS3 protease by RNA aptamers in cells. *Nucleic Acids Res.* **31**:1935-1943.
119. **Nomura-Takigawa, Y., M. Nagano-Fujii, L. Deng, S. Kitazawa, S. Ishido, K. Sada, and H. Hotta.** 2006. Non-structural protein 4A of Hepatitis C virus accumulates on mitochondria and renders the cells prone to undergoing mitochondria-mediated apoptosis. *J. Gen. Virol.* **87**:1935-1945.
120. **Oganesyan, G., S. K. Saha, B. Guo, J. Q. He, A. Shahangian, B. Zarnegar, A. Perry, and G. Cheng.** 2006. Critical role of TRAF3 in the Toll-like receptor-dependent and -independent antiviral response. *Nature* **439**:208-211.
121. **Otsuka, M., N. Kato, M. Moriyama, H. Taniguchi, Y. Wang, N. Dharel, T. Kawabe, and M. Omata.** 2005. Interaction between the HCV NS3 protein and

the host TBK1 protein leads to inhibition of cellular antiviral responses.

Hepatology **41**:1004-1012.

122. **Pang, P. S., E. Jankowsky, P. J. Planet, and A. M. Pyle.** 2002. The hepatitis C viral NS3 protein is a processive DNA helicase with cofactor enhanced RNA unwinding. *EMBO J.* **21**:1168-1176.
123. **Pavlovic, D., D. C. Neville, O. Argaud, B. Blumberg, R. A. Dwek, W. B. Fischer, and N. Zitzmann.** 2003. The hepatitis C virus p7 protein forms an ion channel that is inhibited by long-alkyl-chain iminosugar derivatives. *Proc. Natl. Acad. Sci. U. S. A* **100**:6104-6108.
124. **Penin, F., J. Dubuisson, F. A. Rey, D. Moradpour, and J. M. Pawlotsky.** 2004. Structural biology of hepatitis C virus. *Hepatology* **39**:5-19.
125. **Pflugheber, J., B. Fredericksen, R. Sumpter, Jr., C. Wang, F. Ware, D. L. Sodora, and M. Gale, Jr.** 2002. Regulation of PKR and IRF-1 during hepatitis C virus RNA replication. *Proc. Natl. Acad. Sci. U. S. A* **99**:4650-4655.
126. **Pichlmair, A., O. Schulz, C. P. Tan, T. I. Naslund, P. Liljestrom, F. Weber, and Reis e Sousa.** 2006. RIG-I-Mediated Antiviral Responses to Single-Stranded RNA Bearing 5' Phosphates. *Science*.

127. **Qureshi, S. A.** 2007. Hepatitis C virus--biology, host evasion strategies, and promising new therapies on the horizon. *Med. Res. Rev.* **27**:353-373.
128. **Reed, K. E. and C. M. Rice.** 1998. Molecular characterization of hepatitis C virus. *Curr. Stud. Hematol. Blood Transfus.* 1-37.
129. **Reesink, H. W., S. Zeuzem, C. J. Weegink, N. Forestier, A. van Vliet, van de Wetering de Rooij, L. McNair, S. Purdy, R. Kauffman, J. Alam, and P. L. Jansen.** 2006. Rapid decline of viral RNA in hepatitis C patients treated with VX-950: a phase Ib, placebo-controlled, randomized study. *Gastroenterology* **131**:997-1002.
130. **Reich, N. C.** 2002. Nuclear/cytoplasmic localization of IRFs in response to viral infection or interferon stimulation. *J. Interferon Cytokine Res.* **22**:103-109.
131. **Reiser, M., H. Hinrichsen, Y. Benhamou, H. W. Reesink, H. Wedemeyer, C. Avendano, N. Riba, C. L. Yong, G. Nehmiz, and G. G. Steinmann.** 2005. Antiviral efficacy of NS3-serine protease inhibitor BILN-2061 in patients with chronic genotype 2 and 3 hepatitis C. *Hepatology* **41**:832-835.
132. **Rosenberg, S.** 2001. Recent advances in the molecular biology of hepatitis C virus. *J. Mol. Biol.* **313**:451-464.

133. **Saha, S. K., E. M. Pietras, J. Q. He, J. R. Kang, S. Y. Liu, G. Oganessian, A. Shahangian, B. Zarnegar, T. L. Shiba, Y. Wang, and G. Cheng.** 2006. Regulation of antiviral responses by a direct and specific interaction between TRAF3 and Cardif. *EMBO J.* **25**:3257-3263.
134. **Saito, T. and M. Gale, Jr.** 2007. Principles of intracellular viral recognition. *Curr. Opin. Immunol.* **19**:17-23.
135. **Saito, T., R. Hirai, Y. M. Loo, D. Owen, C. L. Johnson, S. C. Sinha, S. Akira, T. Fujita, and M. Gale, Jr.** 2007. Regulation of innate antiviral defenses through a shared repressor domain in RIG-I and LGP2. *Proc. Natl. Acad. Sci. U. S. A* **104**:582-587.
136. **Sasai, M., M. Shingai, K. Funami, M. Yoneyama, T. Fujita, M. Matsumoto, and T. Seya.** 2006. NAK-associated protein 1 participates in both the TLR3 and the cytoplasmic pathways in type I IFN induction. *J. Immunol.* **177**:8676-8683.
137. **Schafer, S. L., R. Lin, P. A. Moore, J. Hiscott, and P. M. Pitha.** 1998. Regulation of type I interferon gene expression by interferon regulatory factor-3. *J. Biol. Chem.* **273**:2714-2720.

138. **Schneider, D. and D. M. Engelman.** 2004. Motifs of two small residues can assist but are not sufficient to mediate transmembrane helix interactions. *J. Mol. Biol.* **343**:799-804.

139. **Schwer, B., S. Ren, T. Pietschmann, J. Kartenbeck, K. Kaehlcke, R. Bartenschlager, T. S. Yen, and M. Ott.** 2004. Targeting of hepatitis C virus core protein to mitochondria through a novel C-terminal localization motif. *J. Virol.* **78**:7958-7968.

140. **Sen, G. C.** 2001. Viruses and interferons. *Annu. Rev. Microbiol.* **55**:255-281.

141. **Senes, A., M. Gerstein, and D. M. Engelman.** 2000. Statistical analysis of amino acid patterns in transmembrane helices: the GxxxG motif occurs frequently and in association with beta-branched residues at neighboring positions. *J. Mol. Biol.* **296**:921-936.

142. **Servant, M. J., B. Tenoever, and R. Lin.** 2002. Overlapping and distinct mechanisms regulating IRF-3 and IRF-7 function. *J. Interferon Cytokine Res.* **22**:49-58.

143. **Seth, R. B., L. Sun, C. K. Ea, and Z. J. Chen.** 2005. Identification and characterization of MAVS, a mitochondrial antiviral signaling protein that activates NF-kappaB and IRF 3. *Cell* **122**:669-682.

144. **Silverman, E., G. Edwalds-Gilbert, and R. J. Lin.** 2003. DExD/H-box proteins and their partners: helping RNA helicases unwind. *Gene* **312**:1-16.
145. **Silverman, N. and T. Maniatis.** 2001. NF-kappaB signaling pathways in mammalian and insect innate immunity. *Genes Dev.* **15**:2321-2342.
146. **Smith, M. W., Z. N. Yue, M. J. Korth, H. A. Do, L. Boix, N. Fausto, J. Bruix, R. L. Carithers, Jr., and M. G. Katze.** 2003. Hepatitis C virus and liver disease: global transcriptional profiling and identification of potential markers. *Hepatology* **38**:1458-1467.
147. **Smyth, D. J., J. D. Cooper, R. Bailey, S. Field, O. Burren, L. J. Smink, C. Guja, C. Ionescu-Tirgoviste, B. Widmer, D. B. Dunger, D. A. Savage, N. M. Walker, D. G. Clayton, and J. A. Todd.** 2006. A genome-wide association study of nonsynonymous SNPs identifies a type 1 diabetes locus in the interferon-induced helicase (IFIH1) region. *Nat. Genet.* **38**:617-619.
148. **Sulistijo, E. S. and K. R. MacKenzie.** 2006. Sequence dependence of BNIP3 transmembrane domain dimerization implicates side-chain hydrogen bonding and a tandem GxxxG motif in specific helix-helix interactions. *J. Mol. Biol.* **364**:974-990.

149. **Sumpter, R., Jr., Y. M. Loo, E. Foy, K. Li, M. Yoneyama, T. Fujita, S. M. Lemon, and M. Gale, Jr.** 2005. Regulating intracellular antiviral defense and permissiveness to hepatitis C virus RNA replication through a cellular RNA helicase, RIG-I. *J. Virol.* **79**:2689-2699.
150. **Sumpter, R., Jr., C. Wang, E. Foy, Y. M. Loo, and M. Gale, Jr.** 2004. Viral evolution and interferon resistance of hepatitis C virus RNA replication in a cell culture model. *J. Virol.* **78**:11591-11604.
151. **Sun, Q., L. Sun, H. H. Liu, X. Chen, R. B. Seth, J. Forman, and Z. J. Chen.** 2006. The specific and essential role of MAVS in antiviral innate immune responses. *Immunity.* **24**:633-642.
152. **Suzuki, R., T. Suzuki, K. Ishii, Y. Matsuura, and T. Miyamura.** 1999. Processing and functions of Hepatitis C virus proteins. *Intervirology* **42**:145-152.
153. **Szabo, E., G. Lotz, C. Paska, A. Kiss, and Z. Schaff.** 2003. Viral hepatitis: new data on hepatitis C infection. *Pathol. Oncol. Res.* **9**:215-221.
154. **Tan, S. L., Y. He, Y. Huang, and M. Gale, Jr.** 2004. Strategies for hepatitis C therapeutic intervention: now and next. *Curr. Opin. Pharmacol.* **4**:465-470.

155. **Taniguchi, T., K. Ogasawara, A. Takaoka, and N. Tanaka.** 2001. IRF family of transcription factors as regulators of host defense. *Annu. Rev. Immunol.* **19**:623-655.
156. **Taremi, S. S., B. Beyer, M. Maher, N. Yao, W. Prosise, P. C. Weber, and B. A. Malcolm.** 1998. Construction, expression, and characterization of a novel fully activated recombinant single-chain hepatitis C virus protease. *Protein Sci.* **7**:2143-2149.
157. **TenOever, B. R., S. L. Ng, M. A. Chua, S. M. McWhirter, A. Garcia-Sastre, and T. Maniatis.** 2007. Multiple functions of the IKK-related kinase IKKepsilon in interferon-mediated antiviral immunity. *Science* **315**:1274-1278.
158. **Urbani, A., G. Biasiol, M. Brunetti, C. Volpari, S. Di Marco, M. Sollazzo, S. Orru, F. D. Piazz, A. Casbarra, P. Pucci, C. Nardi, P. Gallinari, R. De Francesco, and C. Steinkuhler.** 1999. Multiple determinants influence complex formation of the hepatitis C virus NS3 protease domain with its NS4A cofactor peptide. *Biochemistry* **38**:5206-5215.
159. **Varaklioti, A., N. Vassilaki, U. Georgopoulou, and P. Mavromara.** 2002. Alternate translation occurs within the core coding region of the hepatitis C viral genome. *J. Biol. Chem.* **277**:17713-17721.

160. **Venkataraman, T., M. Valdes, R. Elsby, S. Kakuta, G. Caceres, S. Saijo, Y. Iwakura, and G. N. Barber.** 2007. Loss of DExD/H box RNA helicase LGP2 manifests disparate antiviral responses. *J. Immunol.* **178**:6444-6455.
161. **Voelker, D. R.** 2003. New perspectives on the regulation of intermembrane glycerophospholipid traffic. *J. Lipid Res.* **44**:441-449.
162. **Wakita, T., T. Pietschmann, T. Kato, T. Date, M. Miyamoto, Z. Zhao, K. Murthy, A. Habermann, H. G. Krausslich, M. Mizokami, R. Bartenschlager, and T. J. Liang.** 2005. Production of infectious hepatitis C virus in tissue culture from a cloned viral genome. *Nat. Med.* **11**:791-796.
163. **Wang, C., M. Gale, Jr., B. C. Keller, H. Huang, M. S. Brown, J. L. Goldstein, and J. Ye.** 2005. Identification of FBL2 as a geranylgeranylated cellular protein required for hepatitis C virus RNA replication. *Mol. Cell* **18**:425-434.
164. **Wang, C., J. Pflugheber, R. Sumpter, Jr., D. L. Sodora, D. Hui, G. C. Sen, and M. Gale, Jr.** 2003. Alpha interferon induces distinct translational control programs to suppress hepatitis C virus RNA replication. *J. Virol.* **77**:3898-3912.

165. **Wathelet, M. G., C. H. Lin, B. S. Parekh, L. V. Ronco, P. M. Howley, and T. Maniatis.** 1998. Virus infection induces the assembly of coordinately activated transcription factors on the IFN-beta enhancer in vivo. *Mol. Cell* **1**:507-518.
166. **Wolk, B., D. Sansonno, H. G. Krausslich, F. Dammacco, C. M. Rice, H. E. Blum, and D. Moradpour.** 2000. Subcellular localization, stability, and trans-cleavage competence of the hepatitis C virus NS3-NS4A complex expressed in tetracycline-regulated cell lines. *J. Virol.* **74**:2293-2304.
167. **Wong, J. B., G. M. McQuillan, J. G. McHutchison, and T. Poynard.** 2000. Estimating future hepatitis C morbidity, mortality, and costs in the United States. *Am. J. Public Health* **90**:1562-1569.
168. World Health Organization. Hepatitis C. 2002.

Ref Type: Slide

169. **Wyss, D. F., A. Arasappan, M. M. Senior, Y. S. Wang, B. M. Beyer, F. G. Njoroge, and M. A. McCoy.** 2004. Non-peptidic small-molecule inhibitors of the single-chain hepatitis C virus NS3 protease/NS4A cofactor complex discovered by structure-based NMR screening. *J. Med. Chem.* **47**:2486-2498.

170. **Xu, L. G., Y. Y. Wang, K. J. Han, L. Y. Li, Z. Zhai, and H. B. Shu.** 2005. VISA Is an Adapter Protein Required for Virus-Triggered IFN-beta Signaling. *Mol. Cell* **19**:727-740.
171. **Xu, Z., J. Choi, T. S. Yen, W. Lu, A. Strohecker, S. Govindarajan, D. Chien, M. J. Selby, and J. Ou.** 2001. Synthesis of a novel hepatitis C virus protein by ribosomal frameshift. *EMBO J.* **20**:3840-3848.
172. **Yan, Y., Y. Li, S. Munshi, V. Sardana, J. L. Cole, M. Sardana, C. Steinkuehler, L. Tomei, R. De Francesco, L. C. Kuo, and Z. Chen.** 1998. Complex of NS3 protease and NS4A peptide of BK strain hepatitis C virus: a 2.2 Å resolution structure in a hexagonal crystal form. *Protein Sci.* **7**:837-847.
173. **Yao, N., P. Reichert, S. S. Taremi, W. W. Prosser, and P. C. Weber.** 1999. Molecular views of viral polyprotein processing revealed by the crystal structure of the hepatitis C virus bifunctional protease-helicase. *Structure. Fold. Des* **7**:1353-1363.
174. **Yoneyama, M., M. Kikuchi, K. Matsumoto, T. Imaizumi, M. Miyagishi, K. Taira, E. Foy, Y. M. Loo, M. Gale, Jr., S. Akira, S. Yonehara, A. Kato, and T. Fujita.** 2005. Shared and unique functions of the DExD/H-box helicases RIG-I, MDA5, and LGP2 in antiviral innate immunity. *J. Immunol.* **175**:2851-2858.

175. **Yoneyama, M., M. Kikuchi, T. Natsukawa, N. Shinobu, T. Imaizumi, M. Miyagishi, K. Taira, S. Akira, and T. Fujita.** 2004. The RNA helicase RIG-I has an essential function in double-stranded RNA-induced innate antiviral responses. *Nat. Immunol.* **5**:730-737.
176. **Yoneyama, M., W. Suhara, and T. Fujita.** 2002. Control of IRF-3 activation by phosphorylation. *J. Interferon Cytokine Res.* **22**:73-76.
177. **Yoneyama, M., W. Suhara, Y. Fukuhara, M. Sato, K. Ozato, and T. Fujita.** 1996. Autocrine amplification of type I interferon gene expression mediated by interferon stimulated gene factor 3 (ISGF3). *J. Biochem. (Tokyo)* **120**:160-169.
178. **Zhang, C., Z. Cai, Y. C. Kim, R. Kumar, F. Yuan, P. Y. Shi, C. Kao, and G. Luo.** 2005. Stimulation of hepatitis C virus (HCV) nonstructural protein 3 (NS3) helicase activity by the NS3 protease domain and by HCV RNA-dependent RNA polymerase. *J. Virol.* **79**:8687-8697.
179. **Zhao, T., L. Yang, Q. Sun, M. Arguello, D. W. Ballard, J. Hiscott, and R. Lin.** 2007. The NEMO adaptor bridges the nuclear factor-kappaB and interferon regulatory factor signaling pathways. *Nat. Immunol.* **8**:592-600.

180. **Zhong, J., P. Gastaminza, G. Cheng, S. Kapadia, T. Kato, D. R. Burton, S. F. Wieland, S. L. Uprichard, T. Wakita, and F. V. Chisari.** 2005. Robust hepatitis C virus infection in vitro. *Proc. Natl. Acad. Sci. U. S. A* **102**:9294-9299.